Wave focussing in a laboratory flume

Final report
Master's thesis

M.J.G. van den Boomgaard
June 2003

Preface

This master thesis is the result of my research performed at the Delft University of Technology at the Faculty of Civil Engineering and Geosciences within the scope of my graduation project.

I would like to thank the members of my graduation committee for their support, advice and enthusiasm to complete this graduation work. Especially I would like to thank ir. G. Klopman for sharing his knowledge, direct support and enthusiasm.

I would also like to thank all the people of the Fluid Mechanics Laboratory for the pleasant time and showing their interest. Especially I would like to thank M. van de Meer for his assistance during the experiments.

I hope you enjoy reading this report.

Delft, June 2003

Marloes van den Boomgaard

Committee:

Prof. Dr. Ir. J. A. Battjes
Ir. A van Dongeren
Dr. Ir. H. L. Fontijn
Ir. G. Klopman
Prof. Dr. Ir. J. A. Pinkster

Summary

"Freak" or "rogue" waves are characterised as single, remarkably horizontally asymmetric and extremely high waves, which have an unpredictable nature and appear unexpectedly even in relatively calm seas. These waves have caused serious damage to ships and offshore structures and are therefore hazardous to mariners. Although the occurrence of freak waves has been widely acknowledged, these waves occur in such a short period of time that only a few measurements of these waves in nature are available. It is therefore important that concerted efforts are implemented to provide detailed measurements and analysis. The occurrence of freak waves is ascribed to three different processes:

- Wave-current interactions
- Wave-bottom interactions
- Wave-wave interactions

This research has investigate the generation of breaking waves in deep water in a laboratory flume, due to the process of (non)linear superposition and phasing of different wave components (wave-wave interaction), also referred to as "wave focussing". This process is also one of the processes, which is ascribed to the occurrence of freak waves (wave-wave interaction).

This research focussed on the generation of breaking waves on deep water due to wave focussing under controlled laboratory conditions. The researched questions were: What control signal must be applied to the wave board in order to generate the wave focussing signal? Is the linear theory sufficient to generate an adequate wave focussing signal or are nonlinearities essential?

The main objective of this research was "to develop an offline control signal for a piston wave board for the generation of breaking waves due to wave focussing". The derived objectives of this research were:

1. To develop a user-friendly software package for easy application of the suggested different theories for the generation of the control signal.
2. To carry out experiments to verify and analyse the acquired signals.
3. Investigate the sensitivity of the focussed wave to the variation of the input variables such as:
   Peak frequency
   The ratio of the maximum frequency to the peak frequency
   The focus distance

This research combined different existing theories to develop the desired control signals. These control signals were verified and analysed by experiments. The experiments were performed in a laboratory flume with a piston wave board situated in the laboratory of Fluid Mechanics at the Faculty of Civil Engineering. Furthermore, some film and photo material was generated about the experiments that could be used for a visualisation of the development of the focussing process of the control signals that could be used for further research. After the experiments, which were carried out to assess the control signals, other experiments were carried out in order to see the impact of the generated focussed wave on a ship and a wall. For these only a visual judgement was assigned.

After analysing the experimental results for the developed control signals, there could be concluded that this research succeeded in developing several user friendly software packages, which can be used to generate well-focussed waves in a laboratory flume with a piston wave board. The following conclusions were drawn for the theories which were used to develop these software packages:

- The linear theory was not sufficient to generate an adequate focussed wave.

- The second-order wave maker theory was the most effective theory to generate a well-focussed wave.
- A Lagrangian correction to the first-order wave maker theory, i.e. the wave motion in a Lagrangian frame of reference instead of the Eulerian frame of reference, did improve the wave focussing signal. But this correction was still less than generating the wave focussing signal with the second-order wave maker theory.
- The nonlinear correction due to the mass transport velocity did not improve the wave focussing signal.
- The experiments showed that the choice of the input variables had an effect on the focussed wave, for instance, increasing the distance between the wave board and the place where the wave should focus resulted in an improved focussed wave.
- The experiments for visualising the impact of the developed focussed wave on a ship or a wall had shown that this wave had a huge impact on these constructions.

This research concludes with several recommendations for further research.

CONTENTS

List of Symbols

Roman Letters

Symbol	Description	Unit
a	Wave amplitude	m
a_b	Maximum wave amplitude as a function of time	m
$A(t)$	Envelope of the surface elevation measurement at the focus point as a function of time	m
B_b	Parameter to measure the degree of focussing of the wave signals	-
B_f	Parameter to measure the degree of focussing of the wave signals	-
c	Phase velocity	m/s
c_0	Linear phase velocity for deep water	m/s
c_1	Hedges phase velocity	m/s
c_2	A variation of Hedges phase velocity	m/s
c_3	Kirby and Dalrymple phase velocity	m/s
c_4	A variation of Kirby and Dalrymple phase velocity	m/s
c_S	Stokes phase velocity	m/s
C_g	Group velocity	m/s
$C_{g,d}$	Computation of the group velocity, where the wave amplitude is a dependent variable	m/s
$C_{g,f}$	Group velocity of the first wave, not belonging to the “start function”	m/s
$C_{g,i}$	Computation of the group velocity, where the wave amplitude is an independent variable	m/s
$C_{g,l}$	Group velocity of the last wave, not belonging to the “tail function”	m/s
E	Wave energy per unit area	J/m^2
E_b	Total energy in the breaking wave per unit area	J/m^2
E_f	The wave energy flux per meter width	W/m
f	Frequency	Hz
f_0	Peak frequency	Hz
f_m	Maximum frequency	Hz
g	Gravitational acceleration constant	m/s^2
h	Water depth	m
H	Wave height	m
$H_{e,f}$	Maximum measured wave height at the theoretical focus point	m
$H_{e,m}$	Maximum measured wave height	m
H_l	Theoretical breaking wave height	m

Symbol	Description	Unit
H_m	Maximum wave height at a gauge	m
$H_{\max}$	Maximum wave height	m
k	Wave number	rad/m
k_l	Wave number of the last wave	rad/m
k_p	Wave number of the progressive waves	rad/m
L	Wave length	m
M	Mass transport	kg/m/s
r	Ratio of the maximum frequency to the peak frequency	-
S	Stroke	m
S_{zz}	Power spectral density	m^2/Hz
t	Time	s
t_f	Focus time	s
t_l	Time the last wave is generated	s
t_p	Time where the peak of $A(t)$ occurs	s
$t_{t,b}$	Travelling time of the first wave from the wave board to the focus point	s
$t_{t,e}$	Travelling time of the last wave from the wave board to the focus point	s
T	Wave period	s
U	Depth-averaged time-mean velocity	m/s
U_c	Correction for the mass-transport	m/s
W	Work performed by wave maker	J/m
x	Horizontal co-ordinate	m
x_0	Starting point	m
x_f	Focus point	m
X	Wave board displacement	m
$X_E(t)$	Nonlinearly corrected wave board displacement	m
$X_0(t)$	Linear-theory wave board displacement	m
X_{11}	First-order wave board displacement	m
X_{21}	Second-order first harmonic wave board displacement	m
X_{22}	Second-order superharmonic wave board displacement	m
X_{10}	Second-order subharmonic wave board displacement	m
$X(t,t_1)$	Total second-order wave board displacement	m
z	Vertical co-ordinate	m

Greek Letters

Symbol	Description	Unit
a	Phillips proportionality constant	-
b	Relative wave height	-
dt_t	Difference between Δt_t using the dispersion relation of Hedges and the dispersion relation of Kirby and Dalrymple	s
Δt_t	Difference between the travelling time of the first wave and last wave	s
e	Wave steepness	-
f	Velocity potential	m^2/s
j_A	Slowly varying phase	rad
g	Peak- enhancement coefficient	-
g_b	Breaker index in shallow water	-
l	Wave length	m
l_b	Expected wave length of the breaking wave	m
q_0	Initial wave phase	rad
r	Mass density of water	kg/m^3
s_0	JONSWAP 's shape parameter	-
w	Angular wave frequency	rad/s
$w(t)$	Angular wave frequency as a function of time	rad/s
w_0	Carrier-wave angular frequency	rad/s
w_c	Corrected angular wave frequency	rad/s
w_l	Angular wave frequency of the last wave	rad/s
x_0	Orbital displacement of the Lagrangian point with respect to the rest position x.	m
$x_E(t)$	Nonlinear corrected water surface elevation	m
y	Phase shift	rad
$z(x,t)$	Water surface elevation as a function of space (x) and time (t)	m
$z_0^e(x)$	Even part of the initial water displacement	m
$z_0^o(x)$	Odd part of the initial water displacement	m
$z_E(t)$	Nonlinear corrected water surface elevation	m
z_c	Water elevation of the crest preceding the trough of ζ	m
z_t	Water elevation at a trough	m

List of Figures

List of Tables

Introduction

1 Introduction

1.1 General introduction

For centuries sailors have blamed mysterious surges of water for unexplainable sinking of ships, but the claims were often accompanied by scepticism pointed to bad maintenance or poor seamanship. A classic example is the story of the cargo-ship München (Guardian Weekly,2002):

> *At 7 December 1978 the cargo-ship München, one of the biggest ships ever built (the length of two-and-a half football pitches) suddenly disappeared off the face of the earth from the mid-Atlantic. The ship was never found. A small detail of a lifeboat suggested that it was hit by a wave of more than 60 ft. It was considered as a highly unusual event.*

Satellite images and analysis of numerous disasters with ships and offshore structures in the past decennia have shown that these high steep waves do indeed occasionally occur. Some dramatic examples are shown below:

> *The ship Waratah is lost in 1909 without any trace ever being recovered (211 passengers). The fact that many other ships had been in the area, at the same time without experiencing any difficulties, points towards a spatially localized phenomenon. In 1942 the Queen Mary carrying 15000 soldiers, was hit by a 70 ft wall of water. The ship came within an ace of capsizing, but it was all hushed up at the time. The super tanker World Glory sunk in 1968 after being broken in two by an unexpected giant wave (see fig 1-1). On New Year's Day 1995 a wave of 78 ft was measured hitting the Draupner oil rig placed in the North sea off Norway. In 1998 the superliner Oriana was struck by a 63 ft wave that smashed windows and sent water cascading through the ship, swamping six of its ten decks.*

Fig. 1-1 Damage on the tanker "World Glory" due to a freak wave

There are many more logged sightings of seafarers of these giant waves, taller than tower blocks, which rise out of calm seas and destroy everything in their path. These waves are regularly reported during all sorts of weather including calm days. Eyewitnesses phrase this phenomenon as "the waves from nowhere" or "a very steep wall of water" or "a hole in the ocean".

Fig 1-2 Bow damage on the supertanker "Atlas Pride" due to a freak wave

These unexpectedly large ocean waves are called “freak” or “rogue” waves. They are characterised as single, remarkably horizontally asymmetric and extreme high wave. This phenomenon occurs both in deep and shallow water and they have been observed in coastal and open oceans. Freak waves cannot be predicted by standard methods. A wave of 90 ft could indeed happen, but only once in ten thousand years, but the freak wave events happen much more frequently. Thus it has become clear that other processes are involved in the generation of these freak waves.

Freak waves should not be confused with “tsunamis”. Tsunamis are caused by seismic events, such as earthquakes, landslides, volcanic eruptions or impacts by asteroids or comets. On the open sea they are long and low and might go unnoticed by ships, but as they approach shallow water, they slow down and the wave height increases dramatically.

Because the rogue wave phenomenon is so fleeting, it is difficult to document it for study and analysis, but in spite of that many researches have investigated the cause of freak waves in actual ocean area and many mechanisms of their occurrence have been proposed from different points of view. One explanation is the coincidence of several different wave trains meeting at the same time. In this way, the crests of the waves may be superimposed so that an extremely amplified wave results. Waves generated this way are typically “short-lived” since the wave trains run out of phase as they continue to move on. Another explanation is that wave interaction with an opposing current is a mechanism of the strong wave amplification due to blocking of the wave on the current. Waves generated this way tend to be longer lived and may be very steep as the wave is shortened by the counter current. A last explanation is a mechanism of focussing wave energy due to the effect of the bottom topography.

Freak waves can arise in any ocean in the world, but there are certain areas where they are more common such as:

- South-east coast off South Africa, when there is a strong wind blowing in the opposite direction to the strong Agulhas current.
- Norway, the coast of Norway has a sea bottom which can focus waves together to form freak waves.

Other places are the south east of Japan (Kuroshio current), near the Gulf Stream in the North Atlantic, the Pacific … This indicates that processes such as wave-current interaction and (non)linear superposition of wave components could lead to the generation of these waves.

Although the occurrence of freak waves has been widely acknowledged, these waves occur in such a short period of time that only a few measurements of these waves in nature are available. It is therefore important that concerted efforts should be implemented to provide detailed measurements and analysis.

The understanding of phenomena occurring in nature always starts off with assumptions about the processes involved. Based on these assumptions theories are developed which must be verified under controlled laboratory conditions.

This research has investigate the generation of breaking waves in deep water in a laboratory flume, due to the process of (non)linear superposition and phasing of different wave components (wave-wave interaction), also referred to as “wave focussing”. This process is one of the processes, which is ascribed to the occurrence of freak waves (wave-wave interaction).

1.2 Problem definition

As explained in the introduction, freak or rogue waves, are a phenomenon that can cause serious damage, and should therefore be considered in the design process of ships and offshore constructions. These waves can occur due to three different processes:

- Wave-current interactions
- Wave-bottom interactions
- Wave-wave interactions, i.e. (non)linear superposition and phasing of different wave components.

This research has investigate the generation of breaking waves in deep water in a laboratory flume, due to the process of (non)linear superposition and phasing of different wave components (wave-wave interaction), also referred to as “wave focussing”. This process is one of the processes, which is ascribed to the occurrence of freak waves (wave-wave interaction). In the past efforts have been made to generate focussed waves with a wave generator in a wave flume, but this is not straightforward due to the effects of nonlinearity. Due to frequency dispersion wave components with a longer wave length travel faster than shorter wave length components. Because of that, longer wave components overtake the shorter ones causing a non-periodic wave signal to deform as it travels through the flume. The first effect of wave nonlinearity is amplitude dispersion i.e. higher waves travel faster than lower waves. The second effect of nonlinearity is the generation of higher harmonics because of which a sinusoidal control signal to the wave maker does not lead to a sinusoidal wave train in the flume.

This research focusses on the generation of breaking waves on deep water due to wave focussing under controlled laboratory conditions and tries to solve questions such as: What control signal must be applied to the wave board in order to generate this wave focussing signal? Is the linear theory sufficient to generate an adequate wave focussing signal or are nonlinearities essential?

1.3 Objectives

The main objective of this research is:

To develop an offline control signal for a piston wave board for the generation of breaking waves on deep water due to wave focussing.

The derived objectives of this research are:

4. To develop a user-friendly software package for easy application of the suggested different theories for the generation of the control signal.
5. To carry out experiments to verify and analyse the acquired signals.
6. Investigate the sensitivity of the focussed wave to the variation of the input variables such as: Peak frequency, the ratio of the maximum frequency to the peak frequency and the focus distance.

1.4 Research approach

First the objectives of this research are defined. Subsequently a literature study about the process of wave focussing and the possible accompanying different theories has to be performed. From the available theories the most feasible ones are chosen and by combining those theories several wave focussing signals are generated. The implementations of those signals are programmed in MATLAB, in such a way that a user can easily derive a wave focussing signal by only entering a few parameters.

The theoretical wave focussing signals so obtained are verified by experiments in a wave flume in a laboratory. To determine whether a wave focussing signal correctly results in a well-focussed wave, the experimental data are analysed and compared with the simulation. To evaluate the quality of the wave focussing signals, several parameters are developed besides a visual classification, such as the theoretical wave height at the moment of breaking divided by the experimental wave height at the moment of breaking. From those parameters the most effective combination of the theories to generate the wave focussing signal can be found. Finally, the conclusions and the recommendations for future research are presented. For an overview of this research the approach followed is shown in figure 1-3.

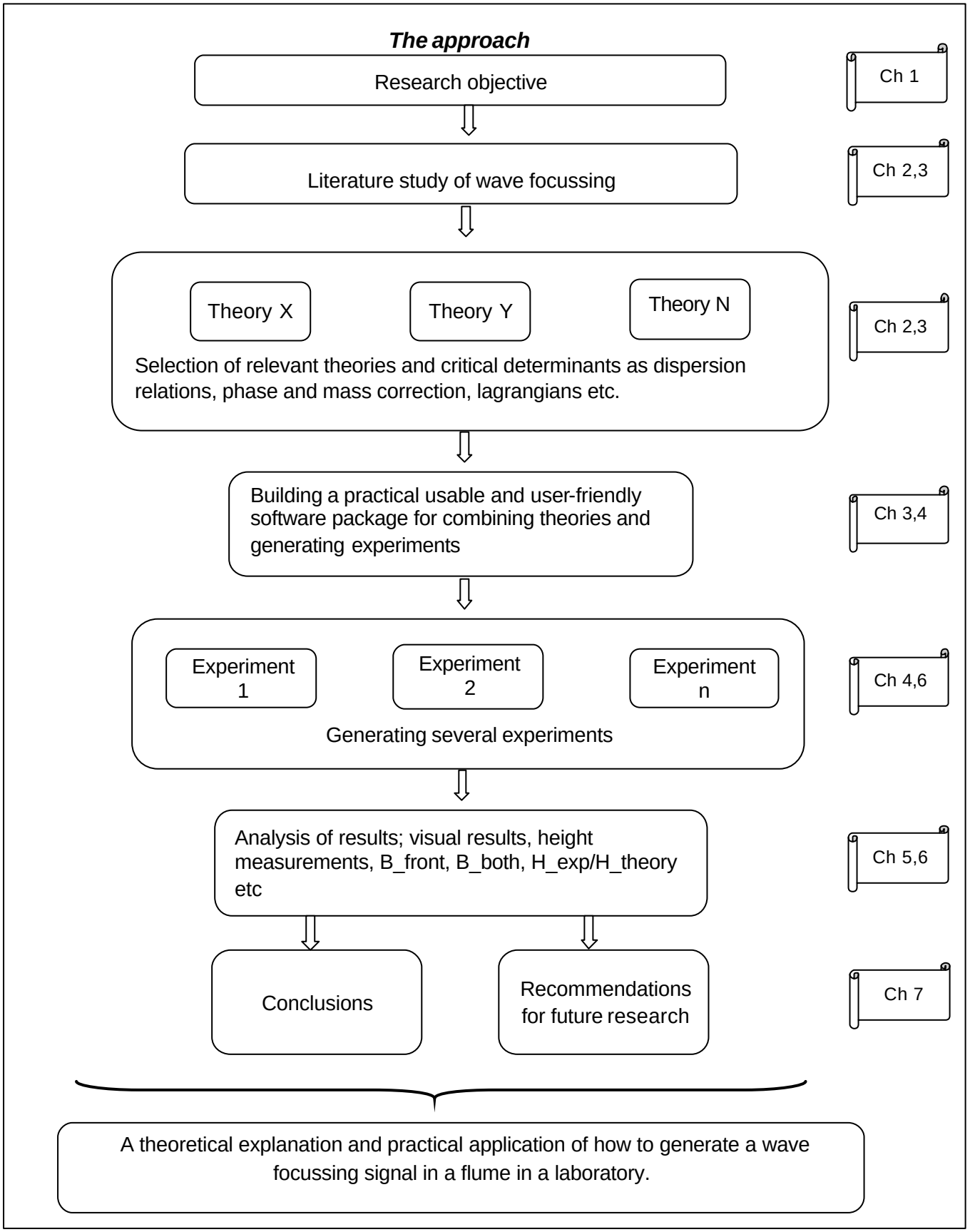

Fig 1-3 The approach followed of this research

1.5 Reading guide

The outline of this report is as follows:

Chapter1
Chapter 1 gives a general introduction about the phenomenon “freak waves” followed by the problem definition and the objectives of this research. This chapter also includes the research approach and this reading guide.

Chapter2
Chapter 2 describes all the theories used to develop focussed waves in a wave flume.

Chapter3
The theory on wave generation in a wave flume in a laboratory is described in chapter 3.

Chapter4
Chapter 4 gives a brief explanation of the experimental set-up and its main components. Also the implementation of the theories is shown in this chapter.

Chapter5
This chapter contains the results and analysis of the experimental data.

Chapter6
Some experiments were carried out only to observe the results and thus without a scientific analysis; these experiments are described in chapter 6.

Chapter7
The conclusions and the recommendations from this research are given in this chapter.

Theory on wave focussing

```
% Computation of some values using the input variables
f_max  = ratio * f_nul;
k_max = disper( 2*pi*f_max, h, g ) ;
kh_max = k_max * h ;

T_max  = tanh( kh_max ) ;

% Compute the minimum group velocity
cgroep_min = 0.5 * (2*pi*f_max) / k_max * ( 1 + kh_max * ( 1
- T_max^2) / T_max ) ;
t_focus      = ( x_focus  - x_nul ) / cgroep_min ;
omega_max    = 2 * pi * f_max ;
omega_min    = 2 * pi * f_nul ;
omega  (       = linspace( omega_min, omega_max, nf ) ;
k              = disper( omega, h, g );

% Define start values for omega and the amplitude
a              = zeros( size( omega ) ) ;
omega_def = omega ;

% Start loop
i              = 1 ;
difference_omega   = 10 * rel_dif ;
```

2. Theory on wave focussing

2.1 Introduction

The objective of this research is to compute an offline control signal for a wave flume with a horizontal bottom and a piston wave board for the generation of a breaking wave due to wave focussing. The wave focussing signal is simulated by developing a breaking wave at a certain point and time in the flume, through sending out a wave train with different frequencies and therefore different speeds, in such a way that all the waves arrive at a specified point in the flume at the same time. The position where the waves come together is called the focus point (x_f) and the time to arrive there is called the focus time (t_f). The wave maker generates short waves first (the high frequency waves) followed by longer waves (the lower frequency waves) which, due to frequency dispersion, are faster and catch up with the shorter waves at the focus point, thus producing a very large wave due to superposition.

The literature study has given a selection of theories to be used for the creation of the offline signal. A global description of the computation of the wave focussing signal is given below. In the remainder of this chapter the different theories are described.

A dispersion relation is needed, in order to describe the way in which a field of propagating waves consisting of many frequencies will disperse due to the different celerities of the various frequency components. In this research the linear and five nonlinear dispersion relations have been evaluated. The linear dispersion relation $\omega(k,h)$ is a function of the wave number k and the water depth h. The nonlinear dispersion relations $\omega(k,h,a)$ include a nonlinear correction to the linear dispersion relation and are designed to mimic the effect of amplitude dispersion, therefore being a function of the wave number k, the water depth h and the amplitude a.

Wave energy will be transmitted when the waves propagate. The speed at which the energy is transmitted is called the group velocity. The group velocity $C_g(\omega,k)$ is likewise a function of the wave frequency and the wave number and can be evaluated from the dispersion relation. The focussing signal consists of many waves, which are generated by the wave board at different times (see figure 2-1). To evaluate the time at which each wave has to be generated by the wave board (t_1, t_2, t_3,….), the group velocity can be used. The first wave generated by the wave board is the wave with the highest frequency and thus travels with the lowest velocity of the whole wave train. This velocity determines the focus time by the following expression:

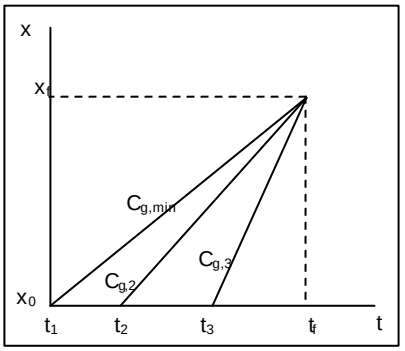

Fig. 2-1 Outline of wave focussing

$$t_f = \frac{x_f - x_0}{C_{g,\min}}$$

where:

x_f = Focus distance (m)

x_0 = Starting point (m)

t_f = Focus time (s)

$C_{g,\min}$ = Group velocity of the wave with the highest frequency (m/s)

The following waves of the wave train are generated after this first wave and therefore have to travel faster in order to arrive in the focus point on time. Knowing the different group velocities of

all the waves in the wave train, the time when each wave has to be generated is determined with these group velocities by:

$$C_{g,i} = \frac{x_f - x_0}{t_f - t_i}$$

where:

$C_{g,i}$ = Group velocity of wave i (m/s)

t_i = Time at which wave i is generated by the wave board (s)

i = 1, 2, 3,…..n

The amplitude of the different waves in the generated wave train is obtained by giving each wave an amplitude that is a certain fraction of the minimum wave height at which waves starts to break. This minimum wave height is empirically given by the Miche criterion an adaptation of this criterion is used. The resulting nonlinear amplitudes are dependent on the wave number k and the water depth h.

To ensure that the last wave of the generated wave train has a wave crest in the focus point at the focus time (in order to get the maximum wave height at the focus point) a phase shift has to be computed. This can be accomplished using the knowledge of the time this last wave is generated by the wave board, the frequency of this wave and the wave number of this wave.

After knowing all the values of the variables (frequency, wave number, group velocity, amplitude, phase shift) for each wave in the wave train the desired water surface elevation at x = 0m can be computed as a function of time. To calculate the wave board motion two theories are applied in this research: the first-order wave maker theory and the second-order wave maker theory. When generating waves in a laboratory wave flume, spurious waves might be generated. With the second-order theory these spurious waves are suppressed in order to create a more accurate signal. Both wave maker theories can compute the wave board motion as a function of time, if all the values of the variables of each wave in the wave train are known.

After knowing all values (frequency, wave number, group velocity, amplitude, phase shift) for each wave in the wave train the desired water surface elevation at x = 0m can be computed as a function of time. To calculate the wave board motion two theories are applied in this research: the first-order wave maker theory and the second-order wave maker theory. When generating waves in a laboratory wave flume, spurious waves might be generated. With the second-order theory these spurious waves are suppressed in order to create a more accurate signal. With both wave maker theories the wave board motion as a function of time can be computed, if all the values of each wave in the wave train are known.

In this research two nonlinear corrections are applied to several control signals in order to create a better focussed wave. First a Lagrangian correction is applied to the first-order wave maker theory. The idea is that the Lagrangian wave motion is less nonlinear than the motion in the Eulerian frame of reference. Second, a nonlinear correction due to the mass-transport velocity is added to the dispersion relation.

Furthermore Cauchy and Poisson have made a theory of waves produced by a local disturbance of the surface, which actually is the reverse of the wave focussing signal we want to create. This theory is used for developing the wave focussing signal, but it did not result in a well-focussed wave. This theory is shown in appendix D and the experiments carried out with this theory can be found on the CD under the name “Lamb”.

Figure 2-1 shows the used theories and their relation for creating the wave focussing signal.

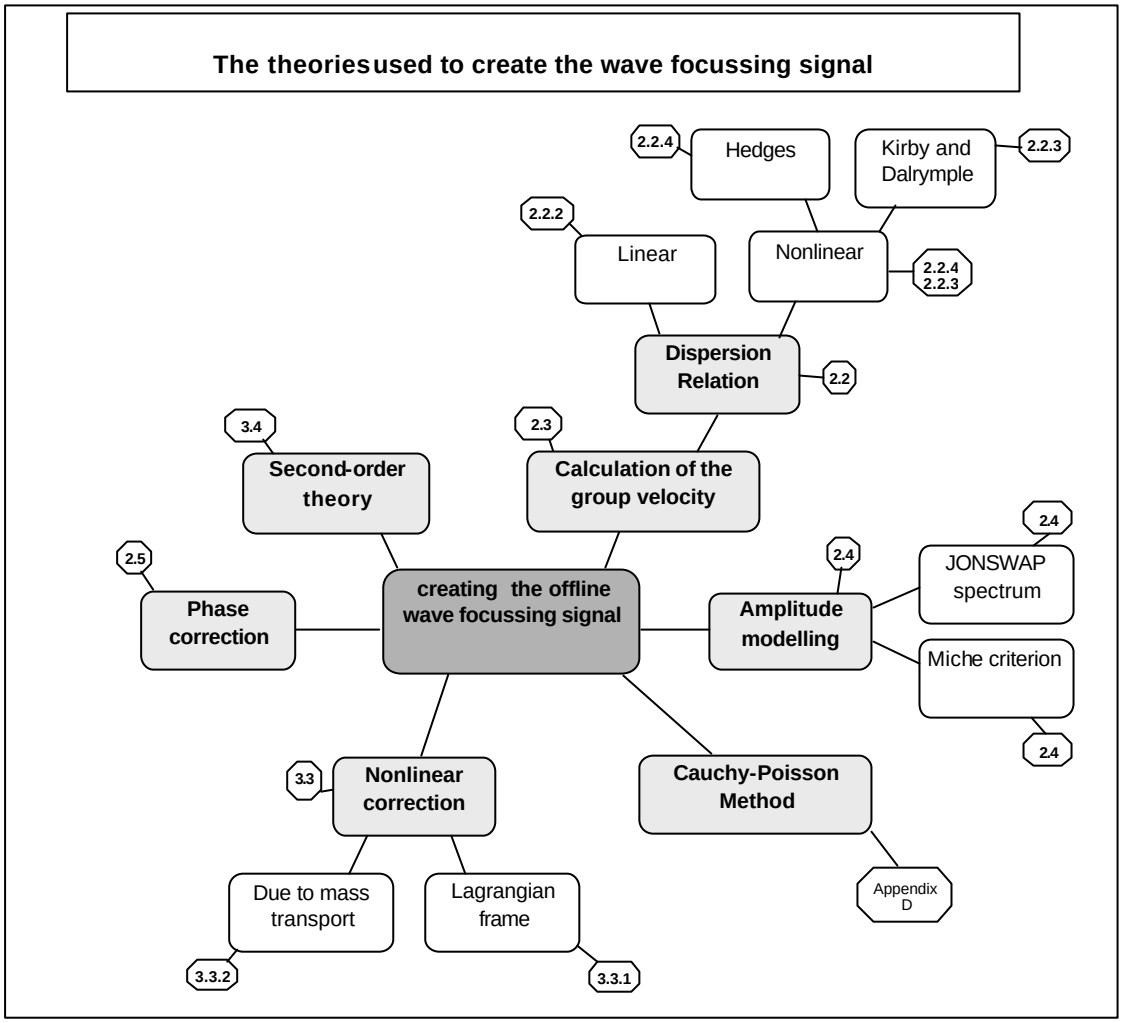

Fig.2-2 The theories used to create the wave focusing signal in this research

2.2 Dispersion relations

2.2.1 Introduction

To describe the manner in which a field of propagating waves, consisting of many frequencies, would disperse due to the different celerities of the various frequency components, a dispersion relation is needed. The dispersion relation describes the relation between the wave frequency and the wave number. There are two kinds of dispersion relations, based on:

1. The linear theory, where the effect of nonlinearity on the wave propagation characteristics is neglected.
2. A nonlinear theory.

Characteristic for all nonlinear theories is the asymmetric profile of the water displacement (like the profile in reality): the crests are sharper than the troughs (see fig.2-3). This asymmetric profile builds up when waves, with a certain wave steepness, come in shallower water (shallow water: $kh << 1$ and deep water: $kh >> 1$, where k is the wave number and h is the water depth). The nonlinear terms become more important when the wave steepness (= wave height divided by depth) increases.

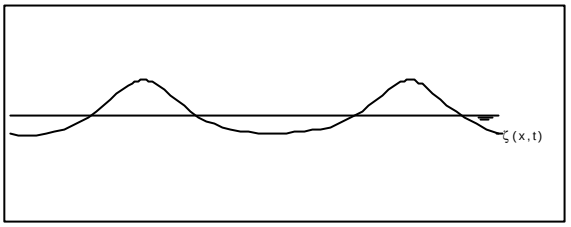

Fig.2-3. z - profile of nonlinear theories.

For creating the control signal for the generation of focussed waves the following five dispersion relationships are used:

1 The linear relation (see 2.2.2)
2-4 Three nonlinear relations developed by Kirby and Dalrymple (see 2.2.3)
5 A nonlinear relation developed by Hedges (see 2.2.4)

The different dispersion relationships can all be put in the following general form:

$$\boxed{w = \Omega(k, h, a)}$$

2.2.2. Linear theory

In the linear theory the terms of quadratic and higher-order are neglected. The equation of Laplace is used, which is linear (in ϕ), as well as, the boundary condition at the bottom. A brief derivation of the linear dispersion with the elemental equations is shown below:

Equation of Laplace:

$$\frac{\partial^2 f}{\partial x^2} + \frac{\partial^2 f}{\partial z^2} = 0 \qquad (2\text{-}1)$$

The boundary conditions at the bottom (z = -h) and at the surface (z = 0) for the linear theory are:

$$\frac{\partial f}{\partial z} = 0 \qquad \text{at } z = -h \qquad (2\text{-}2)$$

$$\frac{\partial f}{\partial z} = \frac{\partial z}{\partial t} \qquad \text{at } z = 0 \qquad (2\text{-}3)$$

$$\frac{\partial f}{\partial t} + gz = 0 \qquad \text{at } z = 0 \tag{2-4}$$

Assuming:

$$z(x,t) = a\sin(wt - kx) \tag{2-5}$$

The equation for the velocity potential results from the equation of Laplace and the bottom boundary:

$$f(x,z,t) = \frac{wa}{k}\frac{\cosh k(h+z)}{\sinh(kh)}\cos(wt - kx) \tag{2-6}$$

substituting equation (2-5) in (2-6) results in the linear dispersion relation:

$$w^2 = gk\tanh(kh) \tag{2-7}$$

where:

f = Velocity potential (m^2/s)
z = Surface evaluation (m)
g = Gravitational acceleration constant (m/s^2)
k = Wave number (rad/m)
w = Wave angular frequency (rad/s)
a = Wave amplitude (m)
x = Horizontal coordinate (m)
t = Time (s)

The general form of this relationship becomes:

$$\boxed{\Omega = \sqrt{gk\tanh(kh)}} \tag{2-8}$$

The obtained dispersion relation is independent of the amplitude, as is to be expected using the linear theory.

2.2.4 Theory of Hedges

Hedges has proposed simple modifications to the linear dispersion relation which are designed to mimic the effect of amplitude dispersion in shallow water (Hedges,1976). This nonlinear dispersion relation is valid for shallow water only (Hedges,1976):

$$\frac{c_1}{c_0} = \tanh(kh + e) \tag{2-9}$$

where

c_1 = Hedges phase velocity (m/s)
$e = ka$ = Wave steepness (-)
c_0 = Linear phase velocity for deep water = $\frac{g}{w}$

In the discussion paper of Kirby and Dalrymple (1987) a new formulation is proposed by Hedges. This new formulation of the nonlinear dispersion relation is valid for the whole range of depths. The validity of this dispersion relation for deep and intermediate water is based on the dispersion relation suggested by Stokes. The result of the Stokes theory is shown below:

Stokes has made the following nonlinear approximation of the dispersion relation which is valid for intermediate and deep water only:

$$\frac{c_S}{c_0} = (1+e^2 D)\tanh(kh) \tag{2-10}$$

with the coefficient:

$$D = \frac{9-12\tanh^2(kh)+13\tanh^4(kh)-2\tanh^6(kh)}{8\tanh^4(kh)} \tag{2-11}$$

where:

c_S = Stokes phase velocity (m/s)

The new formulation of the nonlinear dispersion relation valid for the whole range of depths suggested by Hedges (see Kirby and Dalrymple,1987) is:

$$\frac{c_2}{c_0} = \left(1+e^2\right)\tanh\left(\frac{kh+e}{1+e^2}\right) \tag{2-12}$$

where:

c_2 = a variation of Hedges phase velocity (m/s)

The difference between the two formulations suggested by Hedges and Stokes theory for high nonlinearity (ka=0.4)) is shown in figure 2-4. Because the new formulation proposed by Hedges (equation 2-12) is supposedly valid for the whole range of depths this one is used in this research for developing the wave focusing signal.

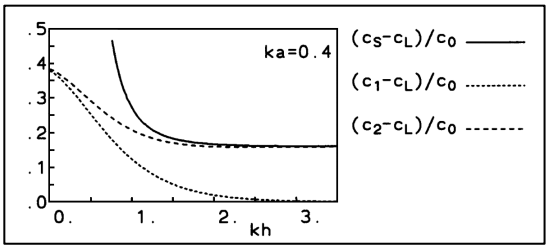

Fig. 2-4 The velocities c_S (Stokes) and c_1 and c_2 according to Hedges (Dingemans,1997)

The general form of this dispersion relation becomes:

$$\Omega = \sqrt{gk\left(1+e^2\right)\tanh\left(\frac{kh+e}{1+e^2}\right)} \tag{2-13}$$

2.2.3 Theory of Kirby and Dalrymple

Kirby and Dalrymple have made an approximate model for nonlinear dispersion in monochromatic wave propagation models (Kirby and Dalrymple, 1986). They propose a simple, empirical extension to the existing methods, which has the effect of smoothly connecting the analytical results for Stokes waves (intermediate and deep water) to the empirical formulation for shallow water of Hedges (equation 2-9):

$$\frac{c_3}{c_0} = \left(1 + f_1 e^2 D\right)\tanh\left(kh + f_2 e\right) \tag{2-14}$$

where:

$$f_1(kh) = \tanh^5(kh) \tag{2-15}$$

$$f_2(kh) = \left(\frac{kh}{\sinh(kh)}\right)^4 \tag{2-16}$$

c_3 = Kirby and Dalrymple phase velocity (m/s)

the general form of the first dispersion relation suggested by Kirby and Dalrymple (1986) becomes:

$$\Omega = \sqrt{\left[gk\left(1 + f_1 e^2 D\right)\tanh\left(kh + f_2 e\right)\right]} \tag{2-17}$$

After comments and suggestions from Hedges they came with a modification of equation 2-17 Kirby and Dalrymple (1987):

$$\frac{c_4}{c_0} = a_k \tanh\left(\frac{kh+e}{a_k}\right) \tag{2-18}$$

where:

c_4 = a variation of Kirby and Dalrymple phase velocity (m/s)

with the coefficient:

$$a_k = 1 + \sqrt{f_1} e^2 D \tag{2-19}$$

the general form of the second dispersion relation suggested by Kirby and Dalrymple (1987) becomes:

$$\Omega = \sqrt{gk\left(a_k \tanh\left(\frac{kh+e}{a_k}\right)\right)} \tag{2-20}$$

In figure 2-5, the difference between the velocities according to Stokes and Kirby & Dalrymple is shown for high nonlinearity (ka=0.4). It can be seen that for deep water ($kh >> 1$) both theories have almost the same solution and for shallow water ($kh << 1$) the Stokes formulation diverges. In this research both dispersion relations suggested by Kirby and Dalrymple are tested, to see the effect of this modification.

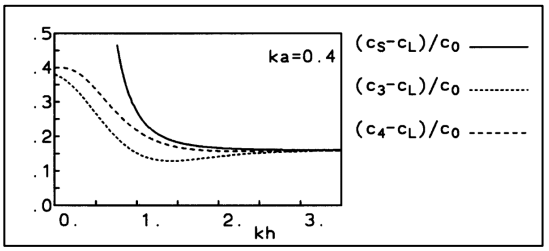

Fig. 2- 5 The velocities c_S (Stokes) c_3 according to Kirby & Dalrymple (1986).and c_4 according to Kirby & Dalrymple (1987).

From the literature study we found that H.Petit (Petit, 1991) has applied the suggested dispersion relation from the discussion paper (equation 2-17), for generation a wave focussing signal, but he has used another formula for the coefficient D:

$$D_P = \frac{9 - 10\tanh(kh)^2 + 9\tanh(kh)^4}{8\tanh(kh)^4} \qquad (2\text{-}21)$$

This coefficient is not the same as suggested in equation 2-11 (they cannot be converted to each other). Therefore this variation is also applied to some signals.

Summary of the dispersion relations used in this research to create the wave focussing signal:

1. *Linear:* $\Omega = \sqrt{gk\tanh(kh)}$ (2.8)

2. *Hedges:* $\Omega = \sqrt{gk\left(\left(1+e^2\right)\tanh\left(\frac{kh+e}{1+e^2}\right)\right.}$ (2.13)

3. *Kirby and Dalrymple (1986*): $\Omega = \sqrt{\left[gk\left(1+ f_1 e^2 D\right)\tanh\left(kh+ f_2 e\right)\right]}$ (2.17)

4. *Kirby and Dalrymple (1987):* $\Omega = \sqrt{gk\left(a_k\tanh\left(\frac{kh+e}{a_k}\right)\right.}$ (2.20)

5. *Kirby and Dalrymple Petit:* $\Omega = \sqrt{\left[gk\left(1+ f_1 e^2 D_P\right)\tanh\left(kh+ f_2 e\right)\right]}$ (2.21)

2.3 Group velocity

The wave focussing signal is a wave motion which consists of superposition of waves with different amplitudes, wave lengths, frequencies and hence with different phase velocities. To assure that all the wave components, generated at different times by the wave board, arrive at a specified point at the same time, the different velocities of the waves have to be computed. The dispersion relation determines the phase velocity (c) of each wave, which is a function of the wave frequency and the wave number:

$$c = \frac{w}{k} \qquad (2\text{-}22)$$

The speed at which the energy is transmitted is called the group velocity. The group velocity is likewise a function of the wave frequency and the wave number and can also be evaluated from the dispersion relation. The definition of the group velocity is:

$$C_g \equiv \frac{\partial w}{\partial k} \qquad (2\text{-}23)$$

In this research two different views on the computation of the group velocity C_g can be distinguished. First, it can be considered that the wave amplitude is an independent variable, which results in a group velocity of:

$$C_{g,i} \equiv \left.\frac{\partial w}{\partial k}\right|_{a=constant} \tag{2-24}$$

This is often called the basic nonlinear group velocity. It is expected to be close to the velocity of the maximum of the wave group. However, the frequency-modulated signal used in this research is highly asymmetrical. This leads to a second definition of the group velocity, more appropriate to the amplitude variation away from the maximum of the wave group. As will be shown in section 2.4, the amplitude is not chosen independently, but as a function of the wave number (k), i.e. a = a(k), so then as a consequence the calculation of the group velocity becomes:

$$C_{g,d} = \frac{\partial w(k,h,a(k))}{\partial k} \cong \frac{\partial w}{\partial k} + \frac{\partial w}{\partial a}\frac{da}{dk} \tag{2-25}$$

Note that in case of a linear dispersion relation both group velocities coincide.

The difference between the two calculations of the group velocity is computed for deep and shallow water and is shown below. For simplicity the difference between $C_{g,i}$ and $C_{g,d}$ is analyzed for the limits of deep and shallow water waves.

For deep water (kh>>1):

The dispersion relation in deep water approaches asymptotically:

$$w = w_0\left(1+\frac{1}{2}(ka)^2\right) \tag{2-26}$$

where:

$$w_0 = \sqrt{gk} \tag{2-27}$$

Substitution of the equations 2-26 and 2-27 into equation 2-24 results in a $C_{g,i}$ of:

$$C_{g,i} = \frac{\partial w}{\partial k} = \frac{\partial w_0}{\partial k}\left[1+\frac{1}{2}(ka)^2\right] + w_0 k a^2$$

$$= \frac{1}{2}\sqrt{\frac{g}{k}}\left[1+\frac{1}{2}(ka)^2 + 2(ka)^2\right] = C_{g0}\left[1+\frac{5}{2}(ka)^2\right] \tag{2-28}$$

with:

$$C_{g,0} = \frac{\partial w_0}{\partial k} = \frac{1}{2}\sqrt{\frac{g}{k}} \tag{2-29}$$

Using 2-26, $\frac{\partial w}{\partial a}$ becomes:

$$\frac{\partial w}{\partial a} = w_0 k^2 a \tag{2-30}$$

assuming waves of constant steepness:

$$ka = cons\tan t \tag{2-31}$$

For a fraction β of the maximum steepness (equal to about 1/7 in deep water) there can be obtained:

$$\frac{H_{\max}}{l} = \frac{ak}{p} = \frac{1}{7}b \Rightarrow ka = \frac{1}{7}pb = e \tag{2-32}$$

therefore:

$$\frac{da}{dk} = -\frac{e}{k^2} \tag{2-33}$$

Equations 2-30 and 2-33 result in:

$$\frac{\partial w}{\partial a}\frac{da}{dk} = -w_0 k^2 a e \frac{1}{k^2} = -\frac{w_0}{k}e^2 = -2C_{g0}e^2 \tag{2-34}$$

Substituting 2-34 in equation 2-24 and 2-25, the difference between the two group velocities for deep water becomes:

$$\boxed{C_{g,d} \cong C_{g,i} - 2C_{g,0}e^2} \tag{2-35}$$

For shallow water (kh<<1):

The dispersion relation in shallow water approaches asymptotically:

$$w = k\sqrt{g(h+a)} \tag{2.36}$$

Equations 2-36 and 2-24 results in a $C_{g,i}$ of:

$$C_{g,i} = \frac{\partial w}{\partial k} = \sqrt{g(h+a)} \tag{2-37}$$

using 2-36, $\frac{\partial w}{\partial a}$ becomes:

$$\frac{\partial w}{\partial a} = k\frac{1}{2}\frac{1}{\sqrt{g(h+a)}}g \tag{2-38}$$

For shallow water and fraction β of maximum steepness:

$$\frac{H_{\max}}{h} = \frac{2a}{h}0{,}833b \tag{2-39}$$

which results in:

$$a = \frac{1}{2} * 0{,}833\,bh \tag{2-40}$$

therefore:

$$\frac{da}{dk} = 0 \tag{2-41}$$

So that for shallow water:

$$\boxed{C_{g,d} \cong C_{g,i}} \tag{2-42}$$

Conclusion:
For deep water a difference between the two calculated group velocities will exist (see equation 2-34)
For shallow water there is no difference between the two calculated group velocities (see equation 2-42)

To estimate the difference for deep water, an example is given:

Example:

$f = 1$ (Hz) *(deep water)*
$h = 0{,}6$ (m) *(as in the experiments)*
$b = 0{,}3$ (-) *(as in the experiments)*
which results in:
$w_0 = 2p$ (rad/s)

$$e = ka = \frac{1}{7}pb = 0{,}135$$

$$C_{g,a} = C_{g,0}\left[1+\frac{5}{2}(ka)^2\right] = 1{,}0456 * C_{g,0}$$

$$\frac{\partial w}{\partial a}\frac{da}{dk} = -2C_{g,0}e^2 = -0{,}0365 * C_{g,0}$$

This results in a difference between $C_{g,i}$ and $C_{g,d}$ of the group velocity for deep water:

Relative difference $= \dfrac{-0{,}0365}{1{,}0456} = -0{,}035$

2.4 Amplitude variation of the control signal

To derive the amplitude variation of the control signal two approaches are considered:

1. As is known from the theory of linear stationary Gaussion random processes of the surface elevation, the neighbourhood of very high waves has approximately the form of the autovariance function. Since this autovariance function is the Fourier transform of the power spectrum characterizing the Gaussion process. Therefore, it is plausible that the shape of the power spectrum influences the focussing. Below a study is carried out about the relationship between a chirp time series and its power spectrum in order to derive the amplitude variation of the control signal.

   Klopman (see Appendix B) has proposed a relationship between a chirp time-series and its power spectrum.
   The assumptions are:
   1. The signal y(t) has to be of finite duration in the interval $t \in [0, T]$
   2. y(t), a(t) and ω (t) have to be finite, continuous and differentiable for all $t \in$ IR
   3. The angular frequency ω (t) has to be a monotonic function of time t

   The chirp signal is described as:

$$z(t) = a(t)\cos\left(\int_0^t w(t)dt + q_0\right) \qquad (2\text{-}43)$$

   where,

   $a(t)$ = Wave amplitude (m)

   $w(t)$ = Angular frequency (rad/s)

   q_0 = Initial wave phase (rad)

   Klopman did obtain the following relationship between the amplitude variation $a(t)$ and the power spectral density:

$$a(t) = 2\sqrt{S_{zz}(w(t))\left|\frac{dw}{dt}\right|} \qquad (2\text{-}44)$$

where:

$$\left|\frac{dw}{dt}\right| = \left|\frac{w(t) - w(t-\Delta t)}{\Delta t}\right| \qquad (2\text{-}45)$$

S_{zz} = Power spectral density (m^2/Hz)

This theory is applied to a software package. It turned out by using the linear dispersion relation the angular frequency (green line) is a monotonic function of time. On the other hand, by using a nonlinear dispersion relation, like suggested by Kirby and Dalrymple the angular frequency (blue line) was not a monotonic function of the time (shown in figure 2-6). This means that the nonlinear dispersion relation comes short of the third assumption. Therefore this method is rejected because of the limited use.

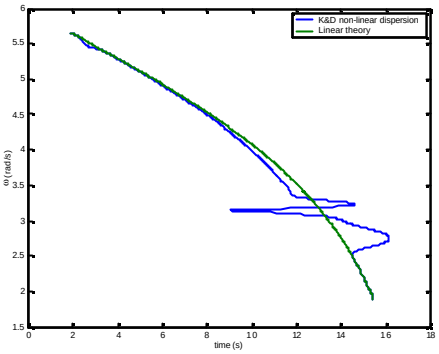

Fig.2-6 The angular frequency as a function of time

2. The second approach considered in this research, to derive the amplitude variation, is to prescribe the amplitude variation of the signal. In this case a plausible approach is to give each wave in the signal initially an amplitude which is a certain (constant) fraction of the minimum wave height at which waves start to break. This minimum wave height is empirically given by the Miche criterion. Breaking of waves occurs because a wave is very steep (on deep water) or because the water is very shallow or a combination of these reasons. Both limits are described with the breaking criterion of Miche. There are many adaptations of this criterion, one is used in this research, modified with a reduction factor b which resulted in:

$$a(t) = b\,\frac{1/2 * 0.88}{k}\tanh\left(\frac{g_b hk}{0.88}\right) \qquad (2\text{-}46)$$

where:

b = Relative wave height $0 \leq b < 1$ [-]

g_b = Breaker index in shallow water = 0,833 [-]

h = Water depth [m]

This second approach is used in this research to determine the amplitude variation of the control signal.

2.5 Wave phase modeling

This section describes the calculation of the wave phase. The next subsection shows the calculation of the phase shift. After the first experiments it is noted that a phase correction is needed such that all the wave crest at the theoretical focus point at the theoretical focus time. This correction is worked out in subsection 2.5.2. This paragraph concludes with the calculation of the total phase.

2.5.1 The phase shift

A phase shift is needed for creating a wave crest of the last wave at the focus point (x_f) at the moment of breaking (t_f). To create this wave crest in the focus point at the focus time (x_f, t_f), the total phase in the focus point has to be zero of multiple of 2 p (cos (0) = 1) so:

$$total\_phase = [kx - wt] - y_0 \tag{2-47}$$

At (x_f, t_f) the total phase of the last wave has to be zero or multiple of 2 p :

$$total\_phase = 0 = k_l(x_f - x_0) - w_l(t_f - t_0) - y_0 \tag{2-48}$$

so that the phase shift can be computed by the following expression:

$$\boxed{y_0 = k_l(x_f - x_0) - w_l(t_f - t_l)} \tag{2-49}$$

y_0 = Phase shift (rad)

t_l = Time the last wave is generated (s)

t_f = Theoretical focus time (s)

k_l = Wave number of the last generated wave (rad/m)

w_l = Angular wave frequency of the last generated wave (rad/s)

x_0 = Starting point (m)

x_f = Theoretical focus point (m)

2.5.2 The phase correction

The first experiments showed that the wave crest of the last wave was not in the focus point at the focus time. Therefore a phase correction has to be added to the control signal. This correction is derived with a theory of Cauchy-Poisson: "*Transient displacement due to an initial displacement on the free surface"*. This theory is described in Mei (1983, section 2.1). Below it is summarized:

The initial displacement $z(x,0)$ is split in an even (= e) and odd (= 0) part with respect to x:

$$z(x,0) = z_0^e(x) + z_0^0(x) \tag{2-50}$$

where:

Even: $$z_0^e(x) = \frac{1}{2}[z(x,0) + z(-x,0)] \tag{2-51}$$

Odd: $$z_0^0(x) = \frac{1}{2}[z(x,0) - z(-x,0)] \tag{2.52}$$

The Fourier transform of $z(x,0)$ is:

$$Z(k) = \int_{-\infty}^{+\infty} z(x,0) e^{-ikx} dx = \int_{-\infty}^{\infty} z(x,0)[\cos(kx) - i\sin(kx)]dx$$

$$= 2\int z_0^e(x)\cos(kx)dx - 2i\int_0^{\infty} z_0^0(x)\sin(kx)dx \tag{2-53}$$

It is split in an even and odd part:

Even: $$Z_0^e(k) = 2\int_0^{\infty} z_0^e(x)\cos(kx)dx = Z_0^e(-k) \tag{2-54}$$

Odd: $$Z_0^0(k) = -2\int_0^{\infty} z_0^0(x)\sin(kx)dx = -Z_0^0(-k) \tag{2-55}$$

The free-surface elevation may be written as:

$$z(x,t) = \frac{1}{2p}\int_{-\infty}^{\infty}(\cos(kx) + i\sin(kx))\cos(w(k)t)[Z_0^e(k) + iZ_0^0(k)]dk$$

$$= \frac{1}{2p}\int_{-\infty}^{\infty} Z_0^e(k)\cos(kx)\cos(w(k)t)dk - \frac{1}{2p}\int_{-\infty}^{\infty} Z_0^0(k)\sin(kx)\cos(w(k)t)dk$$

$$= \frac{1}{2p}\int_{-\infty}^{\infty} e^{ikx}\cos(w(k)t)Z(k)dk \quad \text{(see equation 1-24 in Mei 1983)} \tag{2-56}$$

Assume z_0 odd in x, therefore the free-surface elevation becomes:

$$z(x,t) = -\frac{1}{2p}\int_{-\infty}^{\infty} Z_0^0(k)\sin(kx)\cos(w(k)t)dk \tag{2-57}$$

This may be written as:

$$z(x,t) = -\frac{1}{2p}\int_{-\infty}^{\infty} Z_0^0(k)\frac{e^{ikx} - e^{-ikx}}{2i}\frac{e^{iwt} + e^{-iwt}}{2}dk$$

$$= -\frac{i}{8p}\int_{-\infty}^{\infty} Z_0^0(k)\left(e^{i(kx+wt)} + e^{i(kx-wt)} - CC\right)dk$$

$$= \frac{i}{4p}\int_0^{\infty} Z_0^0(k)\left(e^{i(kx+wt)} + e^{i(kx-wt)} - CC\right)dk \tag{2-58}$$

with:
CC = Complex conjugate

$$z(x,t) = -\frac{1}{2p}\,\mathrm{Im}\int_0^\infty \left(Z_0^0(k)\left(e^{i(kx+wt)} + e^{i(kx-wt)}\right)\right)dk \tag{2-59}$$

The first and second term in the brackets in equation (2-59) represent respectively the left- and right-going waves.
We only consider the right–going waves. For large t, kx-?t varies rapidly and little is contributed to $z(x,t)$ unless there is a point at which the phase is stationary. The method of stationary phase devised by Kelvin is explained in Mei (p25-p26)
Define:

$$g(k) = k\,\frac{x}{t} - w(k) \tag{2-60}$$

then

$$g'(k) = \frac{x}{t} - w'(k) \tag{2-61}$$

$$g''(k) = -w''(k) \tag{2-62}$$

There is a point at which the phase is stationary:

$$g'(k) = \frac{x}{t} - w'(k) = 0 \quad \text{at } k = k_0 \tag{2-63}$$

in that neighbourhood:

$$g(k) \cong g(k_0) + \frac{1}{2}(k-k_0)^2\, g''(k_0) \tag{2-64}$$

So for the right going waves we can write (by substituting equations (2-60), (2-63) and (2-64) into (2-59):

$$z(x,t) = -\frac{1}{2p}\,\mathrm{Im}\int_0^\infty Z_0^0(k)e^{ig(k)t}dk = -\frac{1}{2p}\,\mathrm{Im}\int_0^\infty Z_0^0(k)e^{it\left(g(k_0)+(k-k_0)g'(k_0)+\frac{1}{2}(k-k_0)^2 g''(k_0)\right)}dk$$

$$z(x,t) = -\frac{1}{2p}\,\mathrm{Im}\left(e^{ig(k_0)t}Z_0^0(k_0)\int_0^\infty e^{i\frac{1}{2}(k-k_0)^2 g''(k_0)t}\,dk\right) \tag{2-65}$$

Using the Fresnel integral which is defined as:

$$\int_0^\infty e^{ipv^2}dv = \frac{1}{2}(1+i)\sqrt{\frac{p}{2p}} \tag{2-66}$$

with in this case

$$p = \frac{1}{2}g''(k_0)t \tag{2-67}$$

Equation (2-65) becomes:

$$z(x,t) = -\frac{1}{2p}\,\mathrm{Im}\left(e^{ig(k_0)t} Z_0^0(k_0)(i+1)\sqrt{\frac{p}{g''(k_0)t}} \right)$$
$$= -\frac{1}{2p} Z_0^0(k_0)\sqrt{\frac{2p}{g''(k_0)t}}\sin\left(g(k_0)t + \frac{p}{4} \right) \qquad (2\text{-}68)$$

or:

$$z(x,t) = \frac{1}{2p} Z_0^0(k_0)\sqrt{\frac{2p}{g''(k_0)t}}\sin\left(g(k_0)t - \frac{3}{4}p \right) \qquad (2\text{-}69)$$

Phase correction

In this equation one can recognise the phase correction of -3/4 p.

2.5.3 The total phase

The total phase is described by:

$$total\_phase = [kx - wt] - y_0 + phase\_correction \qquad (2\text{-}70)$$

where:
The phase correction = -3/4 p (equation 2-69)
The phase shift ($?_0$) can be computed with equation 2-49.

Theory on wave generation in a wave flume

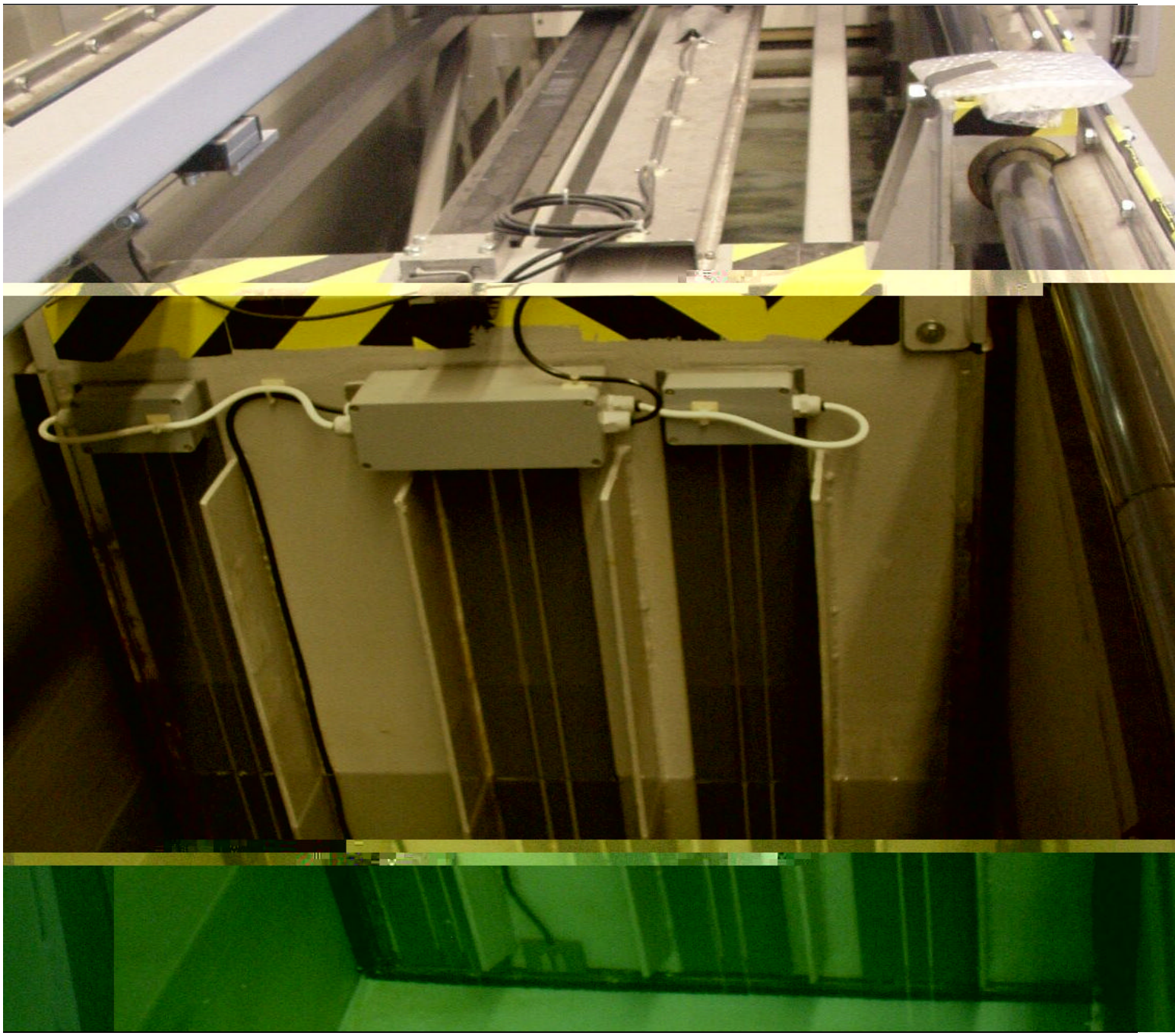

3. Theory on wave generation in a wave flume

3.1 Introduction

To explain how waves are generated in a laboratory environment, the theory proposed by Galvin (1964) is shown briefly (here, specifically for a piston wave board). This theory is valid for shallow water (kh<<1, where k is the wave number and h is the water depth) only. Galvin considered that the volume of water over a whole stroke (S), which is displaced by the wave board, is equal to the crest volume of the propagating wave form. Figure 3-1 shows this for a piston wave board, which is used in this research (see section 4.2).

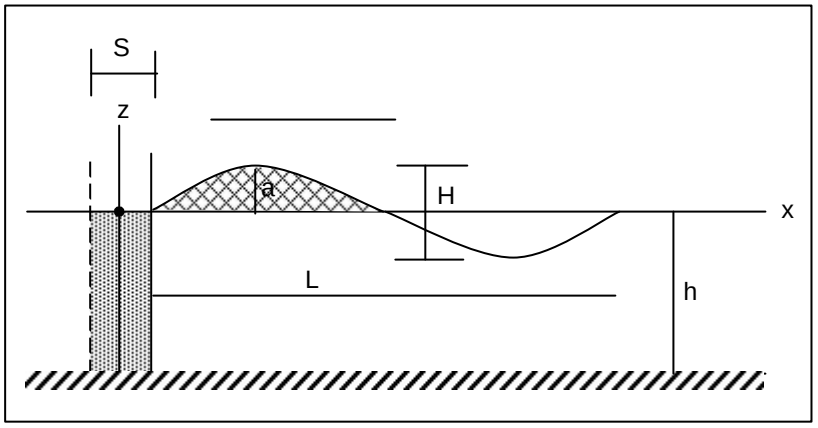

Fig 3-1 Simplified shallow water piston-type wave maker theory of Galvin (Dean and Dalrymple, 1991)

The dotted area is the volume of water displaced by the wave maker and the crosshatched area is the volume of water in a wave crest. According to this theory, these areas are equal to each other.

The volume of water displaced by the wave board $= Sh$ (3-1)

The volume of water in the wave crest $= \int_0^{L/2} a\sin(kx)dx = 2a/k$ (3-2)

where:

S = Stroke, the horizontal displacement of the wave board (m)

L = Wave length, the horizontal distance between two successive wave crests or troughs (m)

which results in:

$$\left(\frac{2a}{S}\right)_{piston} = kh \tag{3-3}$$

A wave maker theory is needed to produce a control signal for the wave board to generate waves in a wave flume. There are different wave maker theories, namely the first-order and the second-order theories. In this research both, the first- and the second- order wave maker theories, are treated. A description of both theories is given in the sections 3.2 and 3.3.

3.2 First-order wave maker theory

The complete first-order wave maker theory (for shallow and deep water) is based on the boundary value problem for two-dimensional waves propagating in an incompressible, irrotational fluid. This is explained by Dean and Dalrymple (1991). Only the result is shown here. The ratio of wave height to stroke for a piston wave board is:

$$\frac{H}{S} = \frac{2\left(\cosh 2k_p h - 1\right)}{\sinh 2k_p h + 2k_p h} \tag{3-4}$$

k_p = Wave number of the progressive waves (rad/m)

In figure 3-2 the ratio of wave height to stroke for a piston wave board (equation 3-4) is plotted and also the ratio wave height to stroke according to the theory of Galvin is plotted.

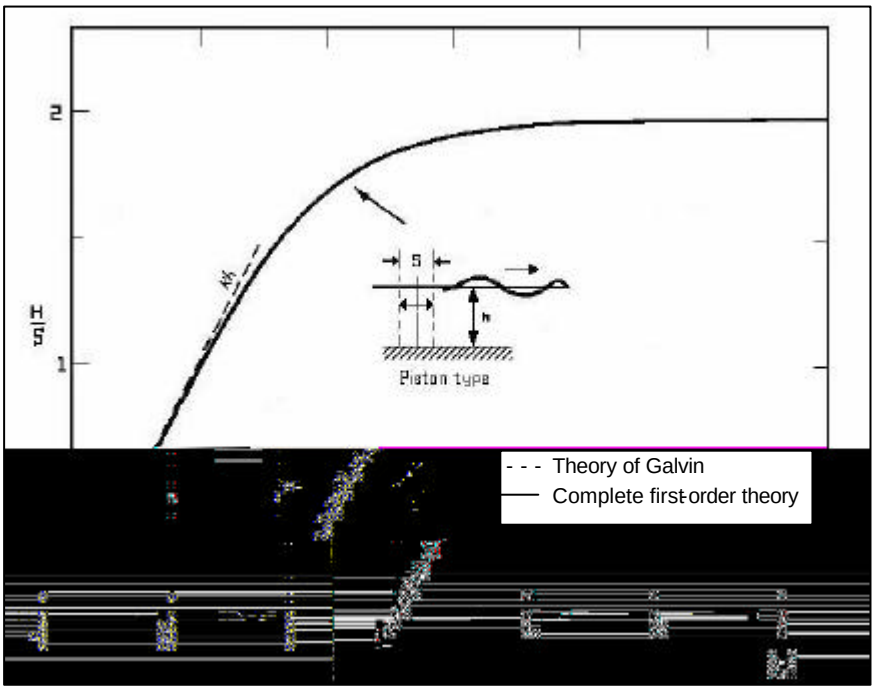

Fig 3-2 Wave height to stroke ratios versus relative depths for a piston wave board. (Dean and Dalrymple, 1991)

The derivation from equation 3-4 to a formula that calculates the wave board displacement is given in appendix E. The result for the first-order wave board displacement is:

$$\boxed{X = -\frac{k(t)C_g(t)a(t)}{w(t)\tanh\left(k(t)h\right)}\sin\left(w(t)t - y\ (t)\right)} \tag{3-5}$$

where:

X = Wave board displacement as a function of time (m)

3.3 Nonlinear corrections

3.3.1 Lagrangian correction

There are different frames of references to describe the wave motion. The Lagrangian frame and the Eulerian frame are discussed here.

Lagrangian frame of reference (total time- derivative)
Using the Lagrangian co-ordinates to describe the wave motion, the co-ordinates are fixed to a given parcel of fluid (so always the same substance) which moves in space. That is why no mass transport will take place through the boundaries.

Eulerian frame of reference (partial time-derivative)
Using the Eulerian co-ordinates to describe the wave motion, the computational cells are fixed in space, while fluid particles move across cell interfaces in any direction. Therefore mass transport can take place through the boundaries of the area (just like flux of momentum and energy)

The wave motion is less nonlinear in a Lagrangian frame of reference than in a Eulerian frame of reference. By transferring the Lagrangian results back to the Eulerian frame of reference, a nonlinear correction has applied to the wave maker theory. This correction on the first-order wave maker theory should be more accurate.

G. Klopman (May 2002) has described a way to apply the nonlinear correction to a wave maker control signal according to the linear wave theory. This can be found in Appendix C. According to this Appendix the Lagrangian correction can be applied to the first-order wave maker theory as follows:

- Compute the orbital displacement of the Lagrangian point with respect to the rest position x:

$$x_0 = -\frac{a}{\tanh(kh)}\sin(y) \tag{3-6}$$

- Compute the nonlinearly corrected water surface elevation:

$$z_E(t) = a\cos(y - kx_0) \tag{3-7}$$

- Compute the first-order wave board displacement:

$$X_0(t) = -\frac{C_g}{C}\frac{1}{\tanh(kh)}a\sin(-wt) \tag{3-8}$$

- Compute the nonlinearly corrected wave board displacement:

$$X_E(t) = -\frac{C_g}{C}\frac{1}{\tanh(kh)}a\sin(-kX_0(t) - wt) \tag{3-9}$$

where:

x_0 = Orbital displacement of the Lagrangian point with respect to the rest position x.

$x_E(t)$ = Nonlinearly corrected water surface elevation (m)

$X_E(t)$ = Nonlinearly corrected wave board displacement (m)

$X_0(t)$ = First-order wave board displacement (m)

3.3.2 Mass transport correction

The individual fluid particles in an irrotational progressive wave do not exactly follow closed paths (ellipses) as predicted in the linear theory. In addition to their oscillatory motion, they have a small net second-order mean velocity in the direction of the wave propagation. This second-order velocity is called the Stokes drift or the mass transport velocity. The surface velocity is periodic, yet faster at the wave crest than at the wave trough (see fig. 3.3). This asymmetry of velocity indicates that more fluid moves in the wave direction under the wave crest than in the trough region. This indicates that there is a small mean velocity in the direction of the waves.

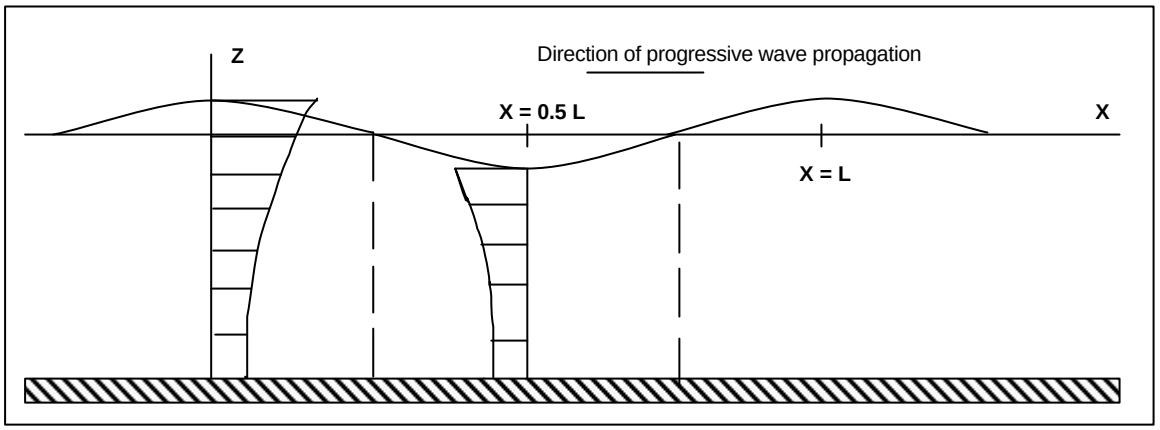

Fig 3-3 Water particle velocities in a progressive wave (Dean and Dalrymple,1991)

The depth- and time-averaged mass transport velocity is:

$$U = \frac{M}{h} \tag{3-10}$$

where

U = Depth-averaged time-mean velocity (m/s)

M = Mass transport (kg/m/s)

with

$$M = \frac{E}{rc} \; ; \; E = \frac{1}{2} r g a^2 \; ; \; c = \frac{w}{k}$$

The depth- and time-averaged velocity due to mass transport becomes:

$$U = \frac{M}{rh} = \frac{1}{2} \frac{gka^2}{wh} \tag{3-11}$$

Therefore the correction due to mass transport velocity becomes:

$$U_c = -\frac{1}{2} \frac{gka^2}{wh} \tag{3-12}$$

To apply this nonlinear correction to the wave focussing signal, it has to be added to the dispersion relation:

$$w_c = w + kU_c \tag{3-13}$$

where:

?$_c$ = Corrected angular wave frequency (due to the mass-transport velocity)

3.4 Second-order wave maker theory

Generating grouped waves in a laboratory wave flume, bound subharmonic (see fig 3-4) and superharmonic (see fig 3-5) waves are generated as well (these arise from the nonlinear interactions of the primary waves). Besides, spurious free waves may occur at subharmonic and superharmonic frequencies, which can disturb the focussing process of the created wave signal and are therefore unwanted. The subharmonics (see fig 3-4) are also called bound long waves. They arise from the wave amplitude modulations and can generate unwanted long period oscillations in medium size harbours.

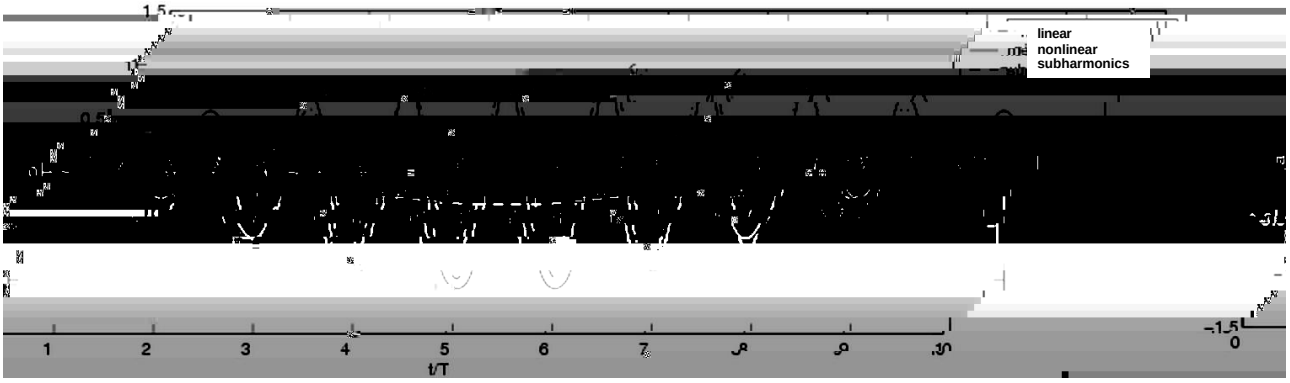

Fig 3.4 Subharmonic

The superharmonics (see fig 3-5) introduce sharper peaked wave crests and flatter troughs. Those harmonics have approximately twice the frequency of the primary wave.

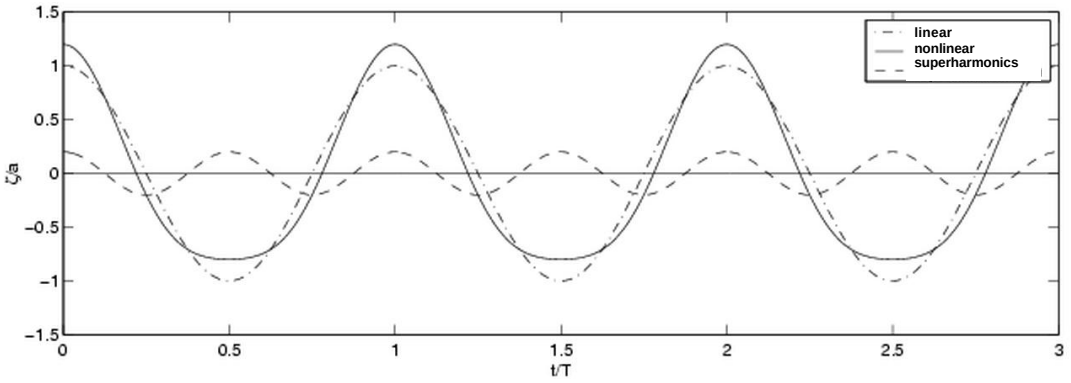

Fig 3-5 Superharmonic

Free waves can be generated at the same frequencies as the bound subharmonics and superharmonics, but are travelling with a different speed. In order to reduce those free subharmonics and superharmonics, the control signal for the wave board can be calculated with higher order theory. Dean and Sharma (1981) and Barthel et al. (1983) have calculated the transfer function for the sub- and superharmonics. Those expressions are exact up to second-order (the nonlinear interactions of all first-order spectral components are taken into account). The disadvantage of these expressions is that they are complex and require long computational time to obtain the second-order signal. Klopman and Van Leeuwen (1996) derive expressions for the wave bound control signal for the generation of second-order waves in a flume, based on the method of multiple scales to reduce those disadvantages. A brief summary of the paper is given.

The assumptions they have made:

- A constant water depth.
- The fluid is homogeneous, inviscid and incompressible.
- The flow is irrotational.
- The surface tension effects and effects of the air above the free surface are neglected.
- The carrier-wave spectrum is narrow banded (the accuracy of the multiple scales method increases as the spectral width decreases).

The carrier waves are assumed to have a narrow banded spectrum, which means that these waves can be described by harmonic functions of which the amplitudes are assumed to vary slowly in space and time. In the method of multiple scales the slow modulation is formalised by the introduction of fast coordinates (x_0, t_0) and sequence of slow co-ordinates (x_1, t_1), (x_2, t_2),.... in the horizontal space and time direction:

$x_0 = x$, $x_1 = ex$, $x_2 = e^2 x$

$t_0 = t$, $t_1 = et$, $t_2 = e^2 t$

where it has been assumed that the modulation effects are of the same order as the nonlinearity effects. e is a small nonlinearity and modulation parameter, which is of the order of the wave-steepness $\approx kA$

Klopman and van Leeuwen (1996) have expanded the surface elevation (z), the velocity potential (f) and the wave board position (X) into the following perturbation series:

$$z = \sum_{n=1}^{\infty} e^n \sum_{m=-n}^{+n} z^{(n,m)} e^{-imw_0 t_0} \quad (3\text{-}14)$$

$$f = \sum_{n=1}^{\infty} e^n \sum_{m=-n}^{+n} f^{(n,m)} e^{-imw_0 t_0} \quad (3\text{-}15)$$

$$X = \sum_{n=1}^{\infty} e^n \sum_{m=-n}^{+n} X^{(n,m)} e^{-imw_0 t_0} \quad (3\text{-}16)$$

with:

$z^{(n,m)} = z^{(n,m)}(x_0, x_1, ...; t_1 t_2, ...)$

$f^{(n,m)} = f^{(n,m)}(x_0, x_1, ...; t_1 t_2, ...)$

$X^{(n,m)} = X^{(n,m)}(x_0, x_1, ...; t_1 t_2, ...)$

Complex-valued amplitude functions and

w_0 = Carrier-wave angular frequency of the first-order waves.

n = Order.

m = Harmonic.

The results of their derivations for the wave board position are:

The first-order wave board motion:

$$X_{11} = \frac{g}{2wB} iA \quad (3\text{-}17)$$

The second-order subharmonic wave board motion:

$$X_{21}=\left[\frac{g}{2w^2B}-\frac{g}{2w^2C_g}\left(1+\sum_{j=1}^{\infty}\left[C_j l_j\left(1+\frac{\tan p_j}{2p_j}\right)-l_j\tan p_j\sum_{i=1}^{\infty}\frac{C_j}{p_j+p_i}\right]\right)\right]\frac{\partial A}{\partial t_1}$$
$$-\frac{X_{10}}{2h}\left(1+i\sum_{j=1}^{\infty}C_j\right)A \qquad (3\text{-}18)$$

The first term on the right side of equation (3-18) describes the frequency modulation and the second term contains the slow wave board motion (X_{10}).

The second-order superharmonic wave board motion:

$$X_{22}=\frac{i}{2wh}\left[\left(\frac{3}{4}\frac{gk}{wsh^2q}-\frac{g}{4B}\right)A^2-\frac{g}{4}\sum_j\frac{C_j}{B^2}iA^2+\frac{1}{4w}\sum_j\frac{C_j}{B}\frac{\left(6w^4-4g^2kl_j-g^2k^2+g^2l_j^2\right)}{4w^2\tan^{-1}\left(p_j+iq\right)+g\left(l_j-ik\right)}A^2\right.$$
$$\left.+\frac{1}{4w}\sum_{ij}\frac{C_iC_j}{B^2}\frac{\left(3w^4+2g^2l_il_j+g^2l_j^2\right)}{4w^2\tan^{-1}\left(p_i+p_j\right)+g\left(l_i+l_j\right)}iA^2\right] \qquad (3\text{-}19)$$

The first-order subharmonic wave board motion:

$$X_{10}=\frac{gC_g\left(2n-1/2\right)|A|^2}{gh-C_g^2} \qquad (3\text{-}20)$$

where:

$|A|$ = slowly varying amplitude of the free-surface elevation

$j_A=\arg\{A\}$ = slowly varying phase

$A=|A|e^{ij_A}$

The magnitude of A ($|A|$) is equal to the envelope of the surface elevation in a time simulation based on the first-order energy–density spectrum, which we want to have in the wave flume. The following coefficients are used:

$$B=\frac{2w}{k\left(sh2q+2q\right)}\left[sh2q\right] \qquad (3\text{-}21)$$

$$C_j=-\frac{2w}{l_j\left(\sin 2p_j+2p_j\right)}\left[\sin 2p_j\right] \qquad (3\text{-}22)$$

where:

$q=kh$

$p_j=l_jh$

k = the positive and real root of $w^2=gk\tanh kh$

l_j = the positive and real root of $-w^2=gl_j\tan l_jh$ with $\left(j-\frac{1}{2}\right)p<l_jh\le jp$ for j=1,2,...

The total second-order wave board motion (in the paper equation 2-88) becomes:

(3-23)

CC denotes the complex conjugate of the preceding terms. The first term on the right hand side of equation (3-23) is the first-order term and the next three terms are second-order.

3.5 Expectations

Before the experiments are carried out, a prediction of the most effective software package, or in other words for the most effective combination of the theories to generate the wave focussing signal, is given. After the analysis of the experiments these expectations are compared with the results. The expectations are:

- *About the used dispersion relation (see 2.2):*
  The nonlinear dispersion relations (Hedges and Kirby and Dalrymple) will probably come out in a better way in comparison with the linear dispersion relation because the effect of nonlinearity on the wave propagation characteristics is neglected in the linear theory.
  The prediction for the best dispersion relation among the three relations created by Kirby and Dalrymple (see 2.2.3.) is the dispersion relation Kirby and Dalrymple (1987), because it is a modification on the dispersion relation Kirby and Dalrymple (1986) and therefore probably more accurate.
  Because of the slight difference between the nonlinear formulations of Hedges and Kirby and Dalrymple (1987) and Kirby and Dalrymple (1986)), it is difficult to predict which of these is more accurate.

- *About the use of the second-order theory:*
  The prediction is that the second-order theory will come out as the most effective theory, because the higher order effects are included (like sub- and super harmonics) which will be developed with the generation of the wave focussing signal and therefore be more accurate.

- *About the calculation of the group velocity:*
  It is expected that the two different ways of the calculated group velocity, respectively $C_{g,i}$ and $C_{g,d}$, will give a difference of 3% at deep water (see section 2.2). The calculated group velocity whereby the amplitude is dependent on k ($C_{g,d}$), is expected to lead to be more approximate to the wave amplitude variation away from the maximum of the wave group, because the frequency-modulated signal used in this research is highly asymmetrical (as explained in section 2.2).

- *About the mass correction*
  An improved signal is expected with this correction, because a nonlinear effect (the small mean motion of the fluid, see 3.3.2) is taken into account. But in comparison with the complete second-order theory it probably will give a poorer signal, because it is a nonlinear correction but will still not be second-order, so less accurate.

- *About the Lagrangian correction*
  The prediction is that this would give an improvement of the signal, because the wave motion is less nonlinear in a Lagrangian frame of references than in an Eulerian frame of reference. But again, in comparison with the complete second-order theory it probably will give a poorer signal, because it is only a nonlinear correction but the theory will still not be second-order, so less accurate.

With those expectations, it is expected that the software packages with the following combination of the theories will result in the most effective wave focussing signals; second-order theory, mass correction, nonlinear dispersion relation of Kirby and Dalrymple (1987). These software packages corresponds with the names “Chirp35duiscussion” and “Chirp37discussion” (see Appendix A).

Experimental set-up

4 Experimental set-up

4.1 Wave flume

The experiments to verify the developed wave focussing signals have been carried out in a wave flume (called “lange speurwerkgoot”) in the Laboratory of Fluid Mechanics at the Faculty of Civil Engineering and Geosciences at Delft University of Technology. This flume has a horizontal bottom and a length of 42 m, a width of 0.8 m and a maximum depth of 1 m. The sidewalls of the flume are made of glass, thus making it possible to view the development of the waves. Five gauges located in the wave flume (described in section 4.5) measure the water surface elevation. The waves are generated by a piston wave board (described in section 4.2) and absorbed by a beach (described in section 4.3). The water depth can be regulated in the wave flume. An overview and a sketch of the wave flume are shown in figure 4-1 and 4-2.

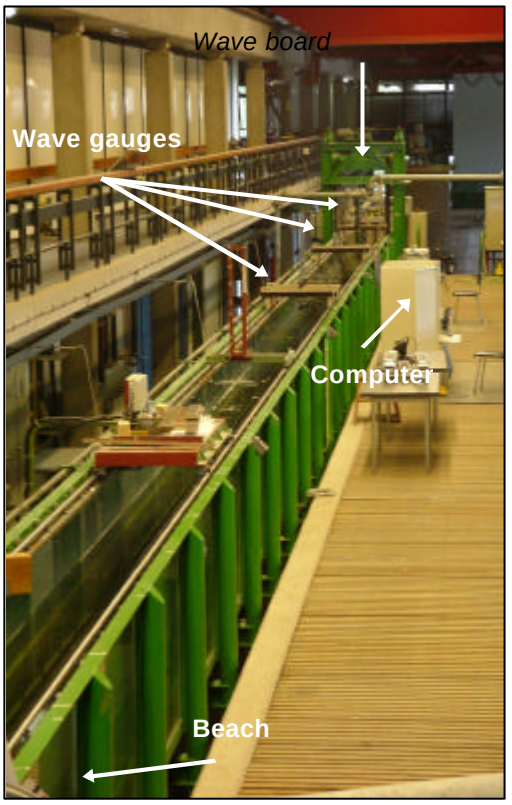

Fig 4-1 Overview of the wave flume

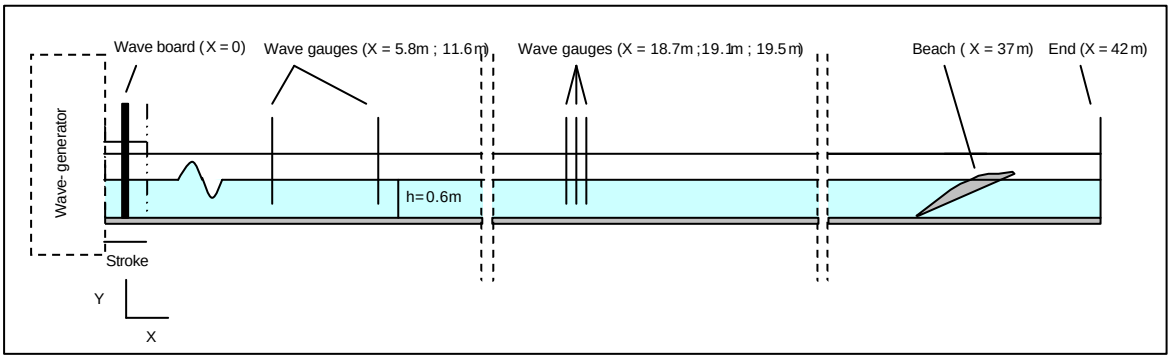

Fig 4-2 Sketch of the experimental set-up

4.2 Wave board

The piston wave board (see fig. 4-3 and fig. 4-4) is positioned at the upstream side of the wave flume. X = 0 m is defined at the midpoint of the wave board (see fig. 4-2). A piston type of wave board moves horizontally while its face remains vertical during its movement. The maximum stroke (the maximum horizontal displacement of the wave board) is one meter on both sides of the midpoint x= 0m (see fig. 4-2).
The wave board is controlled by an offline-calculated control signal. By combining the different theories (explained in chapter 2). several offline-calculated wave focussing control signals are developed. The control signals are time series of the wave board motion. The displacement of the wave board is accomplished by implementing the desired control signal to the wave generator (described in subsection 4.4.1).

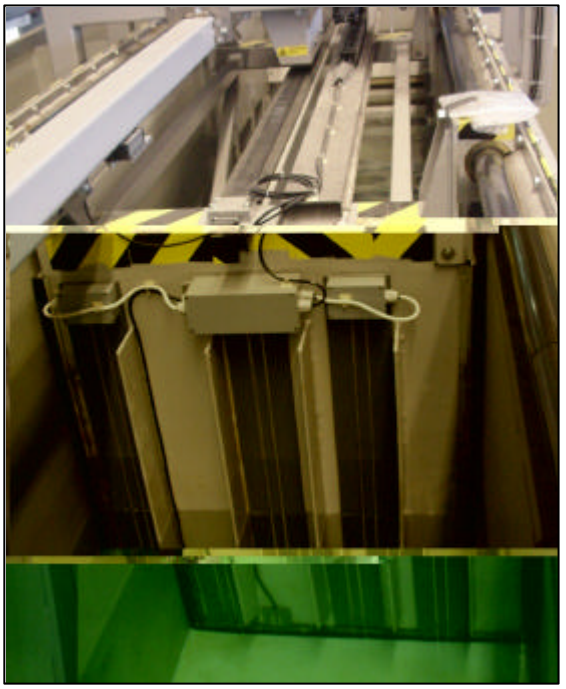

Fig 4-3 The electro-mechanically driven piston wave board

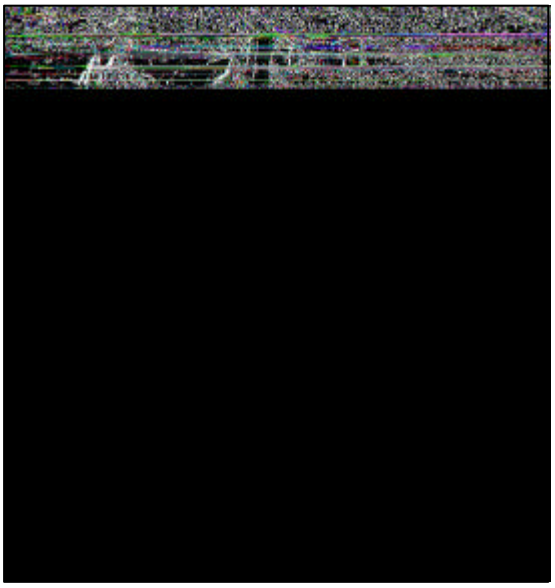

Fig 4-4 Top view of the piston wave board

A special characteristic of the wave board is the Active Reflection Compensation (ARC) algorithm, which compensates the wave board motion for reflected waves. The wave board motion is modified in such a way that the reflected waves are absorbed by the wave machine (= active wave absorption). This ARC can be switched on or off. In the performed experiments this function is switched off, because the interference between the reflected waves and the signal is not possible before the whole signal has passed the focus point.

4.3 Absorbing beach

A parabolic-shaped beach is situated at the downstream side of the wave flume at X = 42 m (see figures 4-2 and 4-5 and 4-6).

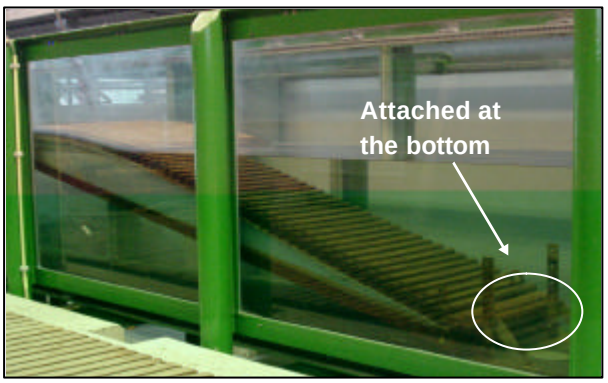

Fig 4-5 Side view of the beach situated at the downstream side of the wave flume

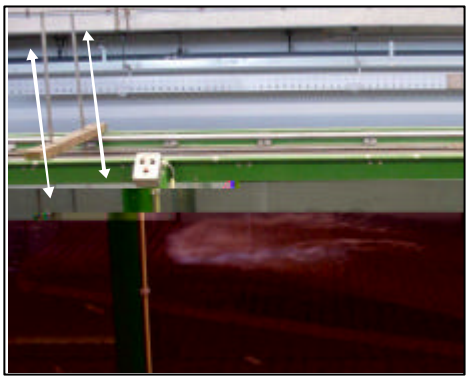

Fig 4-6 Incoming wave on the beach

The beach is attached to the bottom of the wave flume at one end and can rotate around this side. This free movement of the beach minimises the reflection of the incoming waves at the end of the wave flume. The absorption of the waves insures a relative short time needed for the water surface to return to its equilibrium state, thus shortening the time needed between the experiments.

4.4 Wave generation in laboratory flume

4.4.1 Wave generator

The wave board is controlled by a wave generator (Hoffmann, 2002). This wave generator consists of four components (see fig 4-7):

1. The mechanical wave generator (with a surface elevation gauge (=GHM))
2. The motor (2) and its digital controller (2b)
3. The real time processor
4. The operator PC (with the wave generator control application)

The wave generator control application is a computer program (called “control application” for short), that runs on a personal computer (see fig 4-8). This program reads its input from two user specified files (*.dat and *.ifg) and sends the output to the real time processor. The control files are created offline, using MATLAB (a mathematical programming application). In those control files the output values of the surface elevation or the wave board position as a function of time are defined.

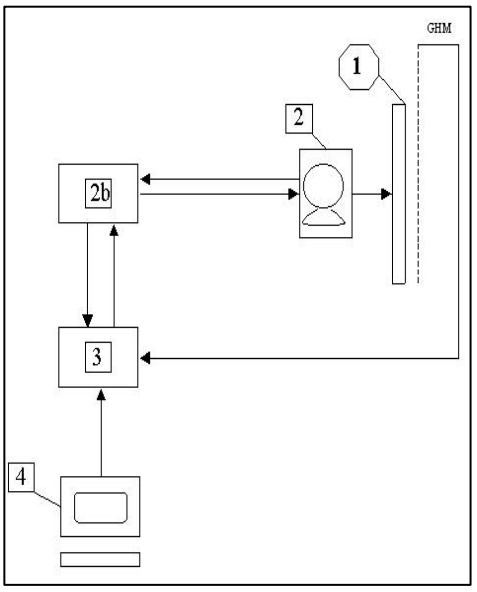

Fig. 4-7 The wave generator

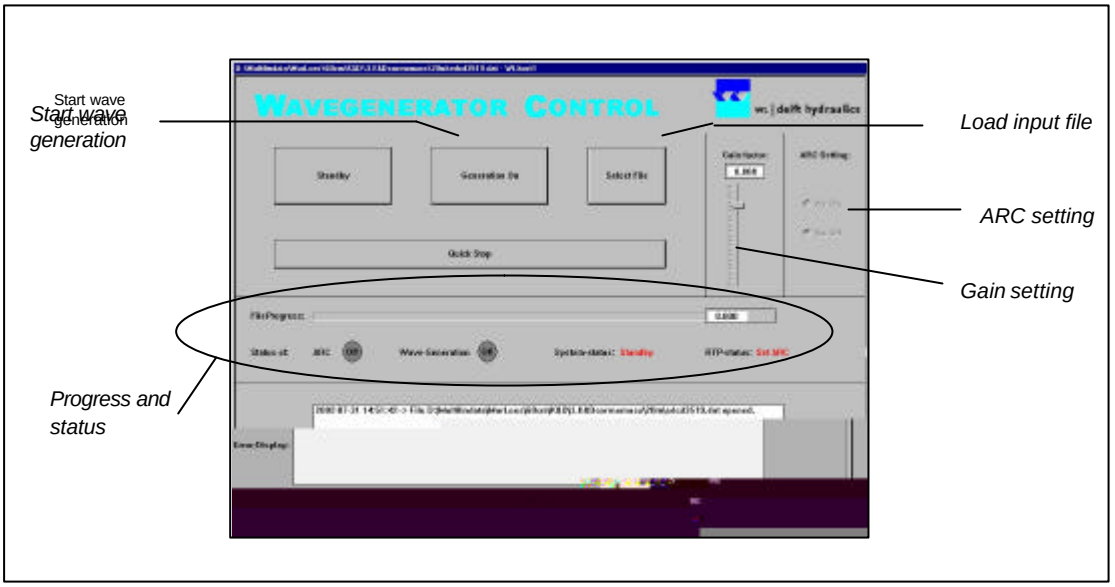

Fig 4-8 Wave generator control application

The input data consist of commands and data such as setpoint information (a setpoint here, is the location of the wave board at a certain time, so (x,t)). When the system generates waves, the control application reads the setpoint file and sends the setpoints to the real time processor. The processor switches the generator and motor on and the wave board starts to make the desired wave signal. The complete description of the operation of this wave generator can be read in Hoffmann (2002).

In this research the control signal for the wave board is calculated offline and can afterwards be enforced on the wave board through the wave generator. In order to make the control signal for the wave board motion, two different approaches are considered:

1. The construction of a control signal using MATLAB, by computing the required wave board motion as a function of time directly.
2. The construction of a control signal using MATLAB that computes the required water surface displacement as a function of time. To obtain the wave board motion corresponding with the water surface displacement the Delft-Auke program (WL|Hydraulics, 2001) is used. This program computes time series for the wave board motion in order to generate a desired wave field.

In this research the first approach is used, because this approach is most challenging and most influential and thereby explainable. Challenging because in this approach the wave board motion has to be calculated, while in the second approach the wave board motion is calculated by the program “Delft Auke”. Most influential and therefore most explainable because the intermediate steps between the calculation of the values of the water surface elevation to the values of the wave board motion can be followed in contrast to the second approach.

In the control application the input values of the time series for the wave board displacement can still be influenced (so after the offline calculated control signal) by a factor called the gain factor. This factor can be regulated in this application. The gain factor has a range from 0.00 till 1.00. The default value is 0.8, which corresponds with the exact input values (the values calculated by the software package). So, for example, when the gain factor is set to 0.2, the input values are multiplied by 0.2/0.8=0.25.

4.4.2 Implementation of the theories

The literature study has given a selection of theories to use for the creation of the offline signal. Before creating the offline signal, some assumptions were made:

- A constant water depth
- The fluid is homogeneous, inviscid and incompressible
- The flow is irrotational
- The surface tension effects and effects of the air above the free surface are neglected
- The carrier-wave spectrum is narrow banded.
- Use of a piston wave board
- Free water surface
- No current

With these assumptions the offline control signal is developed in the computer program MATLAB resulting in different software packages. Except for the wave focussing software package based on the theory of Chaucy-Poisson, all the created software packages have the same global structure, which is described below. An overview of this structure is shown in figure 4.9 and the different steps are briefly described below. A more complete description is shown in appendix K.

The water surface elevation as a function of time at x = 0m can be derived by the following expression:

$$z\left(x_0,t\right)=a(t)*\cos\left(y\ (t)\right) \tag{4-1}$$

To obtain the desired water surface elevation the accompanying wave board displacement has to be computed. This wave board displacement as a function of time at x = 0m can be obtained by
1. The first-order wave maker theory (equation 3-5):

$$X\left(x_0,t\right)=-\frac{kC_g a}{w\tanh\left(kh\right)}\sin\left(y\ (t)\right)$$

2. The second-order wave maker theory (equation 3-23):

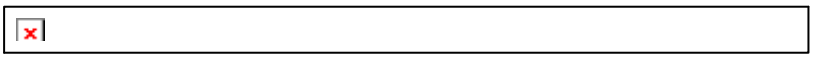

To evaluate the variables dependent on the time, an iterative process is applied in this research by using the input variables. The input variables of the software packages are:
X_0, f_0, h, β and the ratio of the maximum frequency (f_m) to the peak frequency (f_0).
With the input variables the frequency of the wave in the wave train with the lowest celerity (the maximum frequency) can be calculated:

$$f_m = ratio * f_0 \tag{4-2}$$

The wave number of this wave (k_m) can be determined by an iterative computation with the linear dispersion relation (2p f_m, h, g). The focussing signal consists of many waves, which are generated by the wave board at different times. To evaluate the time at which each wave has to be generated by the wave board the group velocity can be used. The first wave generated by the wave board is the wave with the highest frequency and thus travels with the lowest velocity of the whole wave train. Knowing the values of f_m, k_m, h the minimum group velocity can be derived with the definition of the linear group velocity:

$$C_{g,\min} = \frac{1}{2}\frac{2pf_m}{k_m}\left[1 + k_m h \frac{1-\tanh^2(k_m h)}{\tanh(k_m h)}\right] \quad (4\text{-}3)$$

This velocity determines the focus time by the following expression:

$$t_f = \frac{x_f - x_0}{C_{g,\min}} \quad (4\text{-}4)$$

Hereafter an iterative process is applied to obtain the angular frequency, the amplitude, the group velocity for each wave in the wave train and the time when each wave has to be generate by the wave board. First some estimations, for the values of the angular frequency and the amplitude and wave number, are made:

- The estimation for the angular frequency has been derived by linearly spacing between the maximum- and minimum angular frequency with equidistance steps
- The estimation of the wave number is derived iterative with the linear dispersion relation.
- The amplitude is set to zero (which results in neglecting the nonlinear terms in the first iteration)

With these estimations the iterative process starts and ends when the relative difference of the angular frequency between the iterations is small enough (<0,000001). The different steps of this process are:

- Computation of the angular frequency at x = 0m with the desired dispersion relation (see section 2.2)
- Computation of the group velocity at x = 0m from the desired dispersion relation (see section 2.3)
- Computation of the time vector, which means compute the time when each wave has to be generated by the wave board. Each wave, which is generated after the first wave, has to travel faster to arrive at the focus point in time (see fig 2-1, which is repeated here). Therefore the time array can be obtained with the calculated group velocity and the focus time:

$$C_{g,i} = \frac{x_f - x_0}{t_f - t_i} \quad (4\text{-}5)$$

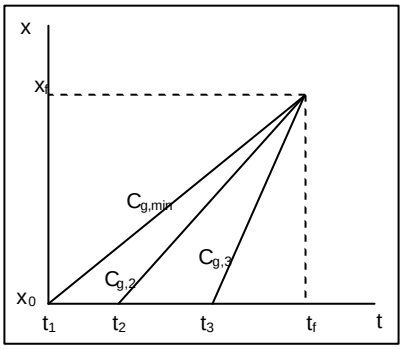

Fig. 2-1 Outline of wave focussing

After this iterative process the total wave phase (?) of each wave can be obtained (see section 2.5). Now all the required arrays are known, the water surface elevation and the wave board displacement at x = 0m can be computed with the equations 3-5 and 3-23 and the control signal is determined.

.

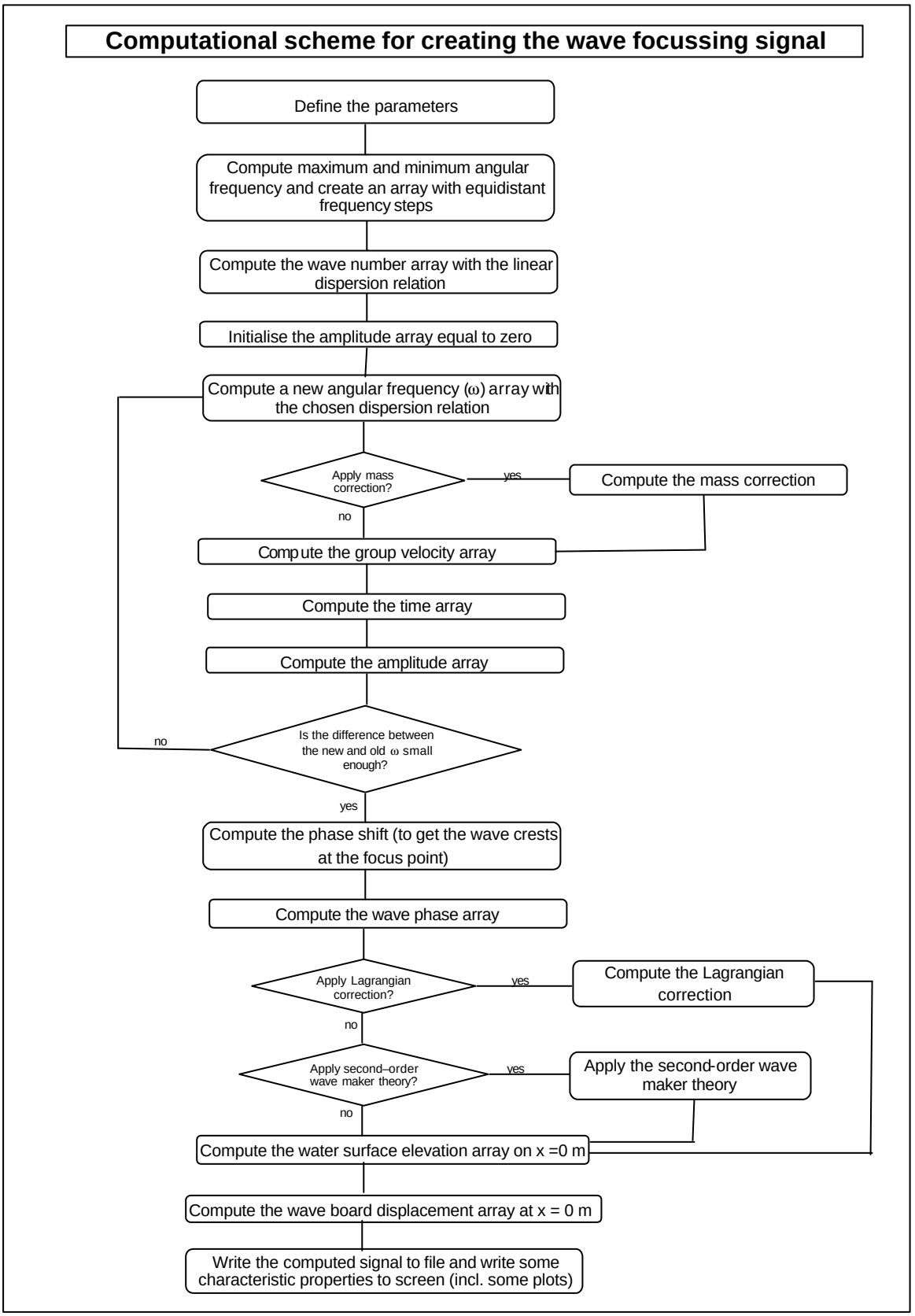

Fig. 4-9 Computational scheme for creating the wave focussing signal

4.5 Instrumentation and data acquisition

In order to observe the water surface elevation as a function of time at a fixed location in the wave flume, wave gauges are used. A wave gauge consists of two parallel stainless steel rods (type 316), placed vertical underneath a small electronic box (see fig. 4-10). The rods act as the electrodes of an electric resistance meter. When voltage is set across the two electrodes the electrical current can be measured and the resistance or conductivity will be calculated. The electrical resistance depends of the column water between the electrodes, the distance between the two electrodes and the conductivity of the water. To avoid the effect of conductivity fluctuations of the water, a third (reference) electrode is mounted at the lower end of the gauge, which has to be at least 4 cm under the water surface.

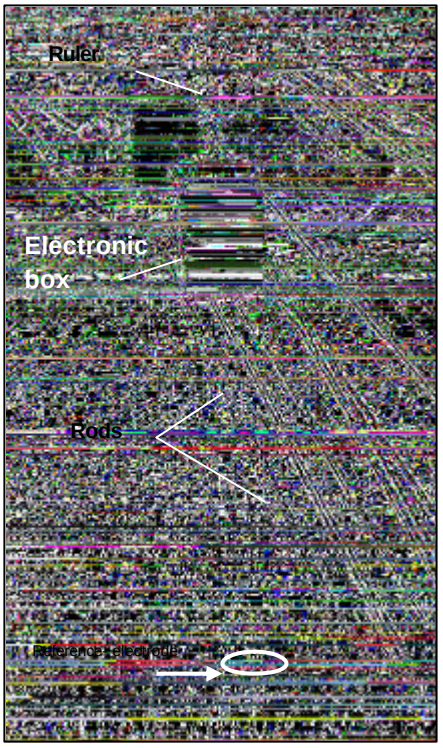

Fig. 4-10 Wave gauge

The probe is connected to a control unit (see fig. 4-11). The control unit displays the voltage on a voltmeter. The output voltage lies between +/– 10 Volt. The range of the control unit can be selected to 5, 10, 20 or 50 cm full scale. This "range" has to be set one position higher than the highest wave height expected.

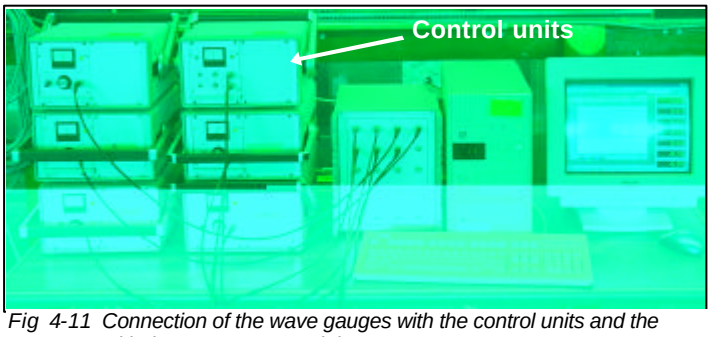

Fig 4-11 Connection of the wave gauges with the control units and the computer with the program "Dasylab"

The measurement accuracy and the non-linearity of the gauge is 0.5 % of the full scale. This means an over-all accuracy, by 50 cm, of 2.5 mm. The gauge has an analogue signal output with a maximum frequency response of 5 Hz. Before starting the experiments, the voltmeter has to be set to centre position (0 Volts) when it is still water, so it can use its maximum range. In the performed experiments the "range" is set at 50 cm which means that 1 Volt corresponds with 2.5 cm (because 20 Volt correspond with 50 cm). This has been checked before the experiments and was found correctly.

Five wave gauges are used in the experiments. The first two wave gauges are situated about five and ten meters from the wave board to get a good view of the development of the generated wave focussing signal far before the theoretical focus point. The other three wave gauges are situated around the theoretical focus point to evaluate the focussing process. Table 4-1 shows the different positions of the wave gauges for the experiments with the different focus points.

	Theoretical focus point at 20 m	**Theoretical focus point at 25 m**
Gauge number	*Distance from wave board (m)*	*Distance from wave board (m)*
1	5.8	5.8
2	11.6	11.6
3	19.6	24.6
4	**20** **(theoretical focus point)**	**25** **(theoretical focus point)**
5	20.4	25.4

Table 4-1 Positioning of the wave gauges for different theoretical focus points

The data from the wave gauges is collected with the program DASYLAB. The measured value of the signal is translated to the computer with an accuracy of 12 bit, which means 50/40.95 = 0.1mm accuracy and the sampling rate is 50 Hz. This data is stored in a file for each experiment and the names of these files are the same as the accompanying control signals, only four or five characters are added as a prefix (see appendix J).

For visualising the focusing process of the waves in the focus point, a digital video/photo camera is used to make movies and pictures of this process. The program “JLIP Video Capture/Producer” is used to transfer the movies and the pictures from the camera to the computer. All the movies and pictures are stored on the CD. The pictures can also be found in appendix-report.

Results and analysis of the experiments

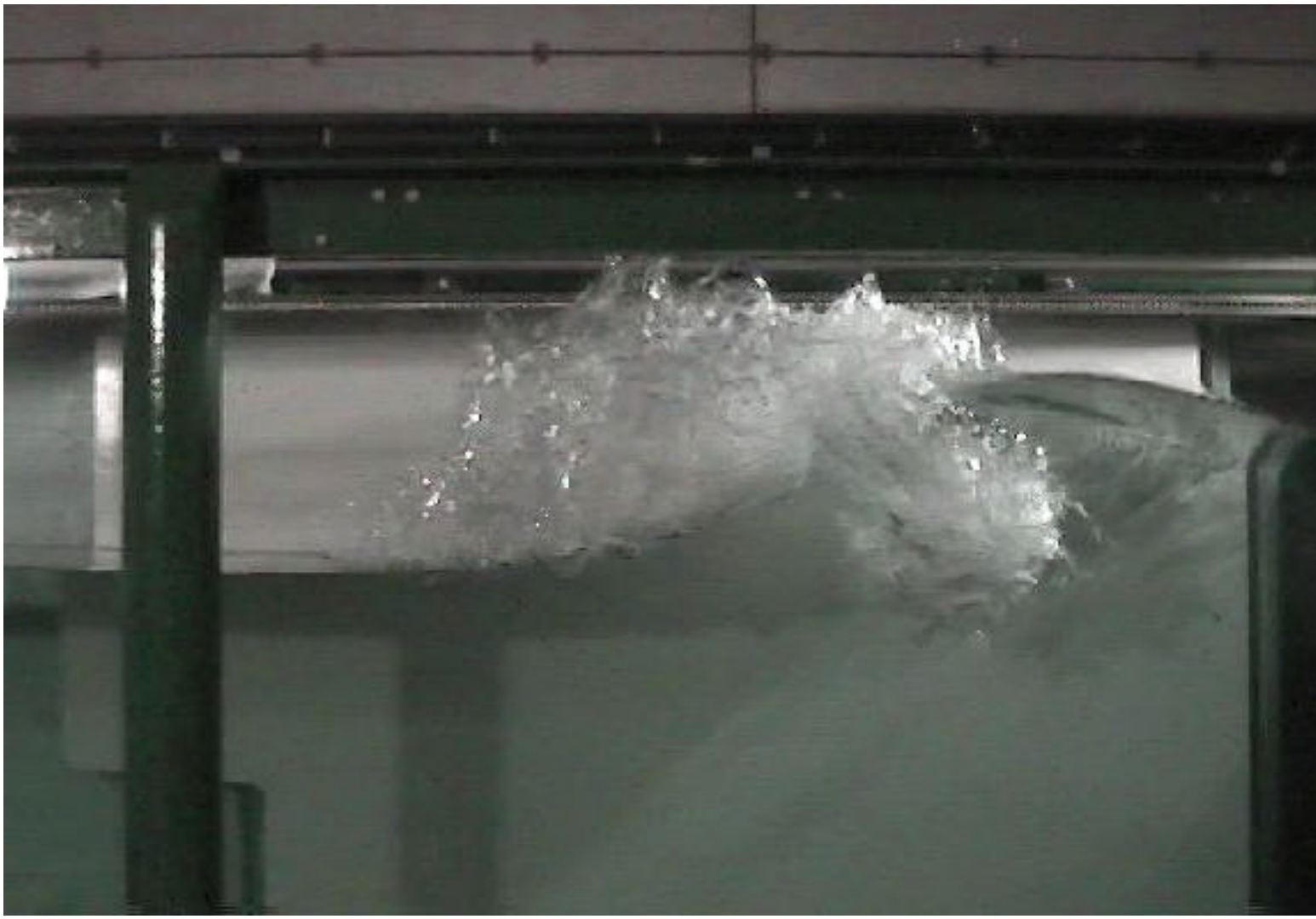

5. Results and analysis of the experiments

5.1 Introduction

In order to verify the created offline signals, experiments were carried out in a laboratory flume. The experiments are performed for each developed software package in order to see which combination of the used theories produces the most effective wave focussing signal. In total 224 experiments are carried out and archived. All the names and the accompanying six input variables are registered and can be found in appendix A. This chapter describes the results and analyses of all the experiments. As will be shown in the following section, the predictive quality of the developed control signals is assessed by two parameters. Each parameter is related to one of the following questions: is the wave height correctly predicted (H_e), does the theory predict the correct location of the wave focussing signal and is the standard deviation small (a large standard deviation means the waves have not correctly accumulated into a well-focussed wave)? In the wave flume the wave height is measured at a limited number of locations. Since the generated wave focussing signal could occur just before (or after) a wave height meter, an assessment solely based on the values of these parameters could lead to incorrect conclusions. To reduce this risk a visual classification of the quality of the signals is also carried out to supplement the numerical evaluation. This visual classification should support the choice of the parameters such as $H_{e,f}/H_l$, the ratio of the experimental wave height ($H_{e,f}$) to the linear theory prediction (H_l). A high classification of a generated wave focussing signal should correspond to a parameter $H_{e,f} / H_l > 1$ as will be shown below. In section 5.3 the values of the derived parameters and the visual classification are clarified and classified. Subsequently the different control signals along with their accompanying experimental data are assessed based on the developed parameters. The influence of the variation of the input variables in the theoretical models is analysed in section 5.4. The conclusions and discussion of the analysis of the experiments are represented in sections 5.5.

5.2 Definitions of the derived parameters

This section contains a description of the dimensionless parameters that have been developed to evaluate the quality of the different control signals. To make comparison possible, all the control signals are generated with the same values for the input variables (reference values):

The reference values for the input variables:	
Theoretical focus distance	$X_f = 25$ *m*
Water depth	$h = 0.6$ *m*
Peak frequency	$f_0 = 0.3$ *Hz*
Ratio of the maximum frequency to the peak frequency	$r = 5$ *(-)*
Relative wave height	$b = 0.3$ *(-)*

In this section only the experiments using these reference values are considered. For all the experiments, the derived parameters and the visual classification are computed and shown in the table 5-1, which is shown on the next page. Each point in the plots of the developed parameters represents a different control signal (modelling a theory or combination of theories).

Software Package	Used theories	Control signal	$H_{e,m}/H_i$ (-)	$H_{e,f}/H_i$ (-)	Visual classification (-)	B_b (-)	B_f (-)
Chirp19c	Hedges + mass corr + $C_{g,d}$				6		
Chirp20c	Hedges + Lagr cor + mass corr + $C_{g,d}$	fhcc3503	1.11	1.11	10	0.81	0.48
Chirp22c	K&D + Lagr corr + mass corr + $C_{g,d}$	fdcc3503	1.05	1.05	10	0.81	0.55
Chirp22cfirstapprox	K&D + Lagr corr + mass corr + $C_{g,d}$	fdcf3503	1.04	1.04	10	0.82	0.57
Chirp22cdiscussion2	K&D + Lagr corr + mass corr + $C_{g,d}$	fdcs3503	1.13	1.13	8	0.81	0.51
Chirp22d	K&D + lagr corr + $C_{g,d}$	fdcd3503	1.22	1.21	8	0.73	0.51
Chirp22dfirstapprox	K&D + lagr corr + $C_{g,d}$	fdcn3503	1.35	1.34	8	0.73	0.52
Chirp22ddiscussion2	K&D + lagr corr + $C_{g,d}$	fdns3503	1.29	1.27	7	0.71	0.45
Chirp22anly	K&D + lagr corr + mass corr + $C_{g,i}$	fdca3503	1.25	1.25	6	0.70	0.50
Chirp22firstapprox	K&D + lagr corr + mass corr + $C_{g,i}$	fdfa3503	0.72	0.71	5.5	0.87	0.55
Chirp22firstapproxumass	K&D + lagr corr + mass corr + $C_{g,i}$	fdgm3503	1.04	0.85	6.5	0.83	0.53
Chirp22discussion2	K&D + lagr corr + mass corr + $C_{g,i}$	fddu3503	0.84	0.84	7	0.87	0.55
Chirp22discussion2umass	K&D + lagr corr + mass corr + $C_{g,i}$	fdug3503	0.98	0.91	7	0.86	0.57
Chirp22lin	K&D + lagr corr + lin + $C_{g,d}$	fdcl3503	1.30	1.30	8	0.72	0.49
Chirp22linfirstapprox	K&D + lagr corr + lin + $C_{g,d}$	fdlf3503	1.21	1.21	7	0.73	0.51
Chirp22lindiscussion2	K&D + lagr corr + lin + $C_{g,d}$	fdlt3503	1.29	1.26	7	0.72	0.46
Chirp23c	Hedges + Lagr corr + $C_{g,d}$	fucc3503	1.30	1.30	6	0.72	0.44
Chirp23d	Hedges + Lagr corr + lin + $C_{g,d}$	fhcl3503	0.89	0.89	6	0.73	0.44
Chirp24c	Hedges + lagr corr + mass corr + $C_{g,i}$	facc3503	0.77	0.76	7	0.85	0.49
Chirp29/0	Hedges + 2nd order + mass corr + $C_{g,i}$	fhaw3503	0.70	0.64	5.5	0.78	0.46
Chirp31	Hedges + mass corr + $C_{g,i}$	fhaa3503	0.82	0.71	7	0.90	0.53
Chirp32/0	Hedges + mass corr + 2nd order + $C_{g,d}$	fhtt3502	0.49	0.49	4	0.91	0.69
Chirp33	K&D + mass corr + $C_{g,d}$	fdnn3503	1.04	1.03	8	0.88	0.60
Chirp33firstapprox	K&D + mass corr + $C_{g,d}$	fdnt3503	1.01	1.01	8.5	0.87	0.59
Chirp33discussion2	K&D + mass corr + $C_{g,d}$	fdkk3503	1.03	1.03	7	0.85	0.53
Chirp34/0	K&D + mass corr + 2nd order + $C_{g,i}$	fdat3503	0.7	0.7	8	0.84	0.52
Chirp34/0firstapprox	K&D + mass corr + 2nd order + $C_{g,i}$	fdtf3503	0.96	0.96	8	0.81	0.51
Chirp34/0discussion2	K&D + mass corr + 2nd order + $C_{g,i}$	fdtr3503	0.79	0.75	7	0.82	0.59
Chirp35/0	K&D + 2nd order + $C_{g,d}$	fdmt3503	1.32\	1.32	10	0.80	0.50
Chirp35/0firstapprox	K&D + 2nd order + $C_{g,d}$	fdmf3503	1.34	1.34	10	0.81	0.52
Chirp35/0discussion2	K&D + 2nd order + $C_{g,d}$	fdms3503	1.32	1.32	6	0.79	0.47
Chirp36	K&D + mass corr + $C_{g,i}$	fdaa3503	0.81	0.77	7	0.90	0.52
Chirp36firstapprox	K&D + mass corr + $C_{g,i}$	fdaf3503	0.89	0.83	5	0.90	0.54
Chirp36discussion2	K&D + mass corr + $C_{g,i}$	fded3503	0.83	0.84	7	0.91	0.55
Chirp37/0	K&D + mass corr + 2nd order + $C_{g,d}$	fdtt3503	1.00	0.95	8	0.78	0.52
Chirp37/0firstapprox	K&D + mass corr + 2nd order + $C_{g,d}$	fdff3503	0.91	0.91	9	0.80	0.52
Chirp37/0discussion	K&D + mass corr + 2nd order + $C_{g,d}$	fddt3503	0.98	0.98	7	0.79	0.58
Chirp38/0	Hedges + 2nd order + $C_{g,d}$	fhmg3503	1.27	1.27	6	0.81	0.35
Chirp40	Linear + mass corr + $C_{g,d}$	flll3503	0.82	0.64	7	0.83	0.52
Chirp41	Linear + mass corr + $C_{g,i}$	flla3503	0.68	0.64	7	0.84	0.52
Chirp42	Linear + Lagr corr + mass corr + $C_{g,d}$	fllc3503	0.67	0.61	7	0.83	0.52
Chirp43	Linear + Lagr corr + mass corr + $C_{g,i}$	flca3503	0.64	0.64	7	0.80	0.56
Chirp44	Linear + lagr corr + $C_{g,d}$	flcn3503	0.71	0.62	7	0.77	0.49
Chirp45	Linear + $C_{g,d}$	flnn3503	0.77	0.77	7	0.85	0.53

Table 5-1 All the experiments with the reference input variables with the accompanying values for the developed parameters

5.2.1 Ratio of the experimental and theoretical wave height

The control signals are developed in such a way that the focussed wave also has to be a breaking wave in the theoretical focus point. Whether the wave actually breaks cannot be assessed by the water surface elevation measurements, this has to be determined visually. The water surface measurements can determine the maximum wave height at each wave gauge. Therefore, the theoretical breaking wave height is compared to the maximum experimental wave height. In order to determine whether the measured wave height is close to the expected theoretical breaking wave height, the following dimensionless parameter is proposed:

$$\frac{H_{e,m}}{H_l} \tag{5-1}$$

where:

H_l = Theoretical breaking wave height (m)

$H_{e,m}$ = Maximum measured wave height (m)

The theoretical breaking wave height is derived from the wave maker control signal by linear wave theory, assuming that all the power provided to the waves concentrates in one wave length at the theoretical focus point. Accordingly:

The expected wave length of the breaking wave (m): $l_b = \frac{2p}{k_l}$ (5-2)

The wave energy per unit area (J/m^2): $E = \frac{1}{2} r g a^2$ (5-3)

The wave energy flux per meter width (W/m): $E_f = EC_g$ (5-4)

The work performed by wave maker (J/m): $W = \int E_f dt$ (5-5)

The total energy in the breaking wave per unit area (J/m^2): $E_b = \frac{W}{l_b}$ (5-6)

where:

k_l = Wave number of the last wave (rad/m)

g = Gravitational acceleration constant (m/s^2)

r = Mass density of water (kg/m^3)

This results in the theoretical breaking wave height of:

$$H_l = \sqrt{\frac{8E_b}{rg}} \tag{5-7}$$

The experimental wave height is derived from the water surface elevation measurements. To determine the maximum experimental wave height, the highest wave height of the four wave gauges nearest to the theoretical focus point, is evaluated. Let ζ_t be the water elevation at a trough and ζ_c the water elevation at the following crest. The maximum wave height at a gauge is then defined as: $H_m=\max(\zeta_c - \zeta_t)$. This maximum wave height is computed for all the four gauges

and the largest wave height of all the gauges ($H_{e,m}$=max(H_m)) is used as the maximum experimental wave height.

The visual classification is graded from 0-10. The resulting grade is used to classify the results as follows:

< 5 poorly-focussed signal
5 – 7 reasonably-focussed signal
> 7 well-focussed signal

The control signals and the corresponding values of the parameter $H_{e,m}$ / H_l are shown in table 5-1 at the end of this section and are plotted against the values of the subjective visual classification in figure 5-1. As will be shown in section 5.3.1 highly nonlinear waves have a wave height larger than predicted by linear theory. In this respect values for the parameter $H_{e,m}$ /H_l are expected to be larger than one for well-focussed waves. Figure 5-1 shows a strong correlation between the visual classification and the parameter $H_{e,m}$ /H_l. High values for $H_{e,m}$ /H_l often correspond to high grades for the visual classification. The same applies for low values of $H_{e,m}$ /H_l and low values for the visual classification. This indicates that the visual classification supports the choice of this developed parameter $H_{e,m}$ /H_l as a predictor of the most effective control signal.

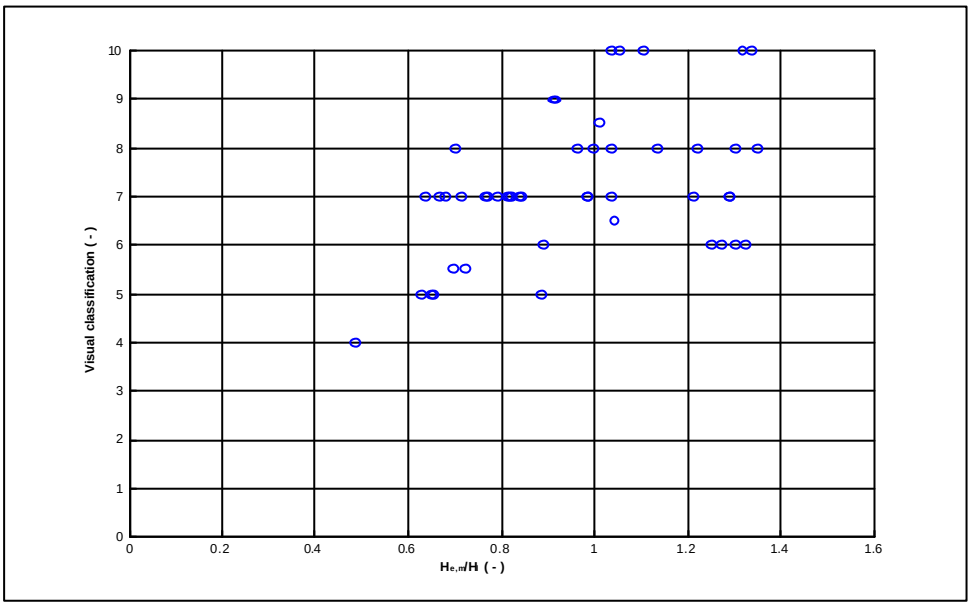

Fig. 5-1 $H_{e,m}$ /H_l plotted against the subjective visual classification (where $H_{e,m}$ / H_l is not necessarily at the theoretical focus point).

From the experimental data it is noticed that the maximum wave height does not always occur at the theoretical focus point. It is important to calculate the maximum experimental wave height at the theoretical focus point for two reasons:

- The ratio of the experimental wave height to the linear theory prediction measures whether the measured wave height is close to the expected theoretical breaking wave height. To make a valid comparison between the theoretical and experimental wave height, both have to be calculated at the same distance from the wave board. The theoretical breaking wave height, H_l, is computed at the theoretical focus point and therefore the experimental wave height has to be computed at the theoretical focus point.
- Wave focussing aims at the generation of a breaking wave at a certain point and time in the flume by sending out a wave train with different frequencies and therefore different speeds in such a way that all the waves arrive at the same time at a certain point in the flume. This is another reason why it is important that the wave focussing signal should acquire its maximum wave height at the theoretical focus point.

Consequently only the highest wave at the gauge in the theoretical focus point should be considered. To take the theoretical focus point into account a new parameter is developed:

$$\frac{H_{e,f}}{H_l} \tag{5-8}$$

where:

$H_{e,f}$ = Maximum of the experimental wave height at the theoretical focus point (m).

The maximum of the experimental wave height at the theoretical focus point is obtained from the surface elevation measurements. To determine this wave height, the highest wave height from the wave gauge at the theoretical focus point is measured (the maximum distance between a trough and the following crest). When the highest wave does not occur at this gauge this obviously results in a lower value of the parameter $H_{e,f}/H_l$ as expected for an incorrectly focussed wave. This is in accordance with the fact that it focussed too early or too late.

The combination of the control signals and the values of the parameter $H_{e,f}$ / H_l are shown in table 5-1. Values of $H_{e,f}$ / H_l are plotted against the values of the subjective visual classification in figure 5-2. Comparing the two figures 5-1 and 5-2 it can be seen that the difference is very small, this in fact indicates that most of the signals focus at or very close to the theoretical focus point. However the analysis above shows that this new parameter is better suited for an assessment of the quality of the control signals. Therefore the parameter $H_{e,m}/H_l$ is rejected from here on.

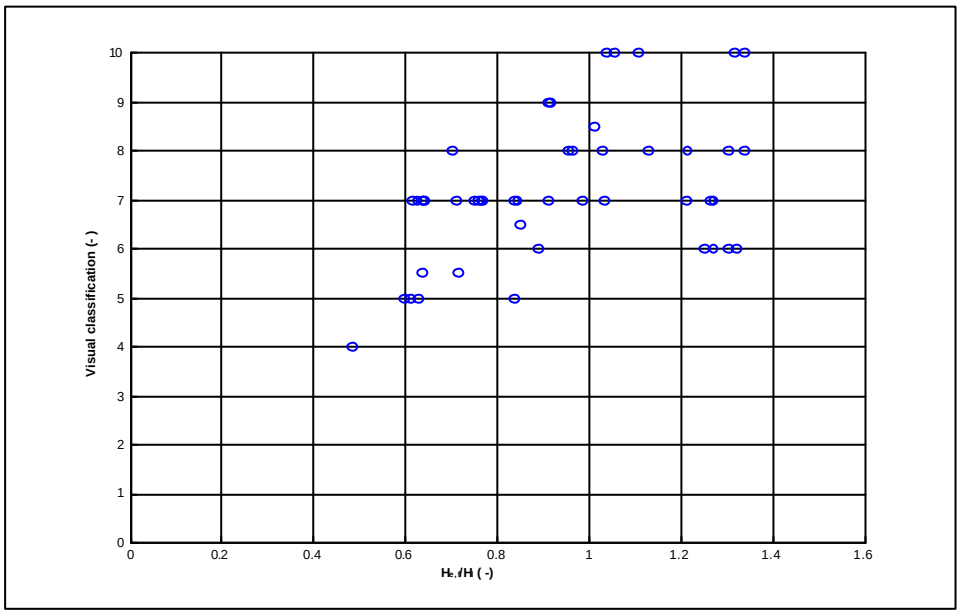

Fig.5-2 $H_{e,f}/H_l$ plotted against the subjective visual classification (where $H_{e,f}/H_l$ is at the theoretical focus point).

5.2.2 "Degree of focussing" parameter

An additional parameter is developed to measure the degree of focussing of the waves (B_b). First the wave envelope is determined for the experimental surface elevation measurements at the theoretical focus point. The standard deviation of this envelope is computed to determine the degree of focussing. The definition of the standard deviation is explained briefly.

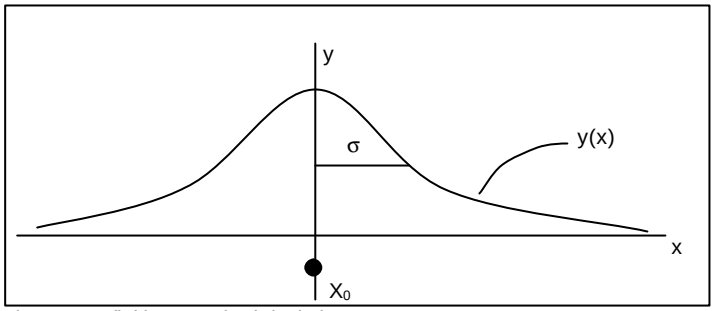

Fig. 5-3 Definition standard deviation

The standard deviation is a measurement of the dispersion or scatter of the values of a function y(x) around its mean at $x = x_0$. In formula this becomes:

$$\text{Standard deviation} = s = \sqrt{\frac{\int_{-\infty}^{+\infty}(x-x_0)^2 y(x)dx}{\int_{-\infty}^{+\infty} y(x)dx}} \qquad (5\text{-}8)$$

The new parameter is computed with the surface elevation measurements as a function of time at fix location (the theoretical focus point). This means that the standard deviation, used to compute the new parameter, is a function of t and ? instead of x and y as shown in the general definition of the standard deviation (see equation 5-8). The envelope of the experimental surface elevation measurements at the theoretical focus point is obtained by using the Hilbert transform. The Hilbert transform introduces a 90° phase shift to the original data; sines become cosines and vice versa.

For example:

Signal $= x(t) = \cos(wt)$

The Hilbert transform $= x_{Hilbert}(t) = \sin(wt)$

The envelope (or wave amplitude) becomes $A(t) = \sqrt{x^2(t) + x^2_{Hilbert}(t)} = 1$

Figure 5-4 shows an example of an envelope of a surface elevation measurement at the focus point, achieved by a Hilbert transform (the blue line is the surface elevation measurement and the red line is the envelope of this signal).

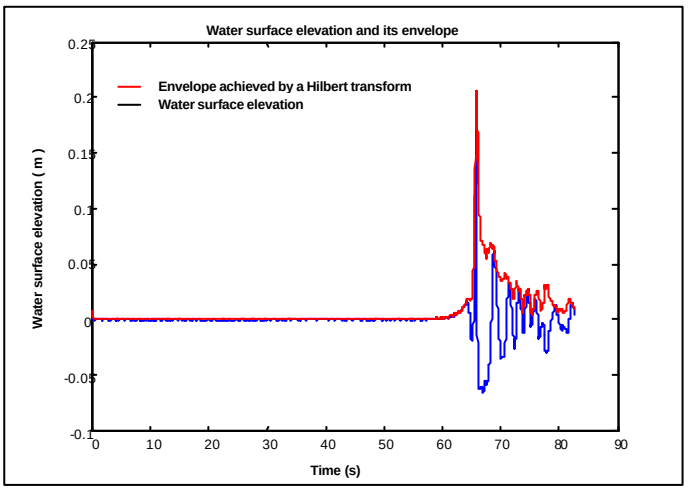

Fig. 5-4 The water surface elevation and its envelope at $x=x_f$ as a function of time.

To determine the degree of focussing of the waves the standard deviation is calculated around the peak of the envelope (t_p). In the computation of the standard deviation of the envelope of the surface elevation measurement at the theoretical focus point an interval [–2T, 2T] is chosen (see fig. 5-5). This interval is large enough to cover all well-focussed waves. It seems a plausible assumption that the contribution to B_b of the signal outside this interval is not relevant to this parameter. Figure 5-5 is an example of a surface elevation of a poorly-focussed signal at the focus point and the used interval in which the standard deviation is calculated. This figure shows that the waves from t_p -2T till t_p are too early at the focus point and the waves from t_p till t_p +2T are too late.

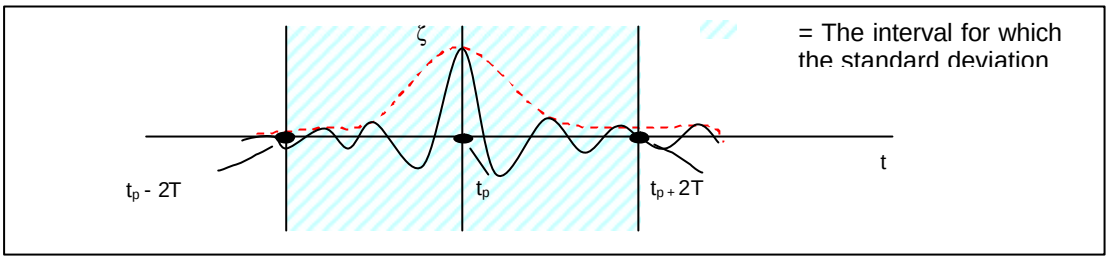

Fig 5-5 The boundaries whereby B_b is calculated

When A(t) describes the envelope of the surface elevation measurement at the focus point and t_p is the peak of this envelope, the standard deviation around t_p, normalised with the frequency f_0 becomes:

$$B_b = \sqrt{\frac{\int_{t_p-2T}^{t_p+2T}(t-t_p)^2 A(t)dt}{\int_{t_p-2T}^{t_p+2T}A(t)dt}} * f_0 \qquad (5\text{-}9)$$

The different values of B_b (dimensionless) of the experiments can be found table 5-1. A low value of B_b should correspond with a better focussing process than a higher one. This is also illustrated in figure 5-6 on the next page. This picture shows the water surface elevation as a function of time at the focus point, and its envelope (the dotted line). Figure 5-6 (a) shows a well-focussed signal and figure 5-6 (b) a less well-focussed signal. Obviously the parameter B_b in figure 5-6 (b) will be larger than in figure 5-6 (a).

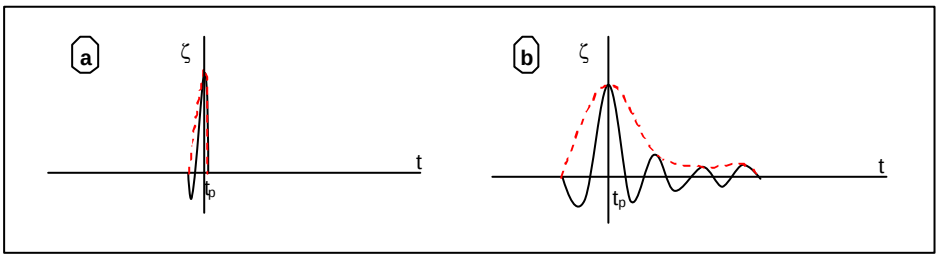

Fig 5-6 The water surface elevation as a function of time and its envelope at the theoretical focus point. Figure (a) is a well-focussed signal and figure(b) is less well-focussed

Values of the parameter B_b are plotted against the values of the subjective visual classification in figure 5-7.

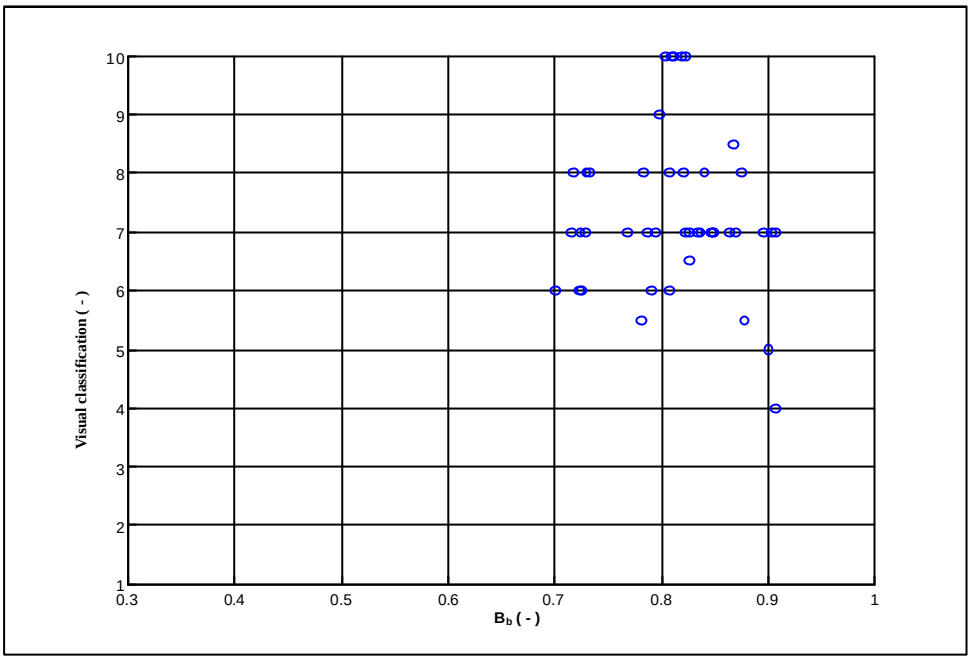

Fig. 5-7 B_b plotted against the subjective visual classification.

Figure 5-7 shows a weak correlation between the visual classification and the parameter B_b. This indicates that the visual classification provides little support to the choice of this developed index B_b, as a predictor for the most effective control signal. An explanation for this weak correlation is described below.

An abrupt ending of the wave focussing signal at a certain level introduces a discontinuity of its derivative, which could possibly cause interference in the generation of the wave focussing signal. To avoid this, the wave focussing signals have been elongated with a tail function. This "tail function" begins with a one-period wave having the same amplitude as the last wave followed by a function that gradually goes to zero. Obviously the waves of the tail function do not have to reach the focus point at t_p since the tail function is only added to avoid interference. However the parameter B_b does include these waves. This could account for the high values for B_b. Figure 5-8 shows a surface elevation measurement at the focus point for one signal with a high value of B_b = 0.87; visual classification = 8.5 and $H_{e,f}/H_i$ = 1.01. The parameter $H_{e,f}/H_i$ and the visual classification qualify this wave as a well-focussed wave, while the parameter B_b qualifies this wave as a poorly-focussed wave. The big difference between the qualification based on B_b and the other two parameters can be attributed to the fact that B_b includes this "tail function".

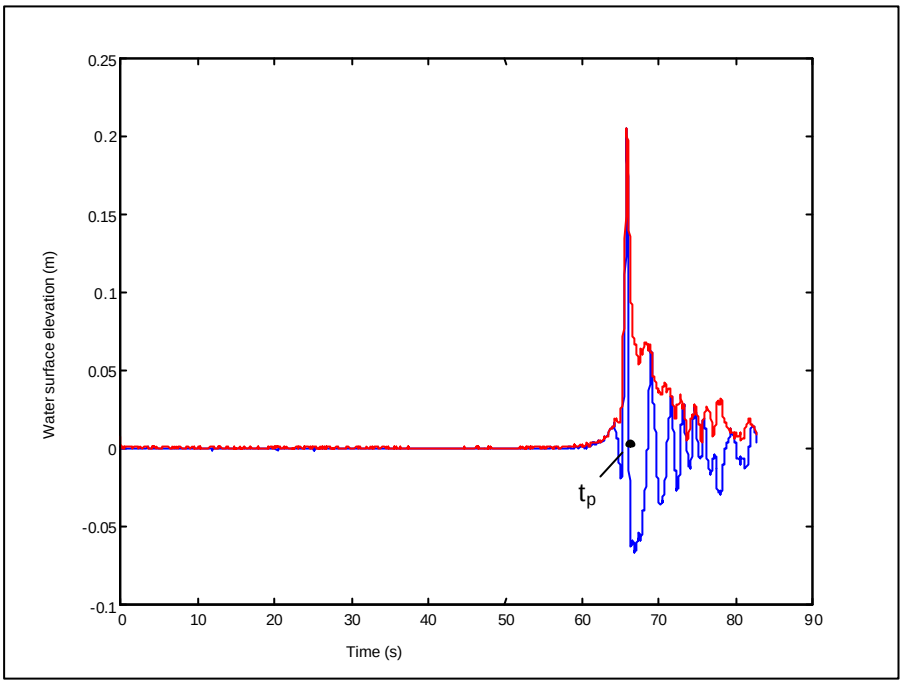

Fig 5-8 A surface elevation measurement at the theoretical focus point for one signal with a high value for B_b (0.87), visual classification (8.5) and for $H_{e,f}/H_i$ (1.01) but it is reasonably-focussed.

The number and the size of the oscillations in the tail, which are generated after the desired focussing signal, is not the same for each signal. This may lead to an incorrect interpretation of the focussing degree of the signal. Therefore a new parameter is evaluated to take this effect into account. This new parameter will be used instead of B_b. The definition of the parameter is actually the same as B_b, but it has different boundaries, whereby only the front of the envelope is taken into account (see fig 5-9).

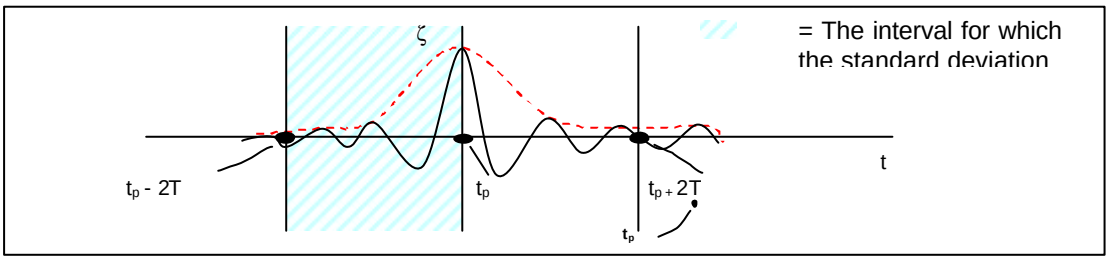

Fig 5-9 The boundaries whereby B_f is calculated

The new dimensionless parameter becomes:

$$B_f = \sqrt{\frac{\int_{t_p-2T}^{t_p} (t-t_p)^2 A(t)dt}{\int_{t_p-2T}^{t_p} A(t)dt}} * f_0 \qquad (5\text{-}10)$$

The combination of the control signals and the values for the parameter B_f are shown in table 5-1. Values of B_f are plotted against the values of the subjective visual classification in figure 5-10.

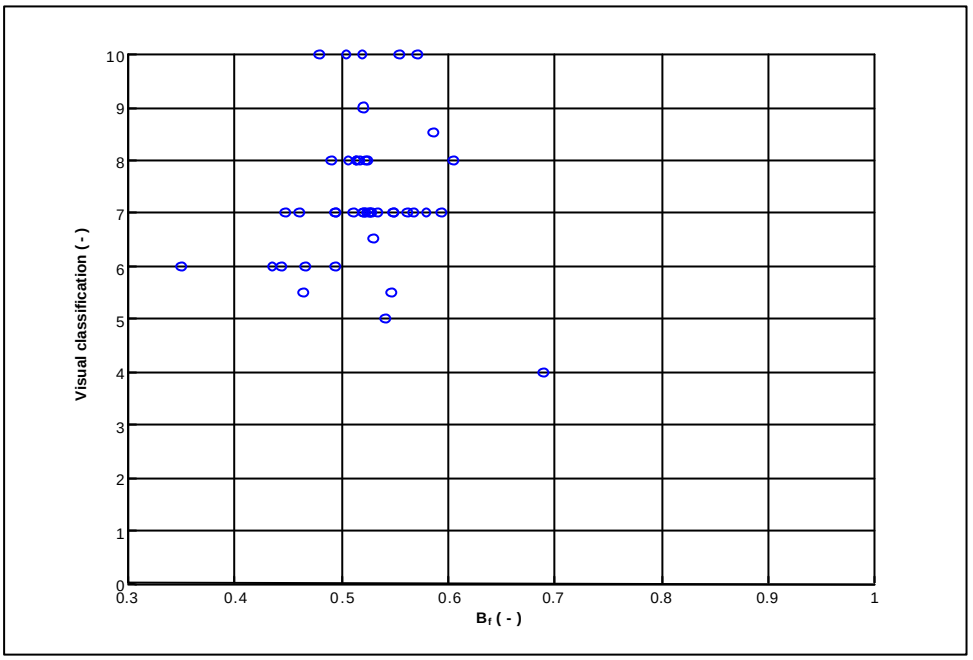

Fig. 5-10 B_f plotted against the subjective visual classification

The values of the new parameter B_f are much lower than the values of the parameter B_b, as comparison of figures 5-9 and 5-10 shows. This is as expected due to the absence of the tail function, i.e. the waves generated at the wave maker after the focussing waves in order to create a smooth transition from maximum wave height to zero. The support of the visual classification to the developed parameter B_f is not much of an improvement compared to the parameter B_b. However, from plots of $H_{e,f}/H_l$ versus B_f and B_b respectively, there is a higher correlation between $H_{e,f}/H_l$ versus B_f than with B_b and therefore we do reject B_b in the remainder of this research. In section 5.3 the parameter B_f and also the other derived parameter $H_{e,f}/H_l$ and the visual classification are assessed as a predictor for the most effective control signal.

5.3 Assessment of the control signals

In the remainder of this chapter only the parameters: $H_{e,f}/H_I$ at the theoretical focus point, B_f and the visual classification are used. In section 5.3.1 the values of the two parameters and the visual classification are determined and they are classified into three areas (well-focussed, reasonably-focussed and poorly-focussed). After this classification, the parameters will be assessed with respect to their usability as a predictor of the most effective control signal and based on the chosen parameters the overall best focussing methods are selected (section 5.3.2).

5.3.1 Classification of the values of the parameters

The values of the derived parameters and the visual classification have to be classified before the quality of the control signals can be evaluated. The waves are classified as follows:

1. Poorly-focussed
2. Reasonably-focussed
3. Well-focussed

The boundaries for the different areas are determined for each parameter and for the visual classification:

- *The visual classification*

The visual classification is graded from 0 – 10. The resulting grade is used to classify the results as follows:

< 5 poorly-focussed signals.
5 – 7 reasonably-focussed signals.
> 7 well-focussed signals.

The wave height, the breaking process, the place of focussing and the presence of waves before or after the breaking wave were observed. Based on those observations the signal was classified. Since waves of the tail function (see 5.2.2) do not have to arrive on time, they have been neglected for the visual classification. When a large number of waves, not belonging to the tail function, arrive after the breaking wave it is obvious that the signal is not well-focussed and therefore the tail of the signal is not neglected in the visual classification. When only one wave, not belonging to the tail function, arrives after the breaking wave, the distinction between the tail function and those waves is much more difficult to observe. This could result in a high value for the visual classification, while it is actually not well-focussed. The resulting grade can cause a discrepancy between the other parameters.

- $H_{e,f}/H_I$

Using linear wave theory, the height of the focussed wave can be estimated, assuming that the time-integrated power provided by the wave maker to the waves is concentrated in one wave length at the focal point. The focal wave length is estimated using linear wave at the wave peak period, assuming that the focussed wave has the same wave period as the last wave generated at the wave maker. With these assumptions for calculation the theoretical breaking height and assuming the experimental waves are linear, the ratio $H_{e,f}/H_I$ of a well focussed wave is expected to lie around one. Since highly nonlinear waves have a larger wave height than the ones predicted by linear theory for the same energy content, it is expected that the ratio $H_{e,f}/H_I > 1$ for well-focussed waves. A twenty-percent lower experimental breaking wave height compared to the theoretical breaking wave height will still be accepted as a reasonably-focussed wave. Therefore a wave signal will be assessed as reasonably-focussed when the ratio lies between 1 and 0.8. If the ratio $H_{e,f}/H_I < 0.8$, the signal will be judged as poorly-focussed.

- B_f

To determine the expected value of this parameter in case the wave is well-focussed a function y(x) needs to be found. This function is created in such a way that it corresponds with a well-focussed wave. In this function, x depends on the peak frequency, the time and a factor that ensures the minimum of y (its trough) at exactly a half wave period. The reference input variables are used as parameters in this function. The envelope of this function is obtained by using a

Hilbert transformation. With the resulting envelope, the parameter B_f is computed and provides the expected value for B_f for a well-focussed wave.

The approach for clarification of the value of B_f:

- Find a function $y(x)$, which looks like a well-focussed wave, in the theoretical focus point. where $x(t, f_0, factor)$
- The factor is determined such that the minimum of y is at exactly a half wave period (see fig. 5-13)
- Compute its envelope $A(t)$ by using the Hilbert transformation (see 5.2.2).
- Compute $B_f = \sqrt{\frac{\int_{t_p-2T}^{t_p}(t-t_p)^2 A(t)dt}{\int_{t_p-2T}^{t_p} A(t)dt}} * f_0$ (5-10)

  using the reference input variables

Three propositions were developed for this function:

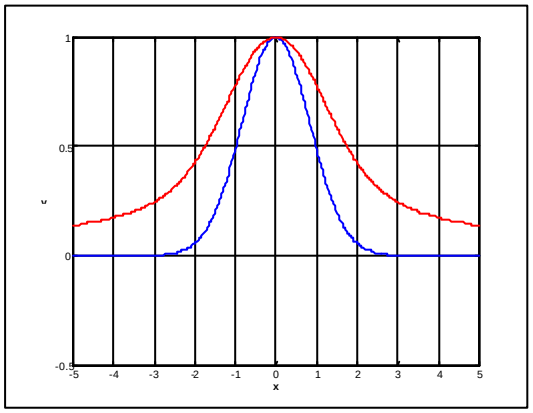

Fig. 5-11 Proposition 1 ($y=e^{-1/2x^2}$)

Proposition 1: Without a trough:

$$y = e^{-\frac{1}{2}x^2} \quad (5\text{-}11)$$

with $x = 4 f_0 t$ (5-12)

$f_0 = 0.3Hz$

$B_f \approx 0.77$ (-)

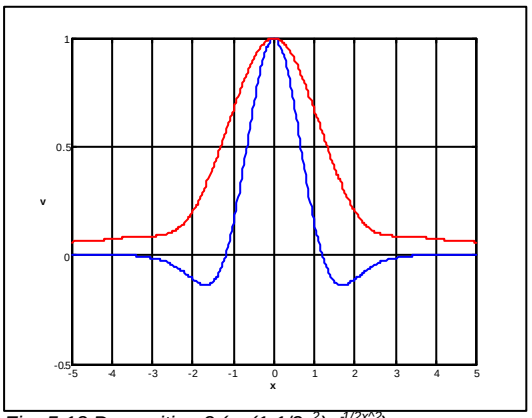

Fig. 5-12 Proposition 2 ($y=(1-1/2x^2)e^{-1/2x^2}$)

Proposition 2: With a small trough:

$$y = \left(1-\frac{1}{2}x^2\right)e^{-\frac{1}{2}x^2} \quad (5\text{-}13)$$

with $x = 3.94 f_0 t$ (5-14)

$f_0 = 0.3Hz$

$B_f \approx 0.63$ (-)

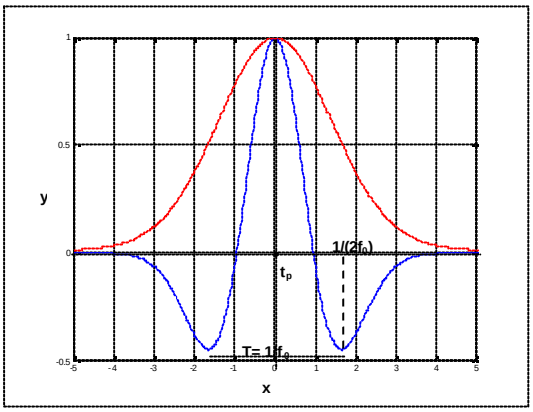

Fig. 5-13 Proposition 3 ($y=(1-x^2)e^{-1/2x^2}$)

Proposition 3: With a deep trough:

$$y = \left(1 - x^2\right) e^{-\frac{1}{2}x^2} \qquad (5\text{-}15)$$

with $x = 3.5\, f_0 t$ (5-16)

$$f_0 = 0.3Hz$$

$$B_f \approx 0.49 \ (\text{-})$$

As described in the introduction, eyewitness reports pictured the freak wave as a deep trough ("hole in the ocean") followed by a steep crest. In this respect the third proposition (with a deep trough) corresponds best with the ideal-focussed wave in the theoretical focus point and is used for the choice of the characteristic value of B_f. The value of B_f for the ideal-focussed wave is therefore about 0.5 (see figure 5-13). The qualification for a reasonably-focussed wave is set between 0.5 and 0.6. Consequently, if B_f exceeds the value 0.6 the signal is qualified as poorly-focussed.

These boundaries are directives for the classification of the different control signals. Table 5-2 shows the boundaries for the different areas of the parameters and the visual classification.

	Well-focussed	Reasonably-focussed	Poorly-focussed
Visual classification	**> 7**	**5 - 7**	**< 5**
$H_{e,f}/H_I$	**> 1**	**0.8 - 1**	**< 0.8**
B_f	**< 0.5**	**0.5 – 0.6**	**> 0.6**

Table 5-2 The boundaries for the different areas of the parameters and the visual classification.

In the figures below the parameters and the visual classification are plotted against each other. Three different rectangular areas are marked; well-focussed, reasonably-focussed and poorly-focussed (figure 5-14 – 5-16). Again, each point in the plots represents a different control signal. The points inside and near the rectangular areas have parameters that agree about the classification of the control signal and those points are specified in the tables 5-3 – 5-5. Consequently, the points outside these areas have parameters that are in disagreement with the classification of the control signals. An attempt to explain these discrepancies is given below each of the figures.

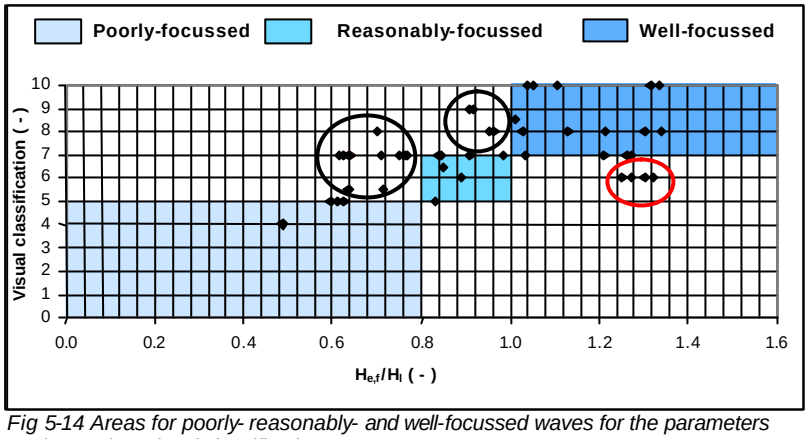

Fig 5-14 Areas for poorly- reasonably- and well-focussed waves for the parameters $H_{e,f}/H_l$ against visual classification.

Possible explanations for the discrepancy between $H_{e,f}/H_l$ and the visual classification (points inside the circular areas) are given below:

- *A high value for the parameter $H_{e,f}/H_l$ and a low value for the visual classification (the red circle).*
  This discrepancy can be a result of a wave focussing signal that focussed too late.
  When this signal passes the focus point it probably already has a high wave height, but it has to catch up one last wave with a small amplitude. This small wave causes the breaking but the difference between the wave height of the signal at the focus point and the one at the moment of breaking is very small. In this respect the parameter $H_{e,f}/H_l$ can be high but the visual classification classifies this signal as a too late focussed wave.
- *A low value for the parameter $H_{e,f}/H_l$ and a high value for the visual classification (the black circles).*
  This discrepancy can be due to the subjectivity of the visual classification.
  The amplitude of the last wave of the wave focussing signal is not the same for every signal. This amplitude can vary from around 0.1 m till around 0.4 m. The visual classification of two signals with the same degree of focussing can differ, because the classification can be influenced by the fact that a big wave makes more impression than a small wave. This could explain a high visual classification and a low value for the parameter $H_{e,f}/H_l$.

Well-focussed	H	V	Reasonably-focussed	H	V	Not-focussed	H	V
Hedges + lagr corr + mass corr + $C_{g,d}$ *(chirp20c)*	1.1	10	Hedges + lagr corr + no mass corr + lin + $C_{g,d}$ *(chirp23d)*	0.89	6	Hedges + 2nd order + mass corr + $C_{g,d}$ *(chirp32)*	0.49	4
K&D + lagr corr + mass corr + $C_{g,d}$			K&D + lagr corr + mass corr + $C_{g,i}$					
Petit *(chirp22c)*	1.05	10	Firstapprox *(chirp22firstapprox)*	0.85	6.5			
Firstapprox *(chirp22cfirstapprox)*	1.04	10	Discussion *(chirp22discussion)*	0.84	7			
Discussion *(chirp22cdiscussion)*	1.13	8						
K&D + lagr corr + $C_{g,i}$			K&D + 2nd order + mass corr + $C_{g,d}$					
Petit *(chirp22d)*	1.21	8	Discussion *(chirp37discussion)*	0.95	8			
Firstapprox *(chirp22dfirstapprox)*	1.34	8						
Discussion *(chirp22ddiscussion)*	1.27	7						
K&D + lagr corr + $C_{g,d}$ + lin			K&D + mass corr + $C_{g,d}$					
Petit *(chirp22lin)*	1.30	8	Firstapprox *(chirp36firstapprox)*	0.83	5			
Firstapprox *(chirp22linfirstapprox)*	1.21	7	Discussion *(chirp36discussion)*	0.84	5			
Discussion *(chirp22lindiscussion)*	1.26	7						
K&D + mass corr + $C_{g,d}$								
Petit *(chirp33)*	1.03	8						
Firstapprox *(chirp33firstapprox)*	1.01	8.5						
Discussion *(chirp33discussion)*	1.03	7						
K&D + 2nd order + $C_{g,d}$								
Petit *(chirp35)*	1.32	10						
Firstapprox *(Chirp35firstapprox)*	1.34	10						

Table 5-3 The control signals, where $H_{e,f}/H_l$ (H) and visual classification (V) have agreement about their quality.

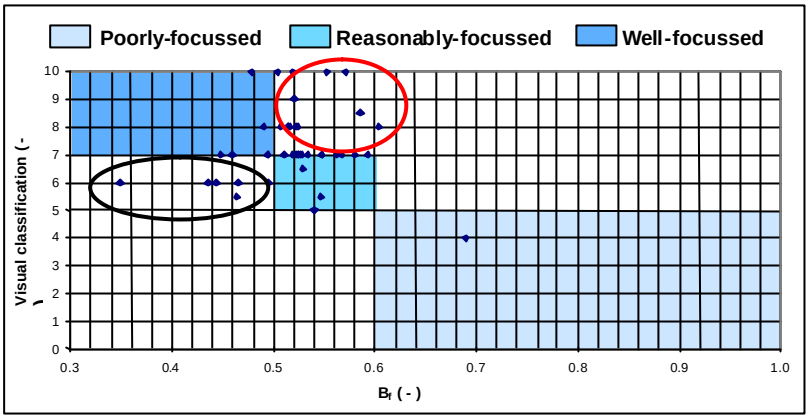

Fig 5-.15 Areas for poorly- reasonably- and well-focussed waves for B_f against the visual classification

Possible explanations for the discrepancy between B_f and the visual classification are given below:

- *A high value for the parameter B_f and a high value for the visual classification (the red circle)*
  This discrepancy can be due to the absence of a trough of the breaking wave.
  The three propositions indicated in subsection 5.3.1, show that in this case the value of B_f is high. Accordingly a well-focussed signal can have a high value of B_f due to the absence of the trough, while the visual classification classifies this signal with a high value, because it breaks at the right place and there are no waves before or after the breaking wave.
  Another possible explanation for this discrepancy can be the subjectivity of the visual classification, as pointed out above. This can be a reason for a high visual classification while the parameter B_f classifies the control signal as reasonably- or even poorly-focussed.
- *A low value for the parameter B_f and a low value for the visual classification (the black circle)*
  This discrepancy can be due to the interval ($[-2T,t_p]$) used for the computation of B_f. Integration over this interval not only neglects the tail function but also the straggler waves, not belonging to the tail function. This in turn results in a low value for B_f, while it is actually not well-focussed. Conversely the visual classification classifies this signal with a low value due to the presence of those straggler waves.

Well-focussed	B_f	V	Reasonably-focussed	B_f	V	Not-focussed	B_f	V
Hedges + lagr corr + mass corr + $C_{g,d}$ *(chirp20c)*	0.48	10	Hedges + mass corr + $C_{g,i}$ *(chirp31)*	0.53	7	Hedges + 2nd order + mass corr + $C_{g,d}$ *(chirp32)*	0.69	*4*
K&D + lagr corr + mass corr + $C_{g,d}$ Discussion*(chirp22cdiscussion)*	0.51	8	K&D + lagr corr + mass corr + $C_{g,i}$ Firstapprox *(chirp22firstapprox)* Discussion *(chirp22discussion)*	0.53 0.57	6.5 7			
K&D + lagr corr + $C_{g,i}$ Petit *(chirp22d)* Firstapprox *(chirp22dfirstapprox)* Discussion*(chirp22ddiscussion)*	0.51 0.52 0.45	8 8 7	K&D + mass corr + $C_{g,i}$ Petit *(chirp36)* Firstapprox *(chirp36firstapprox)* Discussion *(chirp36discussion)*	0.53 0.54 0.55	7 5 7			
K&D + lagr corr + lin + $C_{g,d}$ Petit *(chirp22lin)* Firstapprox *(chirp22linfirstapprox)* Discussion (*chirp22lindiscussion)*	0.49 0.51 0.46	8 7 7	K&D + 2nd order + mass corr + $C_{g,d}$ Discussion *(chirp37discussion)*	0.58	7			
K&D + 2nd order + $C_{g,d}$ Petit *(chirp35)* Firstapprox *(Chirp35firstapprox)*	0.50 0.52	10 10	K&D + 2nd order + mass corr + $C_{g,i}$ Discussion *(chirp34discussion)*	0.59	7			
K&D + 2nd order + mass corr + $C_{g,i}$ Petit *(chirp34)* Firstapprox*(chirp 34firstapprox)*	0.52 0.51	8 8	Linear + mass corr + $C_{g,d}$ *(chirp40)*	0.52	7			
			Linear +mass corr + $C_{g,i}$ *(chirp41)*	0.52	7			
			Linear + lagr corr + mass corr + $C_{g,d}$ *(chirp42)*	0.52	7			
			Linear + lagr corr + mass corr + $C_{g,i}$ *(chirp43)*	0.56	7			
			Linear + $C_{g,i}$ *(chirp45)*	0.53	7			

Table 5-4 The control signals, where B_f and visual classification (V) have agreement about their quality.

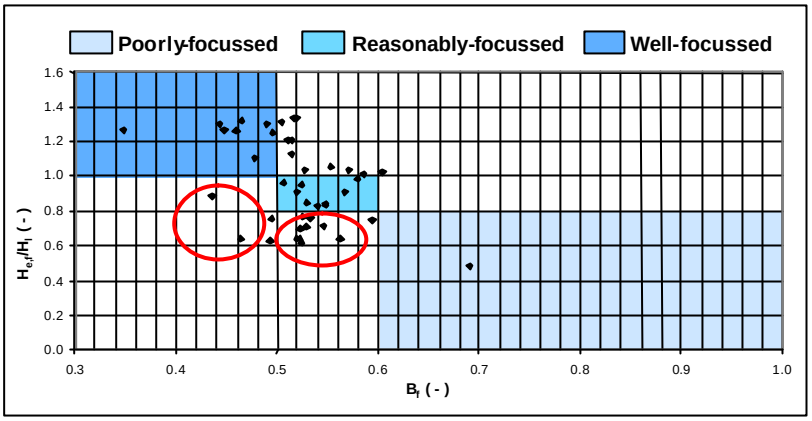

Fig 5-.16 Areas for poorly - reasonably- and well-focussed waves for B_f against the visual classification

A possible explanation for the discrepancy between B_f and $H_{e,f}/H_l$ is given below:

- *A low value for the parameter B_f and a low value for the parameter $H_{e,f}/H_l$ (the red circles)* Computing B_f over the interval ([-2T, t_p]) can results in a low value for B_f for a not well-focussed wave for the same reason as pointed out above. The presence of the straggler waves will also result in a lower experimental breaking wave height at the focus point, which in turn results in a low value of the parameter $H_{e,f}/H_l$.

Well-focussed	B_f	H	Reasonably-focussed	B_f	H	Not-focussed	B_f	H
Hedges + lagr corr + mass corr + $C_{g,d}$ *(chirp20c)*	0.48	1.11	K&D + lagr corr + mass corr + $C_{g,i}$			Hedges + 2nd order + mass corr + $C_{g,d}$		
			Firstapprox *(chirp22firstapprox)*	0.55	0.85	*(chirp32)*	0.69	0.59
			Discussion *(chirp22discussion)*	0.57	0.91			
Hedges + lagr corr + $C_{g,d}$ *(chirp23c)*	0.44	1.30	K&D + mass corr + $C_{g,i}$					
			Firstapprox *(chirp36firstapprox)*	0.54	0.83			
			Discussion *(chirp36discussion)*	0.55	0.84			
K&D + lagr corr + mass corr + $C_{g,d}$			K&D + 2nd order + mass corr + $C_{g,d}$					
Discussion *(chirp22cdiscussion)*	0.51	1.13	Petit *(chirp37)*	0.52	0.95			
			Firstapprox *(chirp37firstapprox)*	0.52	0.91			
			Discussion *(chirp37discussion)*	0.58	0.98			
K&D + lagr corr + $C_{g,d}$								
Petit *(chirp22d)*	0.51	1.21						
Firstapprox *(chirp22dfirstapprox)*	0.52	1.34						
Discussion *(chirp22ddiscussion)*	0.45	1.27						
K&D + lagr corr + mass corr + $C_{g,i}$								
(chirp22analy)	0.50	1.25						
K&D + lagr corr + $C_{g,d}$ + lin								
Petit *(chirp22lin)*	0.49	1.3						
Firstapprox *(chirp22linfirstapprox)*	0.51	1.21						
Discussion *(chirp22lindiscussion)*	0.46	1.26						
K&D + $C_{g,d}$ + 2nd order								
Petit *(chirp35)*	0.50	1.32						
Firstapprox *(Chirp35firstapprox)*	0.52	1.34						
Discussion *(Chirp35discussion)*	0.47	1.32						

Table 5-5 The control signals, where the two parameters B_f and $H_{e,f}/H_l$ (V) have agreement about their quality .

5.3.2 Selection of the overall best control signals.

The discussion above leads to the following conclusions re garding the best parameter as a predictor for the most effective control signal from the considered parameters. First, since B_f does not consider waves arriving too late at the focus point, it is only sensitive in cases where the short waves arrive too early at the focus point. Therefore the parameter B_f is rejected as a focussing parameter. On the other hand the parameter $H_{e,f}/H_I$ and the visual classification react to both late and early waves in a not well-focussed process. Cases for poorly-focussing are waves not belonging to the tail function, arrive too early or too late at the focus point, or the breaking wave does not occur at the focus point but before or after the focus point. These events result in a lower visual classification and a lower experimental breaking wave height at the focus point, which in turn results in a lower value of $H_{e,f}/H_I$. In this respect the parameter $H_{e,f}/H_I$ and the visual classification are accepted as predictors for the performance of a theory. But one should consider the fact that these parameters can in some cases give a wrong impression about the quality of focussing, as explained in subsection 5.3.1.

Therefore the overall best control signals are selected based on the parameter $H_{e,f}/H_I$ and the visual classification. For this reason figure 5-14 and table 5-3 are repeated:

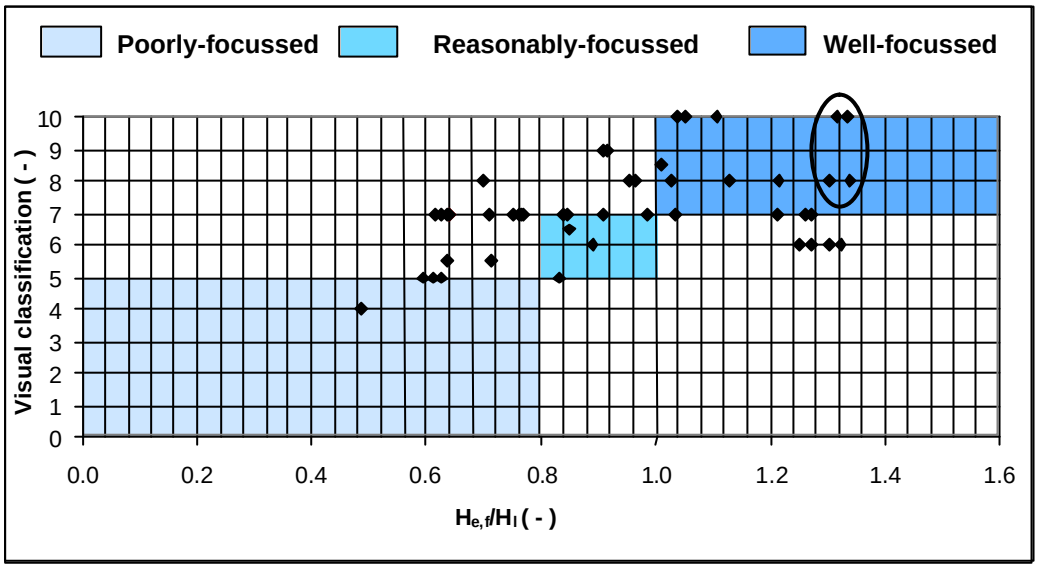

Fig 5-14 Areas for poorly- reasonably- and well-focussed waves for $H_{e,f}/H_I$ against the visual classification.

Well-focussed	H	V	Reasonably-focussed	H	V	Badlyfocussed	H	V
Hedges + lagr corr + mass corr + $C_{g,d}$ *(chirp20c)*	1.1	10	Hedges + lagr corr + $C_{g,d}$ + lin *(chirp23d)*	0.89	6	Hedges + 2nd order + mass corr + $C_{g,d}$ *(chirp32)*	0.49	4
K&D + lagr corr + mass corr + $C_{g,d}$			K&D + lagr corr + mass corr + $C_{g,i}$					
Petit *(chirp22c)*	1.05	10	Firstapprox *(chirp22firstapprox)*	0.85	65			
Firstapprox *(chirp22cfirstapprox)*	1.04	10	Discussion *(chirp22discussion)*	0.84	7			
Discussion *(chirp22cdiscussion)*	1.13	8						
K&D + lagr corr + $C_{g,d}$			K&D + 2nd order + mass corr + $C_{g,d}$					
Petit *(chirp22d)*	1.21	8	Discussion *(chirp37discussion)*	0.95	8			
Firstapprox *(chirp22dfirstapprox)*	1.34	8						
Discussion *(chirp22ddiscussion)*	1.27	7						
K&D + lagr corr + $C_{g,d}$ + lin			K&D + mass corr + $C_{g,i}$ l					
Petit *(chirp22lin)*	1.30	8	Firstapprox *(chirp36firstapprox)*	0.83	5			
Firstapprox *(chirp22linfirstapprox)*	1.21	7	Discussion *(chirp36discussion)*	0.84	5			
Discussion *(chirp22lindiscussion)*	1.26	7						
K&D + mass corr + $C_{g,d}$								
Petit *(chirp33)*	1.03	8						
Firstapprox *(chirp33firstapprox)*	1.01	8.5						
Discussion *(chirp33discussion)*	1.03	7						
K&D + $C_{g,d}$ + 2nd order								
Petit *(chirp35)*	1.32	10						
Firstapprox *(Chirp35firstapprox)*	1.34	10						

Table 5-3 The control signals, where $H_{e,f}/H_I$ (H) and visual classification (V) have agreement about their quality.

The overall best control signals can be found in the upper right corner of figure 5-14 indicated by the black circle. These control signals are classified by both parameters as a well-focussed wave signal.

Filename	Used theories	Control signal	$H_{e,f}/H_i$ (-)	Visual classification (-)
Chirp35firstapprox	K&D + no mass corr + 2nd order	fdmf3503	1.34	10
Chirp35	K&D + no mass corr + 2nd order	fdmt3503	1.32	10
Chirp22dfirstapprox	K&D + lagr corr + no mass corr	fdcn3503	1.34	8
Chirp22lin	K&D + lagr corr + no mass corr + lin	fdcl3503	1.30	8

Table 5-6 The overall best control signals.

5.4 Sensitivity of the focussed wave to the variation of the input variables.

To evaluate the influence of the input variables, some new experiments are carried out with different conditions, resulting in new control signals. In this section these experiments are analysed. These new experiments are carried out before the analysis of the experiments with the reference input variables and for this reason four software packages, which had proved by the visual classification to produce a well-focussed wave, are selected to create the new offline control signals. The chosen software packages are:

- *Chirp22firstapprox*
  Consists of:
  - The nonlinear dispersion relation of Kirby and Dalrymple (1986) (equation 2-22)
  - A Lagrangian correction (equations 3-6 – 3-9)
  - A mass correction (equations 3-10 – 3-13)
  - Calculation of the group velocity by $C_{g,i}$ (equation 2-24)
- *Chirp22dfirstapprox*
  Consists of:
  - The nonlinear dispersion relation of Kirby and Dalrymple (1986) (equation 2-22)
  - A Lagrangian correction (equations 3-6 – 3-9)
  - Calculation of the group velocity by $C_{g,d}$ (equation 2-25)
- *Chirp22ddiscussion*
  Consists of:
  - The nonlinear dispersion relation of Kirby and Dalrymple (1987) (equation 2-26)
  - A Lagrangian correction (equations 3-6 – 3-9)
  - Calculation of the group velocity by $C_{g,d}$ (equation 2-25)
- *Chirp23c*
  Consists of:
  - The nonlinear dispersion relation suggested by Hedges (equation 2-17)
  - A Lagrangian correction (equations 3-6 – 3-9)
  - Calculation of the group velocity by $C_{g,d}$ (equation 2-25)

In order to see the effect of the variation of the input variable, only one variable at a time was changed during each experiment. The red point in all the plots in this section represents the control signal with the reference input values. To evaluate the influence of the variables only the parameters $H_{e,f}/H_i$ and the visual classification are considered (explained in section 5.3) and the values for both are shown in the table 5-6 on the next page. Subsections 5.4.1 until 5.4.3 describe the variation and influence of the different input variables.

File name	Used theories	Control signal	Variation	R_{exp}/R_{lin} (-)	Visual classification (-)
Chirp22firstapprox	**K&D + lagr corr + mass corr +Cg,i**	**fdfa3503**	reference values	0.71	5.5
		fdfa5503	f_0 = 0.5 Hz	0.97	5
		fdfa1503	f_0 = 1 Hz	0.35	1
		fdfa1553	f_0 = 1.5Hz	0.51	1
		fdfa3203	r = 2 (-)	0.23	3
		fdfa3303	r = 3 (-)	0.52	6.5
		fdfa3603	r = 6 (-)	0.79	5.5
		fdfa1303	f_0 = 1 Hz ; r = 3	0.32	1
		fdfa5303	f_0 = 0.5Hz ; r = 3	0.96	5.5
		edfa3503	x = 20 m	0.74	
Chirp22dfirstapprox	**K&D + lagr corr + $C_{g,d}$**	**fdcn3503**	reference values	1.34	8
		fdcn1503	f_0 = 1 Hz	0.37	1
		fdcn1553	f_0 = 1.5Hz	0.30	1
		fdcn3203	r = 2 (-)	0.41	3
		fdcn3303	r = 3 (-)	1.11	9.5
		fdcn3603	r = 6 (-)	1.24	9
		fdcn1303	f_0 = 1 Hz ; r = 3	0.40	1
		fdcn5303	f_0 = 0.5Hz ; r = 3	1.31	9
		edcn3503	x = 20 m	1.00	7
Chirp23c	**Hedges + Lagr corr + $C_{g,d}$**	**fucc3503**	reference values	1.30	6
		fucc5503	f_0 = 0.5 Hz	0.54	6
		fucc1503	f_0 = 1 Hz	0.14	1
		fucc1553	f_0 = 1,5Hz	0.26	1
		fucc3303	r = 3 (-)	1.05	6.5
		fucc3603	r = 6 (-)	1.35	7
		fucc1303	f_0 = 1 Hz ; r = 3	0.86	1
		eucc3503	x = 20 m	1.05	7
Chirp22ddiscussion2	**K&D +lagr corr + $C_{g,d}$**	**fdns3503**	reference values	1.27	7
		fdns5503	f_0 = 0.5 Hz	0.54	6
		fdns3303	r = 3 (-)	1.11	9.5
		edns3503	x = 20 m	1.06	7

Table 5-7 Experiments carried out with variation of the variables and their values of the parameters.

5.4.1 The frequency-range ratio

The variation of the frequency-range ratio i.e. the ratio of the maximum frequency to the peak frequency (r) used in the experiments is:

$r = 6$

$r = 5$ (reference input value)

$r = 3$

$r = 2$

The values of the parameters $H_{e,f}/H_I$ and the visual classification of the experiments with this variation can be found in table 5-6 at the end of this section. These values are plotted against each other as shown in the figures 5-17 - 5-20.

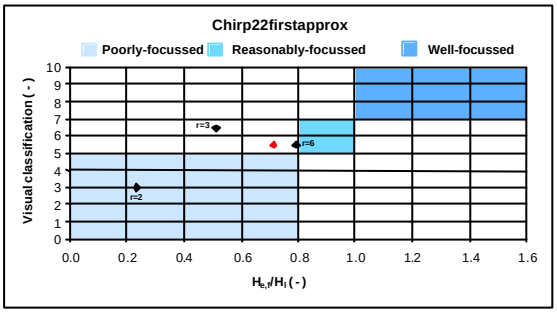

Fig. 5-17 $H_{e,f}/H_I$ plotted against the visual classification for the control signal Chirp22firstapprox with the frequency-range ratio variation.

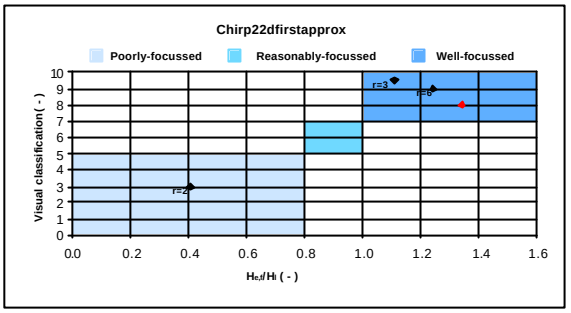

Fig. 5-18 $H_{e,f}/H_I$ plotted against the visual classification for the control signal Chirp22dfirstapprox with the frequency-range ratio variation.

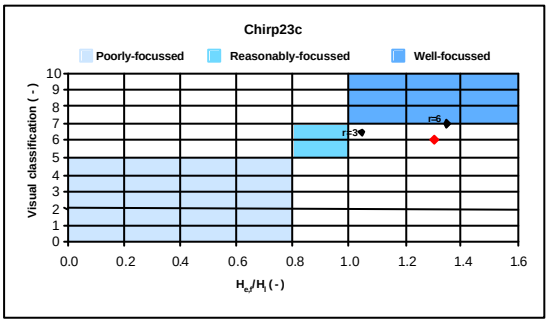

Fig. 5-19 $H_{e,f}/H_I$ plotted against the visual classification for the control signal Chirp23c with the frequency-range ratio variation.

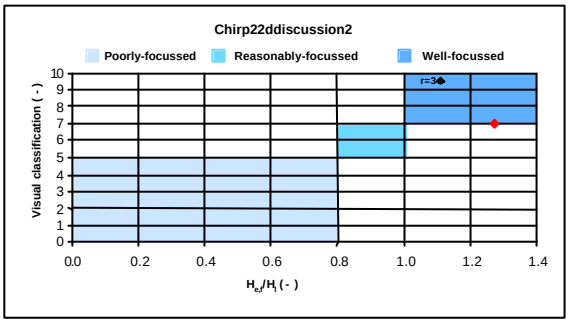

Fig. 5-20 $H_{e,f}/H_I$ plotted against the visual classification for the control signal Chirp22ddiscussion with the frequency-range ratio variation.

From the figures 5-17 – 5-20 it can be concluded that lowering the value of the ratio clearly results in a less-focussed signal. The distribution of the wave energy over the frequencies for a narrow banded signal (ratio equals 2) is apparently too low to result in a pronounced focussed wave. A broader banded spectrum generally leads to a better-focussed wave.

5.4.2 The peak frequency

The variation of the peak frequency used in the experiments is:

$f_0 = 0.3Hz$ (reference input)

$f_0 = 0.5Hz$

$f_0 = 1Hz$

$f_0 = 1.5Hz$

The values of the parameters $H_{e,f}/H_I$ and the visual classification of the experiments with this variation can be found in table 5-6 at the end of this section. These values are plotted against each other as shown in the figures 5-21 - 5-24.

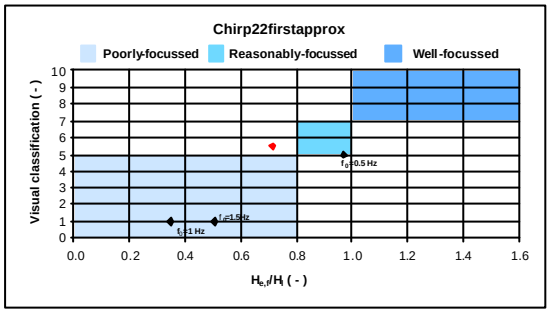

Fig. 5-21 $H_{e,f}/H_I$ plotted against the visual classification for the control signal Chirp22firstapprox with the peak frequency variation.

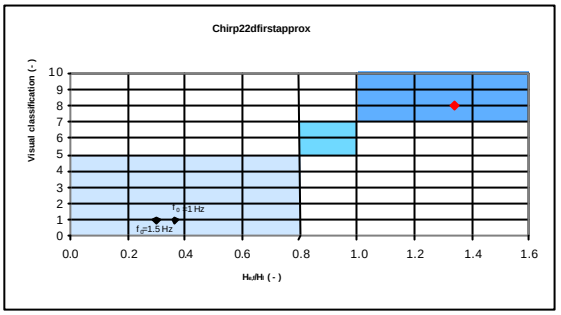

Fig.5-22 $H_{e,f}/H_I$ plotted against the visual classification for the control signal Chirp22dfirstapprox with the peak frequency variation.

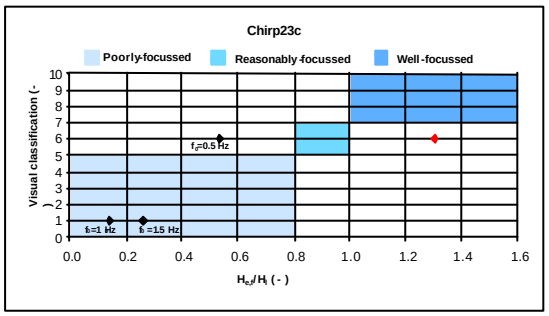

Fig.5-23 $H_{e,f}/H_I$ plotted against the visual classification for the control signal Chirp23 with the peak frequency variation.

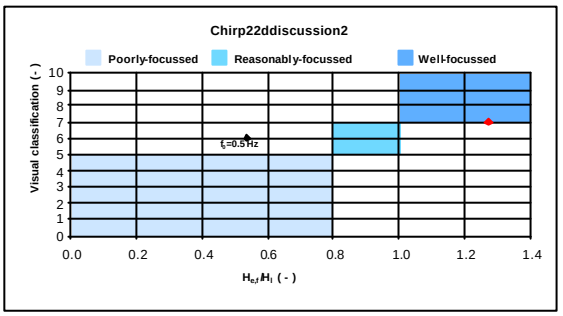

Fig. 5-24 $H_{e,f}/H_I$ plotted against the visual classification for the control signal Chirp22ddiscussion with the peak frequency variation

Figures 5-21 – 5-24 show that an increase of the peak frequency results in a less-focussed wave. This is contrary to the results of the variation of the focus distance. A possible explanation for this result for the high frequencies f_0=1 Hz and f_0=1.5 Hz can be that the focus point is very far from the wave maker in terms of the number of wave lengths and diffraction effects which are not included in the considered theories may become important. But an explanation for the result with a frequency of 0.5 Hz can not be found and further investigation is recommended.

5.4.3 The focus distance

The variation of the peak frequency used in the experiments is:

$x_{focus} = 25m$ (reference input)

$x_{focus} = 20\,m$

The values of the parameters $H_{e,f}/H_I$ and the visual classification belonging to the experiments with this variation can be found in table 5-6 at the end of this section. These values are plotted against each other shown in the figures 5-25 – 5-28.

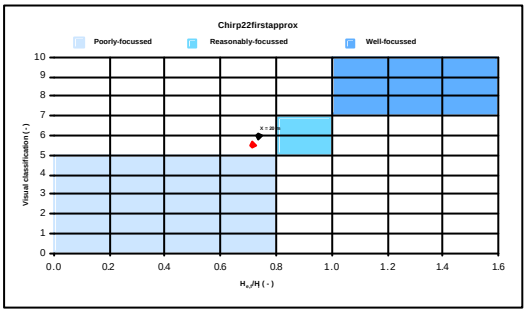

Fig. 5-25 $H_{e,f}/H_I$ plotted against the visual classification for the control signal Chirp22firstapprox with focus distance variation.

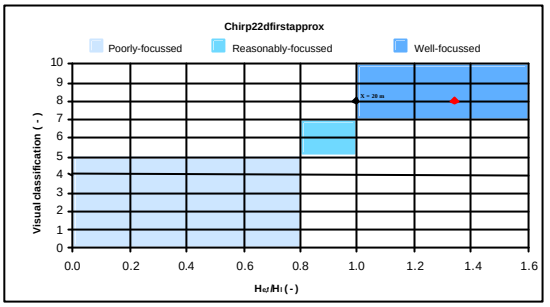

Fig. 5-26 $H_{e,f}/H_I$ plotted against the visual classification for the control signal Chirp22dfirstapprox with the focus distance variation.

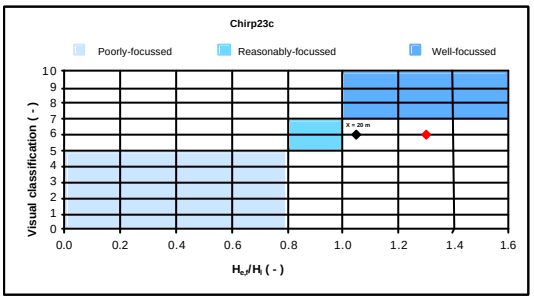

Fig. 5-27 $H_{e,f}/H_I$ plotted against the visual classification for the control signal Chirp23c with focus distance variation.

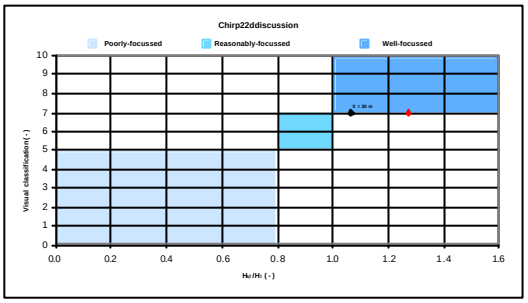

Fig. 5-28 $H_{e,f}/H_I$ plotted against the visual classification for the control signal Chirp22ddiscussion with focus distance variation.

From the figures 5-25 – 5-28 it can be concluded that a decrease of the focus distance results in a less-focussed wave. A longer focus distance implies a longer duration of the control signal and the non-linear effects in the wave dispersion are more important for a longer duration.

5.5 Discussion and conclusions

Conclusions with respect to the results of the experiments with the reference input values (figure 5-14 and the tables 5-2 and 5-5) are:

- *About the used dispersion relationships.*

– From all the used dispersion relations, the nonlinear dispersion relationship of Kirby and Dalrymple (1986) (equation 2-17) and as implemented by Petit (equation 2-21) prove to be the most effective for the modulation of the wave focussing signal.

– The dispersion relation of Kirby and Dalrymple (1986) (equation 2-17) and as implemented by Petit (equation 2-21) turn out to have almost the same results (see table 5-1). The distinction between those relationships is only the definition of the used 3rd order Stokes parameter D (equations 2-11 and 2-21). The definition of the parameter D in equation 2-11 includes the mass correction (see Dingemans, 1997, page 340 equation 3.2.7.7) and equation 2-21 does not include the mass correction (see Dingemans, 1997, page 180 equation 2.4.3.3c). Apparently this correction in the dispersion relationship does not result in an appreciable difference.

– Contrary to the expectations the results show that the new dispersion relation of Kirby and Dalrymple (1987) (equation 2-20) is less effective than the other dispersion relationship of Kirby and Dalrymple (1986) and as implemented by Petit. This is contrary to the expectations, because it is a correction on the previous relationships (see Kirby and Dalrymple,1987).

– The use of the linear dispersion relation (Chirp 40 till Chirp 45) resulted in wave focussing signals that were classified as reasonably- or not-focussed, as expected because of neglecting the effect of nonlinearity on the wave propagation characteristics.

– It turns out that the nonlinear dispersion relationship suggested by Hedges (equation 2-13) is less effective for the modulation of the wave focussing signal than the nonlinear dispersion relationships of Kirby and Dalrymple. To find the relative difference of the two approaches, a "relative focus-mismatch parameter" is developed:

$$t_{t,b} = \frac{x_{fs}}{C_{g,f}} \tag{5-17}$$

$$t_{t,e} = \frac{x_f}{C_{g,l}} \tag{5-18}$$

$$\Delta t_t = x_f \left(\frac{1}{C_{g,f}} - \frac{1}{C_{g,l}} \right) \tag{5-19}$$

$$dt_t = \Delta t_{t,Hedges} - \Delta t_{t,K\&D} \tag{5-20}$$

Relative focus-mismatch parameter = $f_0 * dt_t$ (-) (5-21)

where:

f_0 = Peak frequency (Hz)

$C_{g,l}$ = Group velocity of the last wave, not belonging to the tail function (m/s)

$C_{g,f}$ = Group velocity of the first wave, not belonging to the slow start function (m/s).

$t_{t,b}$ = Travelling time of the first wave from the wave board (x = 0m) to the theoretical focus point (s).

$t_{t,e}$ = Travelling time of the last wave from the wave board (x = 0m) to the theoretical focus point (s).

Δt_t = Difference between the travelling time of the first and last wave to the theoretical focus point (s).

dt_t = Difference between Δt_t using the dispersion relation of Hedges and the dispersion relation of Kirby and Dalrymple (s).

With this relative focus-mismatch parameter the dispersion relationships of Hedges and Kirby and Dalrymple can be compared. One comparison is shown below (with intermediate steps):

Chirp 33 (Kirby and Dalrymple)	*Chirp19c (Hedges)*
$C_{g,l}$ = 2.12 m/s	$C_{g,l}$ = 2.17 m/s
$C_{g,f}$ = 0.53 m/s	$C_{g,f}$ = 0.53 m/s
$t_{t,b}$ = 47.51 s	$t_{t,b}$ = 47.51 s
$t_{t,e}$ = 11.80 s	$t_{t,e}$ = 11.54 s
Δt_t = 35.71 s	Δt_t = 35.97 s
dt_t **= 35.97 s – 35.71 s = 0.26 s** Þ	$f_0 * dt_t$ **= 0.3 Hz * 0.26 s = 0.08 (-)**

The results of other comparisons are shown in table 5-8:

	Relative-mismatch parameter (-)
Chirp22c (K&D + lagr corr + mass corr + $C_{g,d}$) Chirp20c (Hedges + lagr corr + mass corr + $C_{g,d}$)	0.08
Chirp22d (K&D + lagr corr + $C_{g,d}$) Chirp23c (Hedges + lagr corr + $C_{g,d}$)	0.08
Chirp22analy (K&D + lagr corr + mass corr + $C_{g,i}$) Chirp24c (Hedges + lagr corr + mass corr + $C_{g,i}$)	-0.04
Chirp35 (K&D + + $C_{g,d}$ + 2nd order) Chirp38 (Hedges + + $C_{g,d}$ + 2nd order)	0.08
Chirp34 (K&D + + $C_{g,i}$ + 2nd order + mass corr) Chirp29 (Hedges + + $C_{g,i}$ + 2nd order + mass corr)	-0.04
Chirp36 (K&D + mass corr+ $C_{g,i}$) Chirp31 (Hedges + mass corr + $C_{g,i}$)	-0.04

Table 5.8 The relative mismatch parameter for comparing the two dispersion relationships (Kirby and Dalrymple and Hedges)

In combination with the analysis of the results of the experiments, it can be concluded that the nonlinear relationship of Hedges is less effective for the modulation of the wave focussing signal than the nonlinear dispersion relationships of Kirby and Dalrymple

- *About adding nonlinear correction to the dispersion relation*

– A correction due to the mass transport velocity (equation 3-13) does not improve the wave focussing signal, as opposed to the expectations.

- *About the use of the nonlinear wave maker theory*

– The Lagrangian correction to the wave maker signal proved to be more effective than linear wave maker theory, but still less effective than the use of second-order wave maker theory. This is as expected, because the wave motion is less nonlinear in a Lagrangian frame of reference than in a Eulerian frame of reference (see 3.3.1).

– Second-order wave maker theory proved to be the most effective focussing method. This is as expected, because of the theoretically improved accuracy of the second-order wave maker theory with respect to first-order wave maker theory, as described in section 3.3.

- *About the computation of group velocity*
  As expected, the basic nonlinear group velocity ($C_{g,I}$, equation 2-24) is less effective for generating a focussed wave than the second definition of the calculation of the group velocity ($C_{g,d}$, equation 2-25) because in this research the amplitude is not chosen independently but as a function of the wave number.

The experiments with the variation of the input variables clearly show that this variation has an effect on the focussing process. The general conclusions from the experiments with variation of the variables are:

- Decreasing the value of the frequency-range ratio results in a less focussed signal.
- Increasing the value of the peak frequency results in a less focussed signal.
- Decreasing the distance to the focus point results in a less focussed signal.

To find the minimum and maximum values of the variables that still create a well-focussed wave, further research is needed. Also the influence of the water depth requires further investigation.

Observations in the laboratory flume

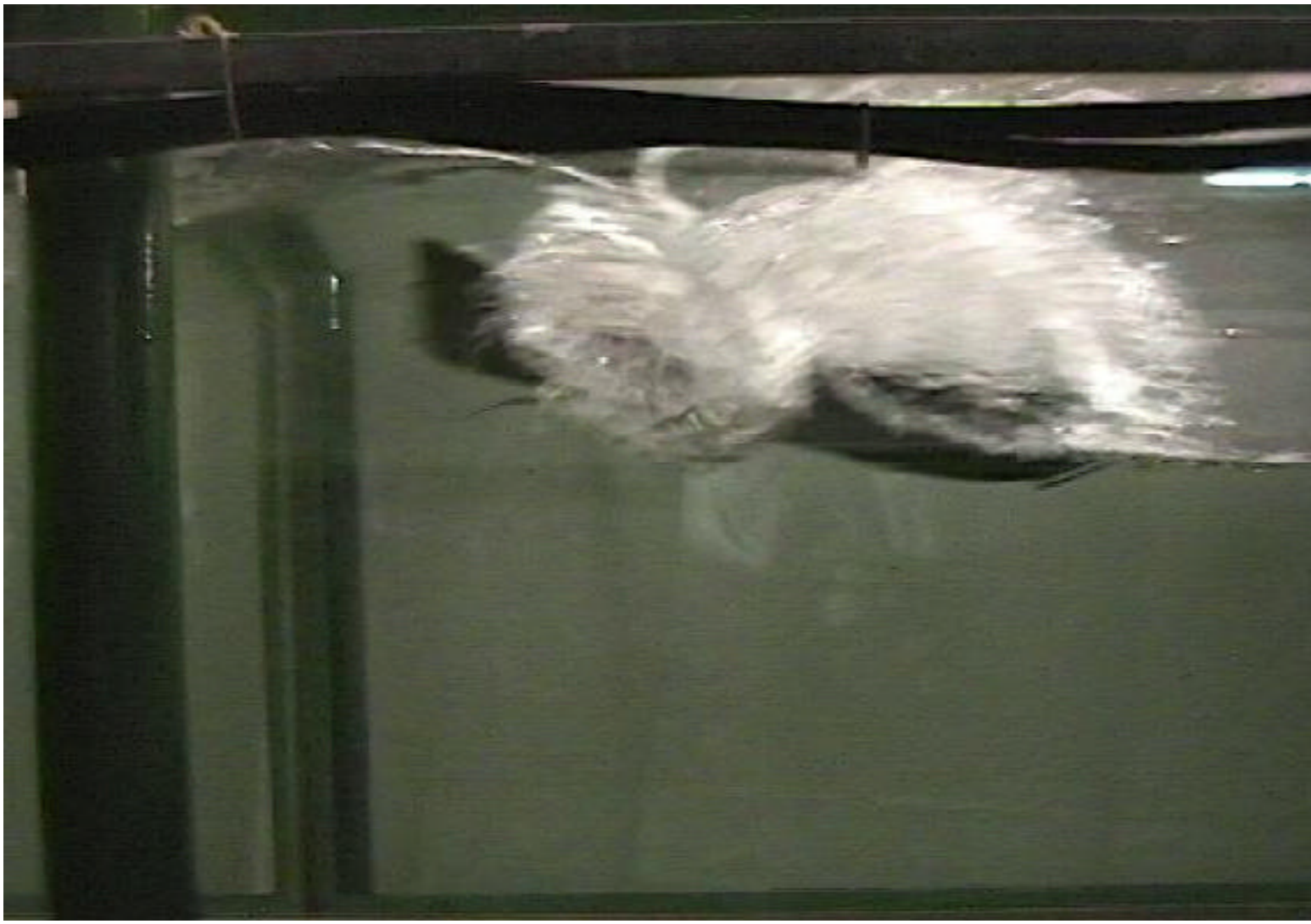

6 Observations in the laboratory flume

6.1 Introduction

Film and photo material is generated about almost all the experiments carried out in this research. This material can be used for a better visualisation of the development of the focussing process and can be found on the CD and the converted pictures can all be found in the appendix-report. In chapter 5 the developed software packages are analysed and verified by using the experiments with the control signals that are the output of the software packages. This analysis resulted in the best four software packages for generating a focussed wave in laboratory flume (see table 5-5). The photographs of the two best control signals are shown in the figures 6-1 and 6-2 on the next two pages. Another figure is shown in figure 6-3 which corresponds with an improved control signal due to another input variable.

After the experiments, which are carried out to assess the control signals, other experiments are carried out to establish the impact of the generated focussed wave, which are treated and discussed in the remainder of this chapter. In reality these waves cause troubles mainly to ships and offshore structures, therefore the experiments are carried out with similar constructions. The scientific analysis of these experiments is outside the scope of this research and for that reason these experiments where only carried out for a visual judgement. In section 6.2 the experiments with a ship placed in the flume are described. The experiments with a wall placed in the flume are treated in section 6.3.

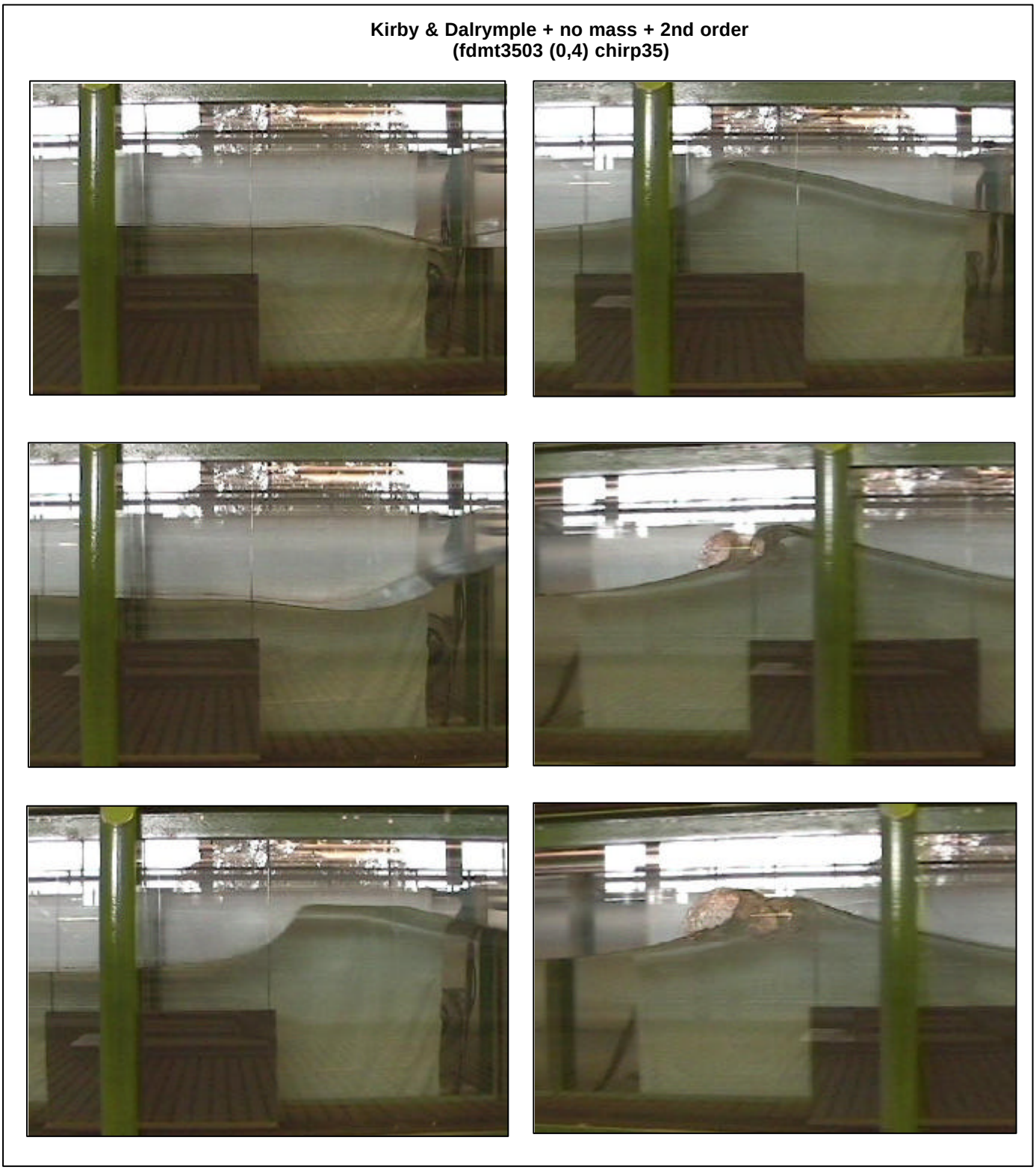

Fig.6-1 The photographs of the experimental results of the control signal Chirp35 (with the reference input variables).

Kirby & Dalrymple + no mass + 2nu order
(fdmf3503 (0,4) chirp35firstapprx)

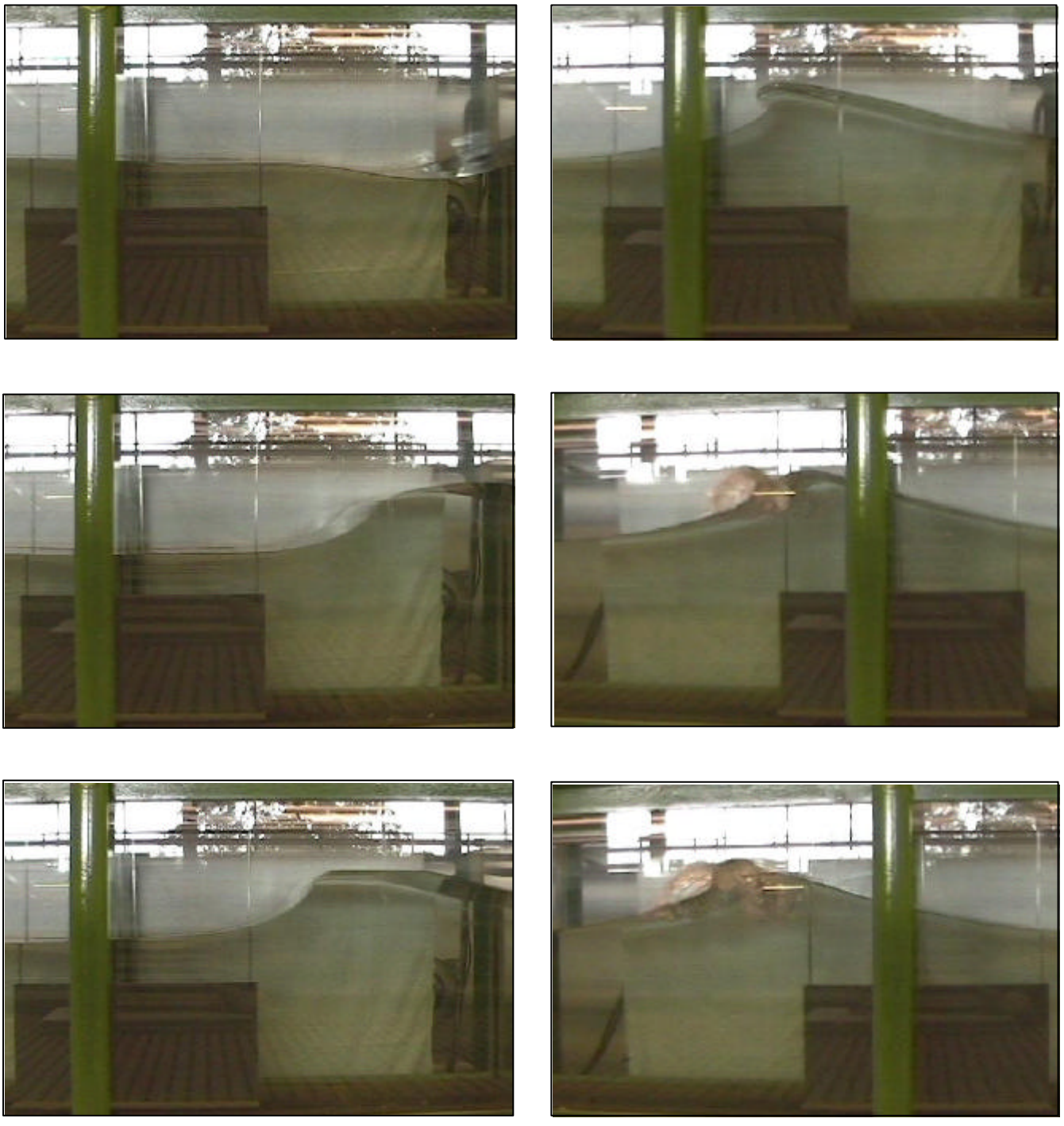

Fig. 6-2 The photographs of the experimental results of the control signalChirp35firstapprox (with the reference input variables).

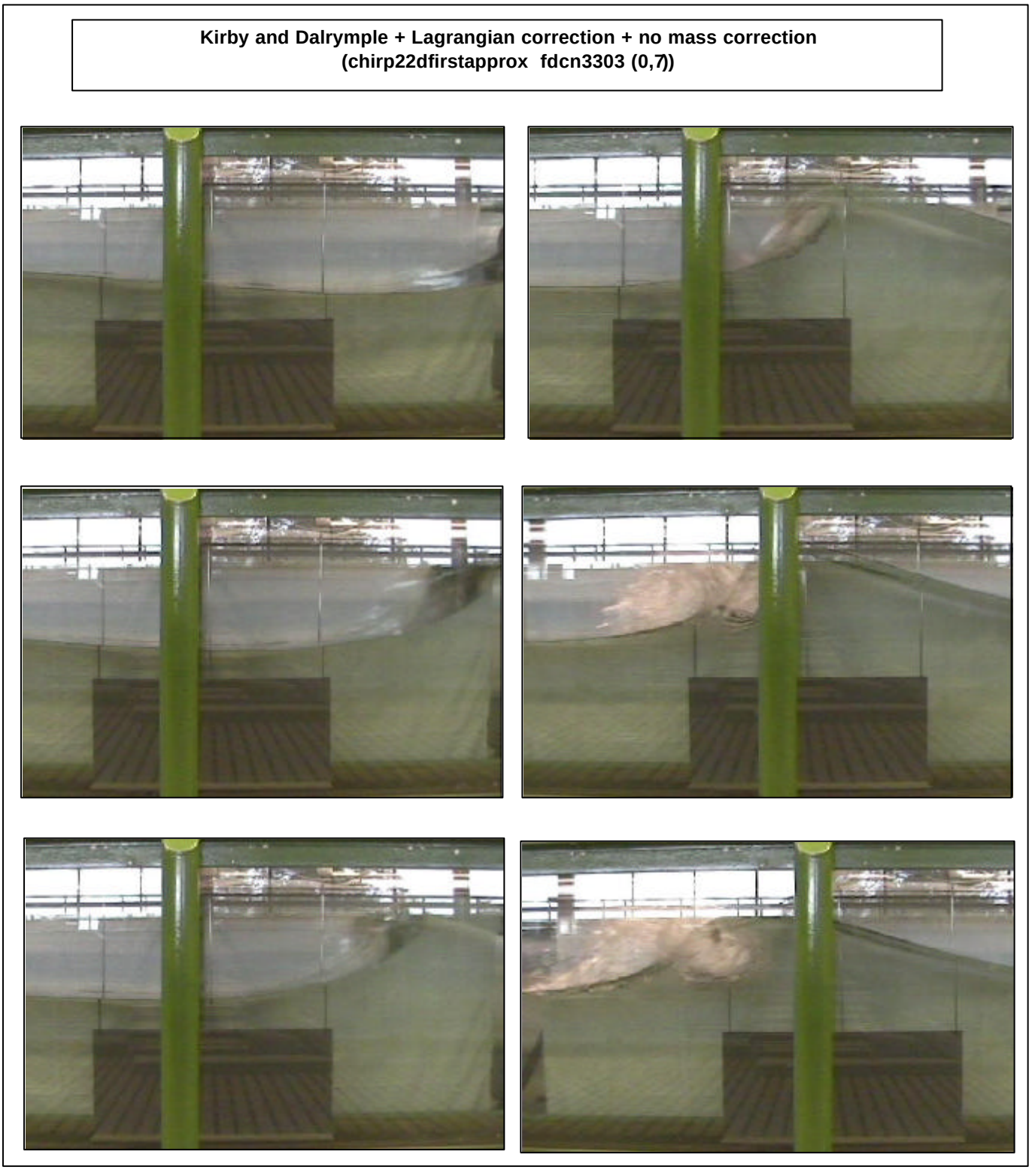

Fig. 6-3 A well wave focussing signal in the wave flume at the theoretical focus point of 25 m

6.2 Experiments with a ship

To establish the impact on a ship placed in the flume at the theoretical focus point several experiments are carried out with a scaled ship. These experiments are executed with a control signal, which had proved that it generated a well-focussed wave. Figure 6-4 shows a picture of the used ship. Its dimensions are:

Length = 75 cm
Width = 25 cm
Height = 15 cm

Fig 6-4 The ship used in the experiments

Eyewitness reports of "freak" waves occurring in nature pointed out that such waves appear "to come out of nothing and occur very fast", so there is not enough time to change the direction of the ship. In order to visualise the possible effects in nature experiments are conducted with the ship placed in two different ways as in a beam sea and a head sea. It appears that the direction of the ship in respect to the focussed wave has a considerable influence on the behaviour of the ship when the focussed wave passes. Placing the ship transversely to the waves caused the ship to sink in almost all the experiments. When the ship is placed in a longitudinal direction to the waves it either sinks rapidly or it is very fast transported in the propagation direction of the waves. Two video records of those experiments are stored on the CD. Figure 6-5 shows one result of the experiment with the ship placed in a longitudinal direction to the waves.

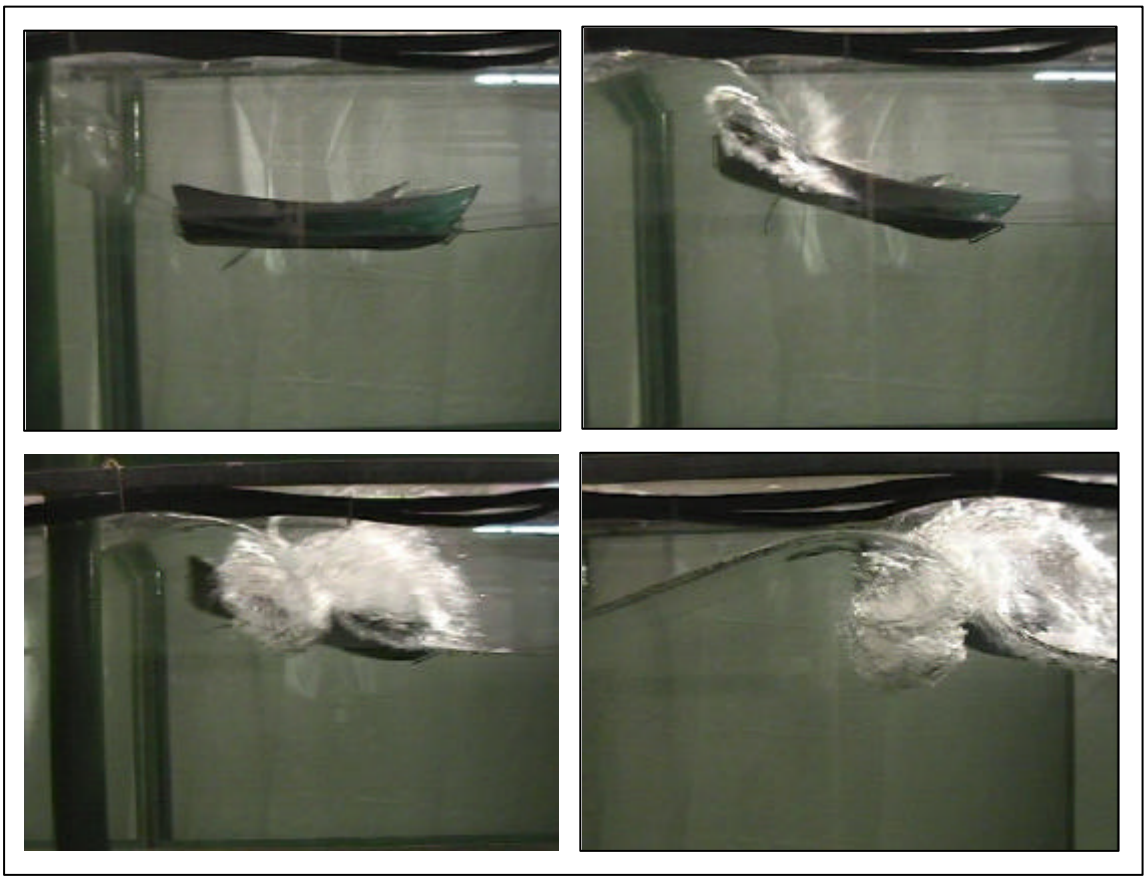

6.3 Experiments with a vertical wall

To establish the impact on an offshore structure a vertical wall is placed in the flume at the theoretical focus point and several experiments are carried out with this wall. These experiments are carried out with the same control signal as used in the experiments with the ship. Figure 6-6 and 6-7 show the side- and front view of the wall in the flume. The wall is made of wood. Its lower edge is placed 0.04 m above the still water level. The width is 0.8 m (the same as the width of the flume). The wall is fixed to the flume with four handscrews (placed at the black circles in figure 6-7) and therefore it could easily be moved to another point.

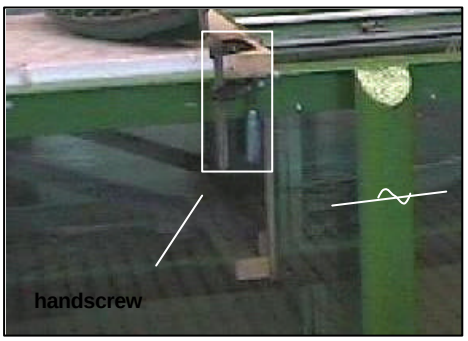

Fig 6-6 Side view of the wall in the flume

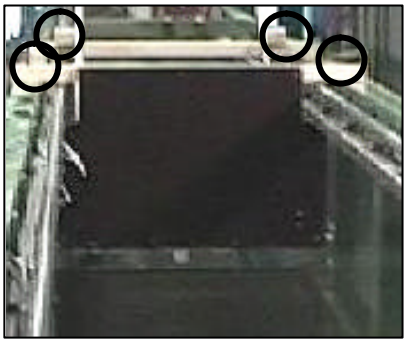

Fig 6-7 Front view of the wall in the flume

Experiments with the wall placed at the theoretical focus point show that when the wave focussing signal reaches the wall a big bang could be heard and the breaking wave came out of the flume. In some experiments the splash reached 2 meter above the flume. Standing next to the flume it looked like the impact of the wave is huge and probably could have caused a lot of damage to a structure. But the wall in the experimental setting is mounted is such a way that it is very stiff. Consequently no movement or damage of the wall could be noted, when it is hit by the wave. In reality the offshore structures will not be as stiff as the wall in the flume. So to see the effect on an offshore structures, it is advisable for future research to use a scaled construction that has is dynamically similar to a real offshore structure. But again these conclusions are based on visual judgement only and have to be investigated further. A video record and pictures of those experiments are stored on the CD. Figure 6-8 on shows a result of such an experiment.

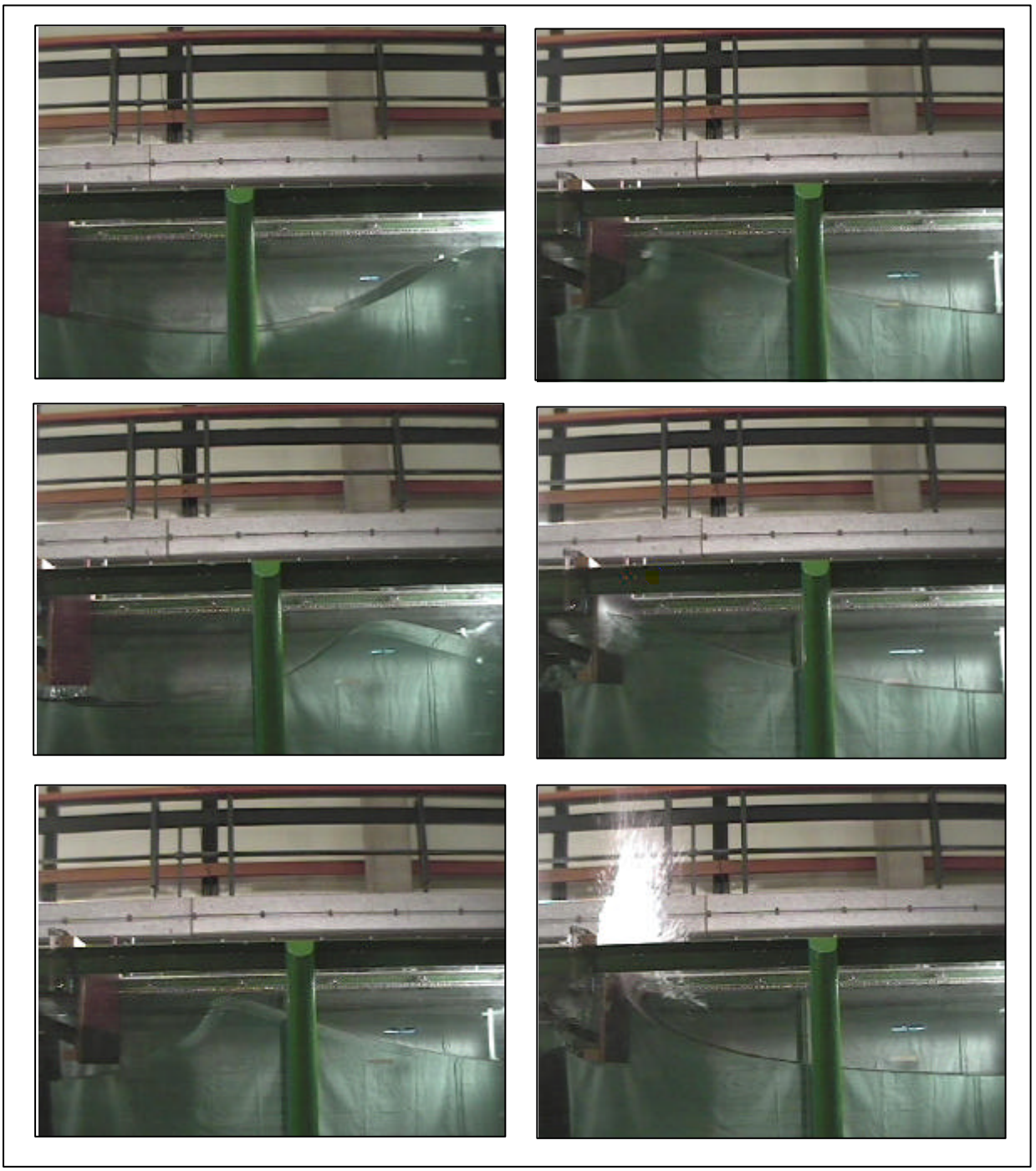

Fig 6-8 The impact on a wall in the wave flume, placed transversely in the theoretical focus point

Conclusions and Recommendations

7 Conclusions and recommendations

This chapter presents the conclusions (section 7.1) of this research and the recommendations for further research (section 7.2).

7.1 Conclusions

This research succeeded in developing several user friendly software packages, which can be used to generate well-focussed waves in a laboratory flume with a piston wave board. The following conclusions could be drawn for the theories that were used to develop these software packages:

- The linear theory is not sufficient to generate an adequate focussed wave.
- The second-order wave maker theory is the most effective way to generate a wave focussing signal.
- The nonlinear correction due to the mass transport velocity does not improve the wave focussing signal.
- The nonlinear Lagrangian correction does improve the wave focussing signal. But this correction is still less than generating the wave focussing signal with the second-order wave maker theory.
- A mass correction to the parameter D_p does not result in an appreciable difference compared with the definition of the parameter D without this correction.
- The use of the two nonlinear dispersion relations developed by Kirby and Dalrymple (1986) and as implemented by Petit are most effective to generate a good wave focussing signal compared with the other dispersion relations that were used.
- The calculation of the group velocity whereby the amplitude is dependent on k ($C_{g,d}$) results, compared with $C_{g,l}$, in an improved wave focussing signal.
- Applying the theory of generating the wave motion at the surface due to initial surface disturbances in the form of initial local elevation or to a local impulse at a point on the free surface developed by Cauchy-Poisson, did not lead to a focussed wave.

The variation of the input variables shows an influence on the resulting wave focussing signal. The following conclusions about the variation of the input variables can be drawn:

- Increasing the value of the frequency-range ratio results in a improved focussed wave
- Decreasing the value of the peak frequency results in a improved focussed wave
- Increasing the distance to the focus point results in a improved focussed wave

The conclusions about the experiments carried out to see the effect of the impact of a focussed wave on a ship or a wall are.

- The direction of the ship with respect to the focussed wave has a considerable influence on the behaviour of the ship when the focussed wave passes.
- When the ship is placed in a longitudinal direction to the waves it either sinks rapidly or it is transported very fast in the propagation direction of the waves.
- Placing the ship transversely to the waves caused the ship to sink in all the experiments.

- The impact on the wall was considerable but impossible to estimate because of the stiffness of the used wall (no movement or damage could be observed).

7.2 Recommendations

Recommendations with respect to the content

- A further investigation about the variation of the variables (the limitations etc.).

- A further investigation about the impact of the focussed waves on ships and offshore structures. Thereby carry out an analysis of the impact and drawn conclusions about the present designs of the ships or offshore structures (do those designs have to be improved etc.).

Recommendations with respect to the experiments

- Care has to be taken of the time between the start of the wave height measurement (in DASYLAB) and the start of the signal (in the control application). Because of the distance between the two measurement tools, it was not possible to start them simultaneous, this makes it very difficult to filter the experimental data to distinguish the focus time.

- It is advised to measure the surface elevation at the wave board, then the theoretical focus time can be determined (see the first recommendation).

- As described in section 3.1 two ways to create the offline control signal have been considered in this research. The first approach i.e. the construction of a control signal using MATLAB, by computing the required wave board motion as a function of time directly, is used. In the future it is more suitable to use the second approach instead, because there is a safety programmed in the Delft-Auke program. This safety looks after the in- and output values and will not accept values, which can not be carried out by the wave board. When using the first approach the user always has to check if the output commands can be carried out by the wave board (does the wave board position lie between the interval [–1m,1m]). The software packages do not verify these values, but they give a plot of the wave board motion as a function of time. The user has to check this plot to see if this motion does not exceed the interval. Exceeding this interval can result in damage to the wave board or the wave board could get stuck.

- To get a better view of the development of the wave focussing signal, it is recommended to use more wave gauges.

8 References

Baldock, T.E., Swan, C., and Taylor, P.H., "*A Laboratory Study of Nonlinear Surface-Waves on Water*," (1995).

Battjes, J.A. *" Korte Golven".* Faculteit Civiele Techniek en Geowetenschappen, Waterbouwkunde, Sectie vloeistofmechanica (August, 1999).

Brillouin.L.*" Wave Propagation and Group Velocity"*. Pure and Applied Physics-Volume 8. Academic Press, New York and London (1960)

Chaplin, J.R., Rainey, R.C.T., and Yemm, R.W., "*Ringing of a Vertical Cylinder in Waves*". Journal of Fluid Mechanics., Volume 350, p119-147 (May, 1997).

Chaplin,J.R. "*On Frequency-Focusing Unidirectional Waves*". International Journal of Offshore and Polar Engineering-Volume 6,No.2, p131-137 (June, 1996).

Clauss, G.F., "*Synthesis of Deterministic Rogue Waves in Extreme Seas*". Design and Operation for Abnormal Conditions II, 6./7. (November, 2001).

Day, R.A., *" How to Write & Publish a Scientific Paper"* , third edition (1989).

Dean, R.G., and Dalrymple, R.A., *"Water Wave Mechanics for Engineers and Scientists*". Advanced series on Ocean Engineering, Volume 2 (1991).

Dingemans, M.W. *"Water Wave Propagation over Uneven Bottoms".* Advanced Series on Ocean Engineering (part one), Volume13 (1997)

Galvin, C.J. *"Wave-Height Prediction for Wave Generators in Shallow Water"*. Tech. Memo 4, U.S. Army, Coastal Engineering Research Center, (Mar., 1964)

Götschenberg, A., and Daemrich,K.F., *"2nd Order Wave Generation and Application to Shoaling Investigations".* Proc. 22nd Int. Conf. Coastal Eng., Delft (1990)

Hedges, T.S., "*An empirical modification to linear wave theory*". Proc. Inst. Civ. Eng. (1976)

Hoffmann,R., " *Wave Generator Control (Userguide)*". WL | Delft Hydraulics (feb, 2002)

Huang, C., Zhang, E., and Lee, J., "*Numerical Simulation of Nonlinear Viscous Wavefields Generated by Piston-type Wavemaker*". Journal of engineering Mechanics-Volume 124, No. 10 p1110-1120 (October, 1998).

Johannessen,T.B., Swan, C. "*A Laboratory Study of the Focusing of Transient and Directionally Spread Surface Water Waves*" . Proceeding Royal Society, p971-1006 (2001).

Kirby, J.T., and Dalrymple, R.A., "*An Approximate Model for Nonlinear Dispersion in Monochromatic Wave Propagation Models*". Coastal Engineering, Volume 9, p545-561 (1986).

Kirby, J.T., and Dalrymple, R.A., "*An Approximate Model for Nonlinear Dispersion in Monochromatic Wave Propagation Models, Discussion*". Coastal Engineering, Volume 11, p87-92 (1987).

Klopman, G., *"Second-order wave generation".* Delft hydraulics (Feb,1996)

Klopman, G., "*On the relationship between a chirp times-series and its power spectrum*". Netherlands Centre for Coastal Research (NCK) Delft University of Technology Faculty of Civil Engineering and Geosciences Fluid Mechanics Section Delft (March, 2002).

Klopman, G., *"A non- linear Lagrangian correction to a wavemaker control signal according to linear wave theory"*. Netherlands Centre for Coastal Research (NCK) Delft University of Technology Faculty of Civil Engineering and Geosciences Fluid Mechanics Section Delft (May, 2002).

Klopman,G., and Van Leeuwen,P.J., *"An Efficient Method for the Reproduction of Non-Linear Random Waves"*. Coastal Engineering (1990)

Lamb,H., *"Hydrodynamics".* Cambridge University Press (6th Edition), Paragraph 238, p.384, (1932)

Longuet-Higgens, M.S., "*Breaking Waves in Deep or Shallow Water*". Proceeding 10th Conference on Naval Hydrodynamics, p597-605 (1974)

McKie, R., Townsend, M. *"Ships face peril of killer waves on the high seas"*. Guardian Weekly, p21 (November, 2002)

Mei,C.K., "*The Applied Dynamics of Ocean Surface Waves*". Advanced series on Ocean Engineering, Volume 2 (1983).

Olagon, M., Athanassoulis, G., *"Rogue waves 2000",* infremer nov 2000

Onorato, M., Osborne, A.R., Serio, M., and Bertone S., *"Freak Waves in Random Oceanic Sea States"*. Physical Review Letters, Volume 86, No. 25, p5831-5834 (June, 2001).

Pelinovsky, E., Kharif, C., Talipova, T., and Slunyaev, A., *"Nonlinear Wave Focusing as a Mechanism of the Freak Wave Generation in the Ocean"*. Rogue Waves

Tucker, M.J. *"Waves in Ocean Engineering"* (1991).

Van Dongeren, A., Klopman, G., Reniers, A., and Petit, H., *"High-quality laboratory wave generation for flumes and basins"*. Ocean wave Measurement and analysis, Volume 2, p1190-1199 (2001).

Van Leeuwen, P.J., and Klopman, G., *" A new method for the generation of second order random waves".* Ocean Engineering, Volume 23, No. 2, p167-192, (1996).

WL | Delft Hydraulics. *"Wave Board Computation Software Manual (Delft-Auke/Generate)*". (Nov, 2001).

Appendixes

Appendix A: The software packages and the corresponding combinations of theories
Appendix B: On the relationship between a chirp time-series and its power spectrum
Appendix C: A nonlinear Lagrangian correction to a wave maker control signal according to linear theory
Appendix D: Cauchy-Poisson method
Appendix E: Derivation of the equation for the wave board motion
Appendix F: User manual
Appendix G: Names of the control signals including the used software packages and the input variables
Appendix H: Software package (the code)
Appendix I: Classification of the control signals by words
Appendix J: Data acquisition
Appendix K: Implementation of the theories
Appendix L: Contents CD

Appendixes

Appendix A: The software packages and the corresponding combinations of theories
Appendix B: On the relationship between a chirp time-series and its power spectrum
Appendix C: A nonlinear Lagrangian correction to a wave maker control signal according to linear theory
Appendix D: Cauchy-Poisson method
Appendix E: Derivation of the equation for the wave board motion
Appendix F: User manual
Appendix G: Names of the control signals including the used software packages and the input variables
Appendix H: Software package (the code)
Appendix I: Classification of the control signals by words
Appendix J: Data acquisition
Appendix K: Implementation of the theories
Appendix L: Contents CD

Appendix A

The software packages and the corresponding combination of theories

Name software package	Dispersion Relation					Lagrangian correction	Mass correction	$C_{g,d}$	$C_{g,i}$	second-order
	Hedges	Kirby and Dalrymple			Linear					
		Petit	First approximate	Discussion						
Chirp19c	X						X	X		
Chirp20c	X					X	X	X		
Chirp22c		X				X	X	X		
Chirp22cfirstapprox			X			X	X	X		
Chirp22cdiscussion2				X		X	X	X		
Chirp22d		X				X		X		
Chirp22dfirstapprox			X			X		X		
Chirp22ddiscussion2				X		X		X		
Chirp22anly		X				X	X		X	
Chirp22firstapprox			X			X			X	
Chirp22firstapproxumass			X			X	X		X	
Chirp22discussion2				X		X			X	
Chirp22discussion2umass				X		X	X		X	
Chirp22lin		X				X	X	X		
Chirp22linfirstapprox			X			X	X	X		
Chirp22lindiscussion2				X		X	X	X		
Chirp23c	X					X		X		
Chirp23d	X					X		X		
Chirp24c	X					X	X		X	
Chirp29/0	X						X		X	X
Chirp31	X						X		X	
Chirp32/0	X						X	X		X
Chirp33		X					X	X		
Chirp33firstapprox			X				X	X		
Chirp33discussion2				X			X	X		
Chirp34/0		X					X		X	X
Chirp34/0firstapprox			X				X		X	X
Chirp34/0discussion2				X			X		X	X
Chirp35/0		X						X		X
Chirp35/0firstapprox			X					X		X
Chirp35/0discussion2				X				X		X
Chirp36		X					X		X	
Chirp36firstapprox			X				X		X	
Chirp36discussion2				X			X		X	
Chirp37/0		X					X	X		X
Chirp37/0firstapprox			X				X	X		X
Chirp37/0discussion				X			X	X		X
Chirp38/0	X							X		X
Chirp40					X		X	X		
Chirp41					X		X		X	
Chirp42					X	X	X	X		
Chirp43					X	X	X		X	
Chirp44					X	X		X		
Chirp45					X			X		

Appendix B:

On the relationship between a chirp time-series and its power spectrum

Gert Klopman

Netherlands Centre for Coastal Research (NCK)
Delft University of Technology
Faculty of Civil Engineering and Geosciences
Fluid Mechanics Section
Delft, The Netherlands

March 26, 2002

Consider a chirp signal $y(t)$, described as:

$$y(t) = a(t) \cdot \cos\left(\int_0^t \omega(\tau)\, d\tau + \theta_0\right), \tag{1}$$

with $a(t)$ the wave amplitude, $\omega(t)$ the wave angular frequency and θ_0 an initial wave phase. The wave amplitude $a(t)$ and angular frequency $\omega(t)$ are slowly varying with time t. Further we assume:

- the signal $y(t)$ to be of finite duration in the interval $t \in [0, \mathcal{T}]$,
- $y(t)$, $a(t)$ and $\omega(t)$ to be finite, continuous and differentiable for all $t \in \mathbb{R}$,
- the angular frequency $\omega(t)$ to be a monotonic function of time t.

In order to determine the relationship between the time series $y(t)$ and its power spectral density $S_{yy}(\omega)$ we consider a time interval $[t, t + \Delta t]$ with amplitude variations $[a(t), a(t) + \Delta a(t)]$ and angular frequency changes $[\omega(t), \omega(t) + \Delta\omega(t)]$. We choose Δt to be one or a few times the momentary wave period $2\pi/\omega(t)$. Since the amplitude $a(t)$ and frequency $\omega(t)$ are only varying slowly in time, the changes $\Delta a(t)$ and $\Delta\omega(t)$ are small compared to $a(t)$ and $\omega(t)$ respectively.

The variance $\sigma_y^2(t)$ of the time series in the interval $[t, t + \Delta t]$ then equals approximately:

$$\sigma_y^2(t) = \int_t^{t+\Delta t} y^2(\tau)\, d\tau \approx \frac{1}{2} a^2(t)\, \Delta t, \tag{2}$$

which should correspond to the integral $m_0(\omega(t))$ of the power spectrum $S_{yy}(\omega(t))$ over the interval $[\omega(t), \omega(t) + \Delta\omega(t)]$:

$$m_0(\omega(t)) \;=\; \left| \int_{\omega(t)}^{\omega(t)+\Delta\omega(t)} S_{yy}(\Omega)\, \mathrm{d}\Omega \right| \;\approx\; S_{yy}(\omega(t)) \;|\, \Delta\omega(t) \,|\,, \tag{3}$$

where the absolute value of $\Delta\omega(t)$ has to be taken because $\omega(t)$ will in general be a decreasing function of time t for the focussing of water waves at a certain focus position and focus time.

Equating these two expressions for the variance in Equations (2) and (3) results in:

$$\frac{1}{2}\, a^2(t)\, \Delta t \;=\; S_{yy}(\omega(t)) \;|\, \Delta\omega(t) \,|\,. \tag{4}$$

In the limit of Δt going to zero, we get the following relationship between the time series expression in Equation (1) and the power spectral density $S_{yy}(\omega(t))$:

$$\frac{1}{2}\, a^2(t) \;=\; S_{yy}(\omega(t)) \left| \frac{\mathrm{d}\,\omega(t)}{\mathrm{d}\,t} \right|, \tag{5}$$

which is the kind of relationship we were looking for.

Appendix C:

A non-linear Lagrangian correction to a wavemaker control signal according to linear wave theory

Gert Klopman

Netherlands Centre for Coastal Research (NCK),
Delft University of Technology, Faculty of Civil Engineering and Geosciences,
Fluid Mechanics Section, Delft, The Netherlands

May 7, 2002

Abstract

It is well known that the wave motion is less non-linear in a Lagrangian frame of reference than in an Eulerian frame of reference. Here we use this knowledge to add a non-linear correction to the Eulerian wavemaker theory by transferring Lagrangian results back to Eulerian frame of reference. Although the results will still be not second-order (in wave steepness) they are expected to be more accurate than the results from linear wave theory in an Eulerian frame of reference.

1 Linear theory in a Lagrangian frame of reference

The wave motion in a Lagrangian frame of reference according to linear wave theory is the same as in an Eulerian frame of reference, see *e.g.* Dean and Dalrymple (1991). However, the results are now to be applied in the (moving) Lagrangian positions (x_L, z_L) instead of the Eulerian positions (x, z).

These two coordinate systems are related by:

$$(x_L,\, z_L) = (x + \xi(x,z,t),\, z + \eta(x,z,t)), \tag{1.1}$$

where ξ and η are the orbital displacements of the Lagrangian points with respect to their still (Eulerian) positions x, z.

For periodic waves we have according to linear wave theory:

$$\zeta_L(x_L, z_L, t) = a\,\cos\psi_L, \tag{1.2a}$$

$$u_L(x_L, z_L, t) = \omega\, a\,\frac{\cosh k(z_L + h)}{\sinh kh}\,\cos\psi_L, \tag{1.2b}$$

$$w_L(x_L, z_L, t) = \omega\, a\,\frac{\sinh k(z_L + h)}{\sinh kh}\,\sin\psi_L, \tag{1.2c}$$

$$\xi(x_L, z_L, t) = -\,a\,\frac{\cosh k(z_L + h)}{\sinh kh}\,\sin\psi_L, \tag{1.2d}$$

$$\eta(x_L, z_L, t) = a\,\frac{\sinh k(z_L + h)}{\sinh kh}\,\cos\psi_L, \tag{1.2e}$$

$$\psi_L(x_L, t) = k\,x_L\,-\,\omega\,t \qquad \text{and} \tag{1.2f}$$

$$\omega^2 = g\,k\,\tanh\,kh, \tag{1.2g}$$

where a is the wave amplitude, k is the wave number, ω is the wave angular frequency, h is water depth, g is the gravitational acceleration, ζ_L is the free surface elevation, $u_L = D\xi/Dt$ and $w_L = D\eta/Dt$ are the components of the wave orbital velocity.

The required motion of a piston-type wavemaker with mean location $x = 0$ to generate these waves is:

$$X_L(t) = -\,\frac{C_g}{C}\,\frac{1}{\tanh kh}\,a\,\sin\psi_L|_{x_L=0}, \tag{1.3a}$$

$$C = \frac{\omega}{k} \qquad \text{and} \tag{1.3b}$$

$$C_g = \frac{1}{2}\,C\,\left(1\,+\,kh\,\frac{1\,-\,\tanh^2 kh}{\tanh kh}\right), \tag{1.3c}$$

where X_L is the linear-theory wavemaker motion, C is the phase velocity of the wave and $C_g \equiv \partial\omega/\partial k$ is the group velocity of the wave.

2 Non-linear correction to the waves and the wavemaker signal

Above the Lagrangian wave motion and associated wavemaker motion are given. In order to transfer these back to the Eulerian frame of reference we use Taylor-series expansions of the Lagrangian quantities f_L around their Lagrangian position:

$$f_E(x, z, t)\;=\;f_L(x_L - \xi, z_L - \eta, t)\;-\;\xi\,\frac{\partial f_L}{\partial x_L}\;-\;\eta\,\frac{\partial f_L}{\partial z_L}\;+\;\mathcal{O}(a^2), \tag{2.4}$$

where the subscript E denotes the quantity in the Eulerian frame of reference. So to lowest order we have:

$$f_E(x, z, t)\;\approx\;f_L(x_L - \xi, z_L - \eta, t). \tag{2.5}$$

Applying this approximation to Equation (1.2) gives:

$$\zeta_E(x,z,t) = a\,\cos\psi_E|_{z=0}, \tag{2.6a}$$
$$u_E(x,z,t) = \omega\,a\,\frac{\cosh k(z-\eta_0+h)}{\sinh kh}\,\cos\psi_E, \tag{2.6b}$$
$$w_E(x,z,t) = \omega\,a\,\frac{\sinh k(z-\eta_0+h)}{\sinh kh}\,\sin\psi_E, \tag{2.6c}$$
$$\psi_E(x,z,t) = k\,(x-\xi_0(x,z,t))\;-\;\omega\,t \qquad \text{and} \tag{2.6d}$$
$$\omega^2 = g\,k\,\tanh\,kh, \tag{2.6e}$$

where ξ_0 and η_0 are the lowest-order approximations of ξ and η:

$$\xi_0(x,z,t) = -\,a\,\frac{\cosh k(z+h)}{\sinh kh}\,\sin\psi_0, \tag{2.7a}$$
$$\eta_0(x,z,t) = a\,\frac{\sinh k(z+h)}{\sinh kh}\,\cos\psi_0, \qquad \text{and} \tag{2.7b}$$
$$\psi_0(x,t) = k\,x\;-\;\omega\,t. \tag{2.7c}$$

For the wavemaker motion we have:

$$X_E(t) = -\,\frac{C_g}{C}\,\frac{1}{\tanh kh}\,a\,\sin(\,-k\,X_0(t)\;-\;\omega\,t\,), \tag{2.8a}$$
$$X_0(t) = -\,\frac{C_g}{C}\,\frac{1}{\tanh kh}\,a\,\sin(\,-\omega\,t\,), \tag{2.8b}$$

where $X_E(t)$ is the non-linear corrected wavemaker motion and $X_0(t)$ is the linear-theory wavemaker motion.

References

Dean, R.G. and Dalrymple, R.A. (1991). *Water wave mechanics for engineers and scientists*. Adv. Series on Ocean Eng., **2**, World Scientific, Singapore.

Appendix D

Cauchy–Poisson method

Cauchy-Poisson have investigated the wave motion generated at the surface due to initial surface disturbances in the form of initial local elevation or to a local impulse at a point on the free surface, assuming linear theory (Lamb,1932). This wave motion is actually the reverse of the wave focussing signal. In this section their theory is explained briefly. For a complete description see Lamb,1932.

They assumed

- the resulting motion to be two-dimensional
- the linear theory to be applicable
- the point load or impulse is concentrated in the origin (x = 0 m)

The solution for the case of initial rest is:

$$z(x,t) = \cos(wt)\cos(kx) \tag{D-1}$$

$$f(x,z,t) = -\sin(wt)\cos(kx)\frac{w}{k}\frac{\cosh k(z+h)}{\sinh(kh)} \tag{D-2}$$

where:

z = Water surface evaluation (m) as a function of space (x) and time (t)

f = Velocity-potential (m^2/s)

$w^2 = gk\tanh(kh)$ = Linear dispersion relation (rad/s)

generalised by Fourier's double-integral theorem:

$$f(x) = \frac{1}{p}\int_0^{\infty} dk \int_{-\infty}^{\infty} f(a)\cos k(x-a)\,da \tag{D-3}$$

with initial conditions:

t=0 $z(x,0) = f(x)$

$f(x,z,0) = 0$

they obtained:

$$z(x,t) = \frac{1}{p}\int_0^{\infty} \cos[w(k)t]dk \int_{-\infty}^{\infty} f(a)\cos k(x-a)\,da \tag{D-4}$$

$$f(x,z,t) = \frac{1}{p}\int_0^{\infty} \sin[w(k)t]\frac{w(k)\cosh k(z+h)}{k\sinh(kh)}dk \int_{-\infty}^{\infty} f(a)\cos k(x-a)\,da \tag{D-5}$$

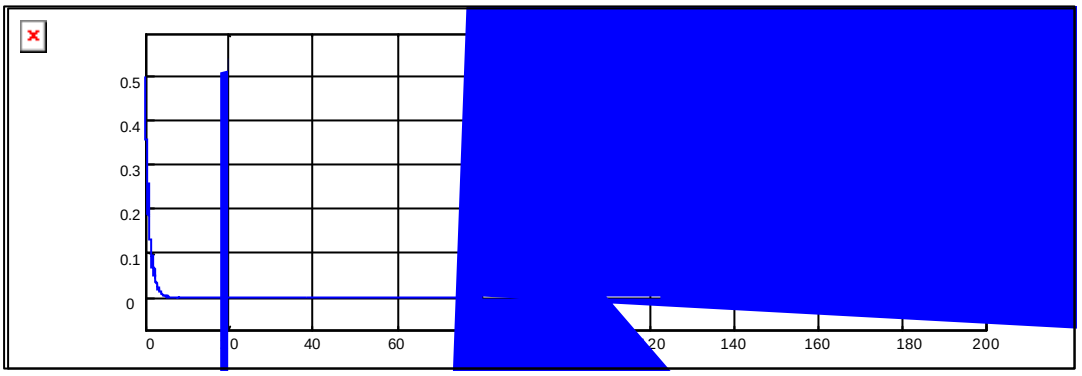

Fig.D-1. Surface elevation at different time levels due to an initial point loaded disturbance using the Cauchy-Poisson wave theory

Figure D-1 shows a wave motion due to an initial point loaded disturbance at different time levels by using the Cauchy-Poisson theory. This figure is not the whole wave motion that would be generated because naturally this motion is also going to the other site of the vertical axis (see fig.D-2). It can be seen that if t increases, the wave signal is stretched out horizontally while vertically the amplitude decreases.

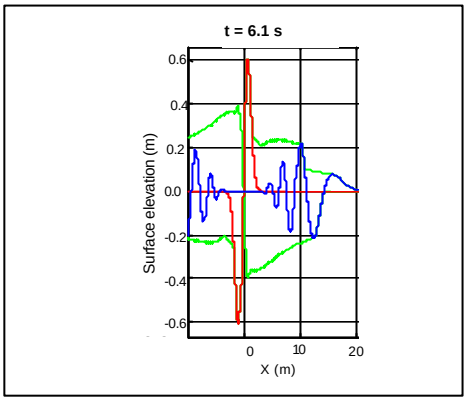

Fig.D-2 The wave motion (blue) due to a initial point loaded disturbance (red)

In this research a software package based on this theory is developed. In this software package, five different initial free surface elevations (freely chosen) were tested. The different elevations with their Fourier transforms are shown below:

		Initial free surface elevation	Fourier transform
1.	Gauss:	$f(x)=ae^{-\frac{1}{2}(k_0x)^2}$	$F(x)=\sqrt{\frac{2}{p}}\frac{a}{k_0}e^{-\frac{1}{2}\left(\frac{k}{k_0}\right)^2}$
2.	Exponential:	$f(x)=ae^{-\lvert k_0x\rvert}$	$F(x)=\frac{1}{p}\frac{ak_0}{k_0^2+k^2}$
3.	Bump:	$f(x)=\frac{a}{1+(k_0x)}$	$F(x)=\frac{a}{2k_0}e^{-\left\lvert\frac{k}{k_0}\right\rvert}$
4.	Odd1:	$f(x)=ak_0xe^{-\lvert k_0x\rvert}$	$F(x)=\left(-2i\frac{1}{p}k_0^2a\right)\left(\frac{k}{\left(k_0^2+k^2\right)^2}\right)$

5. Odd2: $f(x) = ak_0 x e^{-\frac{1}{2}(k_0 x)^2}$ $F(x) = \left(\frac{-ia}{\sqrt{2p}\,k_0}\right)\left(\frac{k}{k_0}\right)e^{-\frac{1}{2}\left(\frac{k}{k_0}\right)^2}$

This software package is verified with experiments. The experiments showed that the resulting control signal did not generate a well-focussed wave. Adaptations were made to the software package but they did not result in a better focussed wave. Therefore this theory is rejected. The software package and the corresponding experiments can be found on the CD under the name “Lamb”.

Appendix E

Derivation of the equation for the wave board motion

The ratio of wave height to stroke for a piston wave board motion given in Dean and Dalrymple (1991, section 6.3 p 177) is (equation 3-4):

$$\frac{H}{S} = \frac{2(\cosh 2kh - 1)}{\sinh 2kh + 2kh} \tag{E-1}$$

With equation E-1 the wave maker displacement can be derived, which is described below:

$$-i\frac{H}{S} = \frac{a}{X} \tag{E-2}$$

Where:

H = The wave height (m)
S = The stroke (m)
a = The amplitude (m)
X = The wave board displacement (m)
k = The wave number (rad/m)
h = The water depth (m)

Using equations E-1 and E-2 and multiplied by $1 = \frac{2\sinh(2kh)}{2\sinh(2kh)}$ becomes:

$$\frac{a}{X} = -i\frac{\left(\frac{2(\cosh(2kh)-1)}{2\sinh(2kh)}\right)}{\left(\frac{\sinh(2kh)+2kh}{2\sinh(2kh)}\right)} = -i\frac{\left(\frac{2\cosh(2kh)-2}{2\sinh(2kh)}\right)}{\frac{1}{2}\left(1+\frac{2kh}{\sinh(2kh)}\right)} \tag{E-3}$$

With: $\sinh^2(x) = \cosh^2(x) - 1$

$$\cosh^2(x) = \frac{1}{2}\cosh(2x) + \frac{1}{2}$$

$$\tanh(x) = \frac{\sinh(x)}{\cosh(x)}$$

$$\sinh(2x) = 2\sinh(x)\cosh(x)$$

The expressions $2\cosh(2x) - 2$ and $4\sinh^2(x)$ can be rewritten as:

$$2\cosh(2x) - 2 = 4\left(\frac{1}{2}\cosh(2x) + \frac{1}{2}\right) - 4 = 4\cosh^2(x) - 4 = 4\sinh^2(x) \tag{E-4}$$

$$4\sinh^2(x) = 2\frac{\sinh(x)}{\cosh(x)}2\sinh(x)\cosh(x) = 2\sinh(2x)\tanh(x) \tag{E-5}$$

The numerator of equation (E-3) substituting expressions E-4 and E-5 becomes:

$$\frac{2\cosh(2kh)-2}{2\sinh(2kh)} = \frac{2\sinh(2kh)\tanh(kh)}{2\sinh(2kh)} = \tanh(kh) \qquad \text{(E-6)}$$

with

$$\frac{C_g}{c} = \frac{1}{2}\left(1+\frac{2kh}{\sinh 2kh}\right) = \frac{kC_g}{w}$$

Resulting in:

$$\frac{a}{X} = -i\frac{\tanh(kh)}{\frac{kC_g}{w}}$$

Therefore the first-order wave board motion is calculated in the experiments with the formula:

$$\boxed{X = -\frac{kC_g a}{w\tanh(kh)}\sin(wt-y)} \qquad \text{(E-7)}$$

Appendix F

User manual

F-1 Introduction

This appendix provides a user manual for the software packages developed in this research, which are produced for generating focussed waves in a laboratory flume. Section F-2 shows the necessary input and the corresponding output. The appendix concludes with a brief description of the implementation of the obtained control signal to the wave generator. Figure F-1 shows the whole process a user has to carry out to generate a wave focussing signal in a wave flume (with a piston wave maker) by using these software packages.

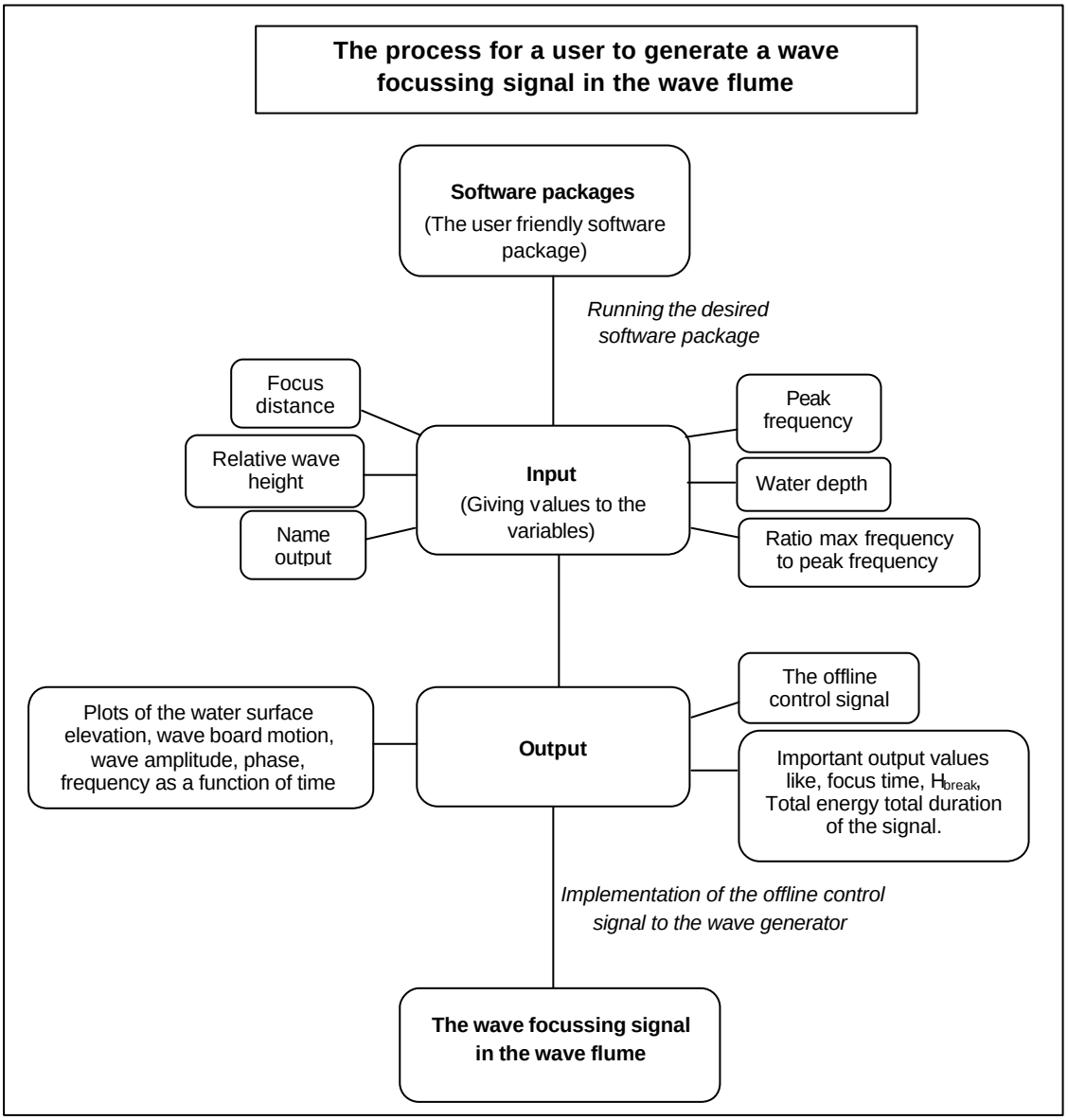

Fig F-1 The process for a user to generate a wave focussing signal in the wave flume by using the developed software packages.

F-2 Creating the offline control signal

One of the objectives of this research is to develop a user friendly software package for easy application of the suggested different theories for the generation of the offline control signal. The different combinations of the theories are programmed in MATLAB and result in so called software packages. These software packages calculate the offline control signal. Appendix A shows the combinations of the theories and the corresponding software package. A user, through running the desired software package and giving values to the asked input variables, can generate the offline control signal. Beside this offline control signal, the software package also produces some important plots and values which are described in subsection F-2.2.

F-2.1 The input

After running one of the software packages the user is asked to give values to six input variables:

1. *The name of the control signal*
   This name can be freely chosen. After the run, the calculated control signal will be stored under this name such as: outputname.ifg and outputname.dat, which are needed to implement the control signal to the wave generator (see subsection 4.1.1)
2. *The focus distance*
   This is the distance between the wave board (x=0m) and the location in the flume where the user wants to produce the focussed wave ($x=x_f$).
3. *The water depth*
   The signals are only designed for a wave flume with a constant water depth. The water depth by which the user wants to do the experiments has to be given.
   (There is a limitation for the water depth (maximum and minimum), but this has still to be investigated for this wave flume. In this research the signals are only tested with a water depth of 0,6 m and 0,7 m).
4. *The peak frequency*
   When the user chooses a high peak frequency more short waves are generated. Those waves travel with a lower velocity than lower frequency waves. Therefore the higher the peak frequency is chosen, the longer the signal will be.
5. *The ratio*
   This is the ratio of the maximum frequency to the peak frequency. In formula:

$$Ratio = \frac{f_{\max}}{f_0} \qquad \text{(F-1)}$$

   with:

   $f_{\max}$ = Maximum frequency (1/s)

   f_0 = Peak frequency (1/s)

   With this input the spectrum is established.
6. *The relative wave height*
   In formula:

$$b = \frac{a}{a_{break}} \qquad \text{(F-2)}$$

   b = The relative wave height (-).

   a_{break} = The maximum wave amplitude as a function of time (m).

   a = The wave amplitude as function of the time (m).

   With a_{break} calculated with the Miche criterum (see section 2.3):

$$a_{break} = \frac{0.5 * 0{,}88}{k} \tanh\left(\frac{ghk}{0{,}88}\right)$$

   g = The breaker index in shallow water = 0,833 (-).

   h = The water depth (m).

   k = The wave number as a function of time (rad/m).

F-2.2 The output

After entering the six variables, the application starts to calculate the control signal corresponding to the user supplied input. Besides the stored control signal the computation also provides some other output, graphical and numerical. This output is presented below, with an example by using the software package “Chirp22c”.

- First the user’s input is repeated:

For example:

Your input is:

output file name	*= x*
focus distance	*= 25 m*
peak frequency	*= 0.3 Hz*
waterdepth	*= 0.6 m*
relative wave height	*= 0.3*
ratio max. to peak frequency	*= 5*

- Afterwards the number of iteration steps, to come to the control signal, is shown with a minimum of one and a maximum of five iteration steps (which is programmed in the software package).

For example:

Iteration 1
Iteration 2
Iteration 3

Subsequently some important output values are calculated and presented:

For Example:

The wave is expected to break after 50 s at x = 25 m
The expected breaking wave height is 0.384 m
The total wave energy input by the wave maker is 1.41e+003 J/m
The total duration of the signal is 70 s
The number of records written to file is 1750

- Two figures are produced:
  The first figure is a plot of the water surface elevation (ζ) and the wave board motion (X) as a function of time at X = 0 m.

For example:

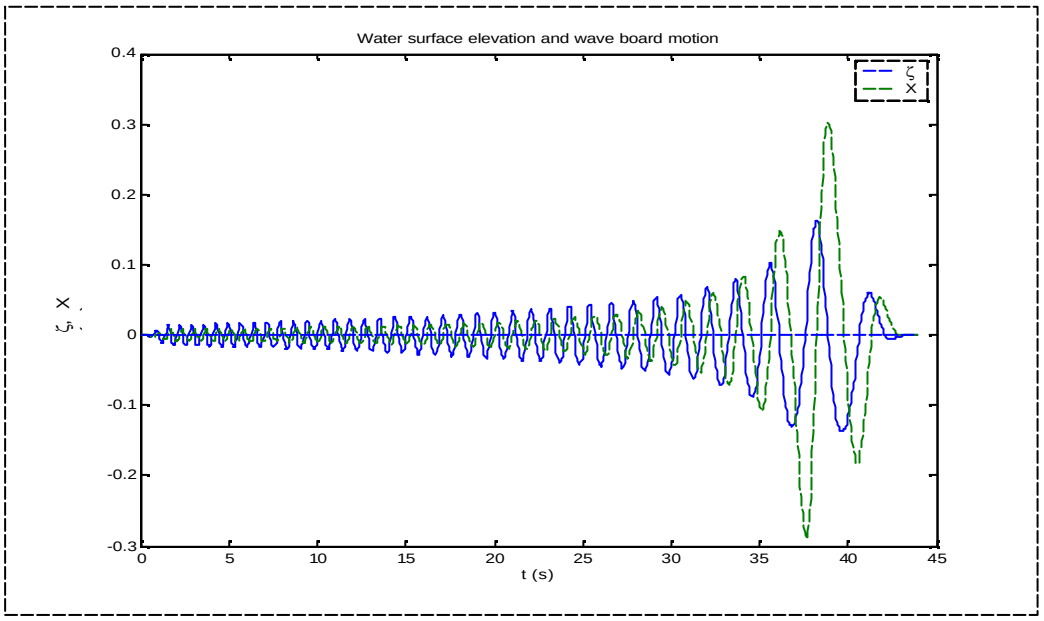

Fig F-2 Water surface elevation and wave board motion as function of time at X= 0m

N.B. The wave board can maximally move one meter forwards and one meter backwards from its mean position (the maximum stroke). Because of the choice for the approach to create the wave signal without using the program “Delft-Auke”, the results for the wave board displacement have to be checked for not exceeding this limit, which can be verified in the figure giving the output, like figure F-2. (So X may not exceed the value of 1 m).

The other figure shows plots of the water surface elevation (ζ), wave amplitude (a), angular frequency (ω) and phase (ψ) all as a function of time at X = 0m (an example is given in figure F-3):

For example:

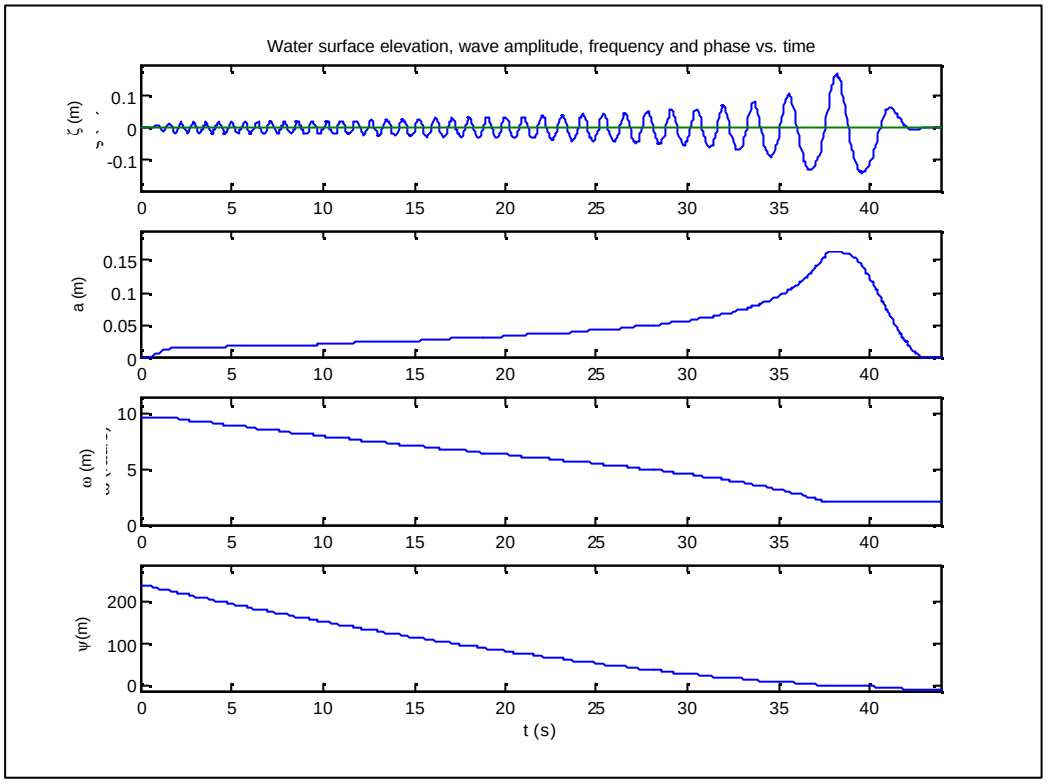

Fig F-3 Water surface elevation, wave amplitude, frequency and phase as a function of time at X = 0m

5.2 Implementation

The output files with the extensions *.ifg and *.dat contain the wave board motion as a function of time for generating the desired wave focussing signal. This offline control signal has to be enforced to the wave generator. Therefore both files have to be implemented to the computer with the wave generator control application. By running this control application the user can select the desired control signal by pressing the ¨select file¨ button (see fig 4-8) and select the desired output file. Afterwards the gain factor has to be set on the desired value and the ARC setting has to be set on “off”. Finally the user has to press the ¨generation on¨ button in the control application resulting in the generation of the desired wave signal in the wave flume (as explained in section 4.4).

Appendix G

The names of all the control signals including the used software packages and the input variable

Software package	theory	control signal	x_f	h	f_0	r	b
Chirp19c	Hedges + mass corr + $C_{g,d}$	ehhh3502	20	0.6	0.3	5	0.2
		ehhh3503	20	0.6	0.3	5	0.3
		fhhh3503	25	0.6	0.3	5	0.3
Chirp20c	Hedges + lagr corr +mass corr + $C_{g,d}$	ehcc3502	20	0.6	0.3	5	0.2
		ehcc3525	20	0.6	0.3	5	0.25
		ehcc3503	20	0.6	0.3	5	0.3
		fhcc3502	25	0.6	0.3	5	0.2
		fhcc3525	25	0.6	0.3	5	0.25
		fhcc3503	25	0.6	0.3	5	0.3
Chirp22c	K&D + lagr corr + mass corr + $C_{g,d}$	edcc3502	20	0.6	0.3	5	0.2
		edcc3525	20	0.6	0.3	5	0.25
		edcc3503	20	0.6	0.3	5	0.3
		fdcc3502	25	0.6	0.3	5	0.2
		fdcc3525	25	0.6	0.3	5	0.25
		fdcc3503	25	0.6	0.3	5	0.3
Chirp22cfirstapprox	K&D + lagr corr + mass corr + $C_{g,d}$	edcf3502	20	0.6	0.3	5	0.2
		edcf3503	20	0.6	0.3	5	0.3
		fdcf3503	25	0.6	0.3	5	0.3
Chirp22cdiscussion2	K&D + lagr corr + mass corr + $C_{g,d}$	edcs3503	20	0.6	0.3	5	0.3
		fdcs3503	20	0.6	0.3	5	0.3
Chirp22d	K&D + lagr corr + $C_{g,d}$	edcd3502	20	0.6	0.3	5	0.2
		edcd3525	20	0.6	0.3	5	0.25
		edcd3503	20	0.6	0.3	5	0.3
		fdcd3502	25	0.6	0.3	5	0.2
		fdcd3525	25	0.6	0.3	5	0.25
		fdcd3503	25	0.6	0.3	5	0.3
Chirp22dfirstapprox	K&D + lagr corr + $C_{g,d}$	edcn3502	20	0.6	0.3	5	0.2
		edcn3503	20	0.6	0.3	5	0.3
		edcn5503	20	0.6	0.5	5	0.3
		edcn1503	20	0.6	1	5	0.3
		edcn1553	20	0.6	1.5	5	0.3
		edcn3203	20	0.6	0.3	2	0.3
		edcn3303	20	0.6	0.3	3	0.3
		edcn3603	20	0.6	0.3	6	0.3
		edcn5303	20	0.6	0.5	3	0.3
		fdcn5503	25	0.6	0.5	5	0.3
		fdcn1503	25	0.6	1	5	0.3
		fdcn1553	25	0.6	1.5	5	0.3
		fdcn3303	25	0.6	0.3	3	0.3
		fdcn3603	25	0.6	0.3	6	0.3
		fdcn3203	25	0.6	0.3	2	0.3
		fdcn1303	25	0.6	1	3	0.3
		fdcn5303	25	0.6	0.5	3	0.3
		fdcn3503	25	0.6	0.3	5	0.3
Chirp22ddiscussion2	K&D + lagr corr + $C_{g,d}$	edns3503	20	0.6	0.3	5	0.3
		edns5503	20	0.6	0.5	5	0.3
		edns3303	20	0.6	0.3	3	0.3
		fdns3503	25	0.6	0.3	5	0.3
		fdns5503	25	0.6	0.5	5	0.3
		fdns3303	25	0.6	0.3	3	0.3

Software package	theory	control signal	x_f	h	f_0	r	b
Chirp22analy	K&D + lagr corr + mass corr + $C_{g,d}$	edca3503	20	0.6	0.3	5	0.3
		edca5503	20	0.6	0.5	5	0.3
		fdca3503	25	0.6	0.3	5	0.3
		fdca5503	25	0.6	0.5	5	0.3
chirp22firstapprox	K&D + lagr corr + mass corr + $C_{g,d}$	edfa3502	20	0.6	0.3	5	0.2
		edfa3503	20	0.6	0.3	5	0.3
		edfa3203	20	0.6	0.3	2	0.3
		edfa3303	20	0.6	0.3	3	0.3
		edfa3603	20	0.6	0.3	6	0.3
		edfa1303	20	0.6	1	3	0.3
		edfa5303	20	0.6	0.5	3	0.3
		fdfa3503	25	0.6	0.3	5	0.3
		fdfa5503	25	0.6	0.5	5	0.3
		fdfa1503	25	0.6	1	5	0.3
		fdfa1553	25	0.6	1.5	5	0.3
		fdfa3303	25	0.6	0.3	3	0.3
		fdfa3603	25	0.6	0.3	6	0.3
		fdfa3203	25	0.6	0.3	2	0.3
		fdfa1303	25	0.6	1	3	0.3
		fdfa5303	25	0.6	0.5	3	0.3
chirp22firstapproxumass	K&D + lagr corr + mass corr + $C_{g,d}$	edgm3502	20	0.6	0.3	5	0.2
		edgm3503	20	0.6	0.3	5	0.3
		fdgm3503	25	0.6	0.3	5	0.3
chirp22discussion2	K&D + lagr corr + mass corr + $C_{g,d}$	eddu3503	20	0.6	0.3	5	0.3
		fddu3503	25	0.6	0.3	5	0.3
chirp22discussion2umass	K&D + lagr corr + mass corr + $C_{g,d}$	edug3503	20	0.6	0.3	5	0.3
		fdug3503	25	0.6	0.3	5	0.3
Chirp22lin	K&D + lagr corr + mass corr + $C_{g,id}$+ lin	edcl3502	20	0.6	0.3	5	0.2
		edcl3525	20	0.6	0.3	5	0.25
		edcl3503	20	0.6	0.3	5	0.3
		edcl5503	20	0.6	0.5	5	0.3
		fdcl3502	25	0.6	0.3	5	0.2
		fdcl3525	25	0.6	0.3	5	0.25
		fdcl3503	25	0.6	0.3	5	0.3
		fdcl5502	25	0.6	0.5	5	0.2
		fdcl5503	25	0.6	0.5	5	0.3
chirp22linfirstapprox	K&D + lagr corr + mass corr + $C_{g,id}$+ lin	edlf3502	20	0.6	0.3	5	0.2
		edlf3503	20	0.6	0.3	5	0.3
		fdlf3503	25	0.6	0.3	5	0.3
chirp22lindiscussion2	K&D + lagr corr + mass corr + $C_{g,id}$+ lin	edlt3503	20	0.6	0.3	5	0.3
		fdlt3503	25	0.6	0.3	5	0.3
Chirp23c	Hedges + lagr corr + $C_{g,d}$	bucc3502	20	0.7	0.3	5	0.2
		bucc5502	20	0.7	0.5	5	0.2
		eucc3502	20	0.6	0.3	5	0.2
		eucc3525	20	0.6	0.3	5	0.25
		eucc3503	20	0.6	0.3	5	0.3
		eucc3303	20	0.6	0.3	3	0.3
		eucc3603	20	0.6	0.3	6	0.3
		eucc3203	20	0.6	0.3	2	0.3
		eucc5503	20	0.6	0.5	5	0.3
		eucc1503	20	0.6	1	5	0.3
		eucc1553	20	0.6	1.5	5	0.3
		eucc1303	20	0.6	1	3	0.3
		eucc5303	20	0.6	0.5	3	0.3

Software package	theory	control signal	x_f	h	f_0	r	b
Chirp23c	Hedges + lagr corr + $C_{g,d}$	fucc3502	25	0.6	0.3	5	0.2
		fucc3525	25	0.6	0.3	5	0.25
		fucc3503	25	0.6	0.3	5	0.3
		fucc3303	25	0.6	0.3	3	0.3
		fucc3603	25	0.6	0.3	6	0.3
		fucc3203	25	0.6	0.3	2	0.3
		fucc5503	25	0.6	0.5	5	0.3
		fucc1503	25	0.6	1	5	0.3
		fucc1553	25	0.6	1.5	5	0.3
		fucc1303	25	0.6	1	3	0.3
		fucc5303	25	0.6	0.5	3	0.3
Chirp23d	Hedges + lagr corr +$C_{g,d}$ + lin	bucd3502	20	0.7	0.3	5	0.2
		ehcl3502	20	0.6	0.3	5	0.2
		ehcl3503	20	0.6	0.3	5	0.3
		fhcl3503	25	0.6	0.3	5	0.3
		fhcl3502	25	0.6	0.3	5	0.2
Chirp29/0	Hedges + 2nd order + $C_{g,i}$ + mass corrl	ehaw3503	20	0.6	0.3	5	0.2
		fhaw3503	25	0.6	0.3	5	0.2
Chirp30	Hedgs + 2nd order + $C_{g,d}$	ehmt3502	20	0.6	0.3	5	0.2
		ehmt3503	20	0.6	0.3	5	0.3
		fhmt3502	25	0.6	0.3	5	0.2
		fhmt3503	25	0.6	0.3	5	0.3
Chirp31	Hedges + mass corr + $C_{g,i}$	ehaa3502	20	0.6	0.3	5	0.2
		ehaa3503	20	0.6	0.3	5	0.3
		ehaa5502	20	0.6	0.5	5	0.2
		ehaa5503	20	0.6	0.5	5	0.3
		fhaa3502	25	0.6	0.3	5	0.2
		fhaa3503	25	0.6	0.3	5	0.3
Chirp32	Hedges + 2nd order + $C_{g,d}$ + mass corr	ehtt3502	20	0.6	0.3	5	0.2
		ehtt3503	20	0.6	0.3	5	0.3
		fhtt3502	25	0.6	0.3	5	0.2
		fhtt3503	25	0.6	0.3	5	0.3
Chirp33	K&D + mass corr + $C_{g,d}$	ednn3503	20	0.6	0.3	5	0.3
		ednn5503	20	0.6	0.5	5	0.3
		fdnn3503	25	0.6	0.3	5	0.3
		fdnn5503	25	0.6	0.5	5	0.3
Chirp33firstapprox	K&D + mass corr + $C_{g,d}$	ednt3502	20	0.6	0.3	5	0.2
		ednt3503	20	0.6	0.3	5	0.3
		ednt3519	20	0.6	0.3	5	0.188
		fdnt3503	25	0.6	0.3	5	0.3
Chirp33discussion2	K&D + mass corr + $C_{g,d}$	edkk3503	20	0.6	0.3	5	0.3
		edkk3517	20	0.6	0.3	5	0.169
		fdkk3503	25	0.6	0.3	5	0.3
Chirp34	K&D + mass corr + $C_{g,i}$ + 2^{nd} order	fdat3503	25	0.6	0.3	5	0.3
Chirp34firstapprox	K&D + mass corr + $C_{g,i}$ + 2^{nd} order	edtf3502	20	0.6	0.5	5	0.2
		edtf3503	20	0.6	0.5	5	0.3
		fdtf3503	25	0.6	0.3	5	0.3
Chirp340discusion2	K&D + mass corr + $C_{g,i}$ + 2^{nd} order	edtr3503	20	0.6	0.3	5	0.3
		fdtr3503	25	0.6	0.3	5	0.3
Chirp35	K&D + $C_{g,d}$ +2nd order	edmt3503	20	0.6	0.3	5	0.3
		fdmt5503	25	0.6	0.5	5	0.3
Chirp35firstapprox	K&D + $C_{g,d}$ +2nd order	edmf3502	20	0.6	0.3	5	0.2
		edmf3503	20	0.6	0.3	5	0.3
		fdmf3503	25	0.6	0.3	5	0.3

Software package	theory	control signal	x_f	h	f_0	r	b
Chirp35discussion2	K&D +$C_{g,d}$ +2nd order	edms3503	20	0.6	0.3	5	0.3
		fdms3503	25	0.6	0.3	5	0.3
Chirp36	K&D + $C_{g,i}$ +mass corr	fdaa3503	25	0.6	0.3	5	0.3
Chirp36firstapprox	K&D + $C_{g,i}$ +mass corr	edaf3502	20	0.6	0.5	5	0.2
		edaf3503	20	0.6	0.5	5	0.3
		fdaf3503	25	0.6	0.3	5	0.3
Chirp36discussion2	K&D + $C_{g,i}$ +mass corr	fded3503	25	0.6	0.3	5	0.3
Chirp37	K&D +mass corr + $C_{g,d}$ +2nd order	fdtt3503	25	0.6	0.3	5	0.3
Chirp37firstapprox	K&D +mass corr + $C_{g,d}$ +2nd order	edff3502	20	0.6	0.3	5	0.2
		edff3519	20	0.6	0.3	5	0.19
		edff3503	20	0.6	0.3	5	0.3
		fdff3503	25	0.6	0.3	5	0.3
Chirp370discussion2	&D +mass corr + $C_{g,d}$ +2nd order	eddt3503	20	0.6	0.3	5	0.3
		eddt3515	20	0.6	0.3	5	0.15
		fddt3503	25	0.6	0.3	5	0.3
Chirp38	Hedges + $C_{g,d}$ + 2nd order	fhmg3503	25	0.6	0.3	5	0.3
Chirp39	K&D + mass corr +$C_{g,d}$ + 2nd order	fdtg3503	25	0.6	0.3	5	0.3
Chirp39firstapprox	K&D mass corr +$C_{g,d}$ + 2nd order	edfg3502	20	0.6	0.3	5	0.2
		edfg3503	20	0.6	0.3	5	0.3
		fdfg3503	25	0.6	0.3	5	0.3
Chirp39discussion2	K&D + mass corr +$C_{g,d}$ + 2nd order	edgt3503	20	0.6	0.3	5	0.3
		fdgt3503	25	0.6	0.3	5	0.3
Chirp40	Linear + mass corr + $C_{g,d}$	elll3503	20	0.6	0.3	5	0.3
		flll3503	25	0.6	0.3	5	0.3
Chirp41	Linear + + $C_{g,i}$ + mass corr	ella3503	20	0.6	0.3	5	0.3
		flla3503	25	0.6	0.3	5	0.3
Chirp42	Linear + larg corr + mass corr + + $C_{g,d}$	ellc3503	20	0.6	0.3	5	0.3
		fllc3503	25	0.6	0.3	5	0.3
Chirp43	Linear +lagr corr + mass corr + + $C_{g,i}$	elca3503	20	0.6	0.3	5	0.3
		flca3503	25	0.6	0.3	5	0.3
Chirp44	Linear + lagr corr + $C_{g,i}$	elcn3503	20	0.6	0.3	5	0.3
		flcn3503	25	0.6	0.3	5	0.3
Chirp45	Linear + $C_{g,d}$	elnn3503	20	0.6	0.3	5	0.3
		flnn3503	25	0.6	0.3	5	0.3

Appendix H

Software package (the code)

% Signal for focussing waves in a wave flume with a piston wave maker

% Theories: Dean & Dalrymple (dispersion relation from approximation(1986)) + analytical computation of the group velocity + Lagrangian correction

```
% a                 % wave amplitude (m)
% beta              % relative waveheight (-)
% cgroep            % nonlinear group velocity (m/s)
% cgroep_min        % lowest groupvelocity (m/s)
% difference_omega  % relative differences in omega
% d_omega           % angular frequency step (rad/s)
% dt                % time step (s)
% E                 % wave energy (J/m^2)
% E_flux            % wave energy flux (W/m')
% f_max             % maximum frequency (Hz)
% f_name            % output file
% f_nul             % peak frequency (Hz)
% g                 % gravitational acceleration constant (m/s^2)
% gamma             % breaker index in shallow water (-)
% h                 % water depth (m)
% k                 % wave number (rad/m)
% k_max             % maximum wave number (rad/m)
% max_it            % max number of iterations (-)
% omega             % wave angular frequency compute from the input frequency (rad/s)
% omega_def         % wave angular frequency after loop (rad/s)
% omega_max         % maximum wave angular frequency (=2*pi*f_max) (rad/s)
% omega_min         % minimum wave angular frequency (rad/s)
% psi               % wave phase (rad)
% psi_nul           % phase shift (rad)
% ratio             % the ratio of the max. frequency to the peak frequency (-)
% rel_dif           % max. allowed relative differences in omega between iterations (-)
% rho               % mass density (kg/m^3)
% t_focus           % focus time (s)
% theta             % initial wave phase (rad)
% Umass             % correction for the mass-transport velocity
% W                 % work performed by wave maker (J/m')
% x_focus           % focus point (m)
% x_nul             % starting point (m)
% zeta              % desired surface elevation at x_nul (m)


x_nul   =   0;      % starting point (m)
g       =   9.81;   % gravitational acceleration constant(m/s2)
dt      =   0.04;   % time step (s)
gamma   =   0.833;  % fixed value (-)
rho     =   1000.;  % density (kg/m3)
nf      =   1000;   % number of frequency steps
rel_dif =   1.0e-6; % max. allowed relative differences in omega between iterations
```

```
max_it  =    5;                                    % max. number of iterations
amplif  =    0.80;                                 % gain/amplification factor (-)
setp_res =   0.00005;                              % wavemaker calibration (m/unit)


% Input variables
f_name = input('What is the name of the output file?\n','s');   % input f_name

 while ischar(f_name) == 0
          disp( 'Please give a file name' ) ;
          f_name      = input('What is the name of the output file?\n');          % input f_name
 end


x_focus = input('Where do you want to focus the waves in the flume (m)?\n');      % input x_focus

while x_focus > 35 |  x_focus < 10                                                % boundary
     disp('The distance has to lie between 10 and 35 meters');
     x_focus        =input('Where do you want to focus the waves in the flume (m)?\n');
end


h                   =input('What is the water depth (m)?\n');                     % input depth

 while h < 0.2 | h > 0.8                                                          % boundary
      disp('the depth has to lie between 0.2 and 0.8 meter');
      h             =input('What is the water depth (m)?\n');
 end


f_nul               =input('What is the peak frequency (Hz)?\n');                 % input f_nul

while f_nul > 2 |  f_nul < 0.05                                                   % boundary
f_nul
     disp('The peak frequency has to lie between 0.05 Hz and 2 Hz');
     f_nul          =input('What is the peak frequency (Hz)?\n');                 % input f_nul
  end

ratio               =input('What is the ratio of the maximum frequency to the peak frequency?\n');

while  ratio < 1
     disp('The ratio of maximum to peak frequency has to be greater than 1');
     ratio          =input('What is the ratio of the maximum frequency to the peak frequency?\n');
  end


beta                =input('What is the relative wave height?\n');                % input beta

 while  beta > 1 |  beta < 0                                                      % boundary
disp('The relative wave height has to lie between 0 and 1');
     beta           =input('What is the relative wave height?\n');                % input beta
  end
```

```
% Computation of some values using the input variables
f_max           = ratio * f_nul;                                    % compute f_max
k_max           = disper( 2*pi*f_max, h, g ) ;                      % compute k_max
kh_max          = k_max * h ;                                       % compute kh_max
T_max           = tanh( kh_max ) ;                                  % compute  T_max
% Compute the minimum group velocity
cgroep_min      = 0.5 * (2*pi*f_max) / k_max * ( 1 + kh_max * ( 1 - T_max^2) / T_max ) ;
% Compute t_focus
t_focus         = ( x_focus - x_nul ) / cgroep_min ;

% Write input to screen
fprintf( 1, '\n' ) ;
fprintf( 1, 'Your input is:\n' ) ;
fprintf( 1, '  output file name           = %s\n'     , f_name  ) ;
fprintf( 1, '  focus distance             = %.5g m\n' , x_focus ) ;
fprintf( 1, '  peak frequency             = %.3g Hz\n', f_nul   ) ;
fprintf( 1, '  waterdepth                 = %.3g m\n' , h       ) ;
fprintf( 1, '  relative wave height       = %.3g\n'   , beta    ) ;
fprintf( 1, '  ratio max. to peak frequency = %.3g\n'   , ratio   ) ;
fprintf( 1, '\n' ) ;

%  aa             =input('Do you want to change one of these variable? (Y/N)','s');


omega_max       = 2 * pi * f_max ;                                  % Compute omega_max
omega_min       = 2 * pi * f_nul ;                                  % Omega_min
omega           = linspace( omega_min, omega_max, nf ) ;            % Vector omega (first estimate)
k               = disper( omega, h, g );                            % Linear dispersion relation
%(linear dispersion  = omega.^2 = g*k.*tanh(k*h),futher k stays fixed/constant )

% Define start values for omega and the amplitude
a               = zeros( size( omega ) ) ;                          % Startvector for the amplitude
omega_def       = omega ;                                           % used for the loup first time

% Start loop
i               = 1 ;
difference_omega    = 10 * rel_dif ;

while  ( ( abs(difference_omega) > rel_dif )  & ( i <= max_it ) ) | ( i <= 2 ) % max iterations 5
   fprintf( 1, 'Iteration %2i\n', i ) ;
   omega_try    = omega_def;                                        % omega_try=omega before last loup
   sigma        = tanh(k*h);
   f1           = sigma.^5;
   f2           = ((k*h)./(sinh(k*h))).^4;
   D            = (cosh( 4 * k * h) + 8 - 2 * (sigma).^2) ./ ( 8 * (sinh(k*h)).^4);
   alpha        = 1 + ((f1).*(k.*a).^2.*D);
   P1           = ( g * k .* alpha .* tanh ( (k*h) + (f2 .* k .*a))).^(1/2);

   % Correction for the mass-transport velocity -E/(rho*c*h)
   Umass        = -1 * (0.5 * g * a.^2) ./ ( ( P1 ./ k ) * h ) ;

  % Computation of the wave angular frequency
   omega_def    = P1 + k .* Umass ;          % Nonlinear dispersion relation (kirby & dalrymple)
```

```
    v1              = k .* a;
    v2              = v1.^2;
    v3              = k * h ;
    v4              = k .* (a).^2 ;

    s1              = sigma;
    s2              = sigma.^4;
    s3              = sigma.^5;
    s4              = ( sinh(k * h) ).^4;
    s5              = ( sinh(k * h) ).^5;
    s6              = 1-sigma.^2;
    s7              = cosh(k * h);
    s8              = sigma.^2;

    o4              = ( (k).^5 * (h)^4 .* a) ./ (s4) ;
    o1              = tanh(k * h + o4);
    o2              = cosh(4 * k * h) + 8 - 2 * s8;
    o3              = (s3 .* v2 .* o2) ./ (8 * s4);
    o5              = (4 * sinh(4 * k * h) * h) - (4 * sigma .* s6 * h) ;
    o6              = ( (k).^5 * (h)^5 .* a .* s7) ./ s5 ;
    o7              = ((k).^4 * (h)^4 .* a) ./ (s4);

    % calculation of the group velocity (analytical)
    C_groep     = ((g *( 1 + o3 ) .* o1) ...
                  + (g * k .* ( ( ( 5 * s2 .* v2 .* o2 .* s6 * h) ./ (8 * s4) ) ...
                  +( (s3 .* v4 .* o2) ./ (4 * s4) ) + ( (s3 .* v2 .* o5) ./ (8 * s4) ) ...
                  -((s3 .* v2 .* o2 .* s7 * h) ./ (2 * s5))) .* o1) ...
                  + (g * k .* (1 + o3) .* (1 - (o1).^2) .* ( h + 5 * o7 - (4 * o6)))) ...
                  ./ (2 * (g * k .* (1 + o3) .* o1).^(1/2) )%+Umass;

    t               = t_focus - ( ( x_focus - x_nul ) ./ C_groep ) ;          % Compute t

    P               = 0.5 * beta * 0.88 ;
    R               = ( gamma * h ) / 0.88 ;
   % The wave amplitude (constant steepness)
    a               = ( P ./ k ) ;
    % a                     = ( P ./ k ) .* tanh( R * k ) ;    % The wave amplitude ("miche" equation 3)
    difference_omega    = ( omega_def - omega_try ) ./ omega_try ;
    i               = i+1 ;
    if      i == max_it
            disp('The solution of omega is not converged but the computation has now done five
            times the loop')
    end
end



% Expected wave length of breaking wave
lambda_b        = 2*pi / k(1) ;

% Compute the phase shift needed for creating a wave crest of the last wave at the focus
position
psi_nul         = k(1) * ( x_focus - x_nul ) - omega_def(1) * ( t_focus - t(1) ) ;

% Interpolate to an equidistant time step
t_inter         = [ min(t) : dt : max(t) ] ;
```

```
a_inter          = interp1( t, a,         t_inter ) ;
omega_inter      = interp1( t, omega_def, t_inter ) ;
k_inter          = interp1( t, k,         t_inter ) ;
Cg_inter         = interp1( t, C_groep,   t_inter ) ;
t_inter          = t_inter - min(t_inter) ;
N                = length( t_inter ) ;

% Compute the wave phase
psi              = -cumsum( omega_inter * dt ) ;
psi              = psi - psi( length( psi ) ) ;

% Make a slow start of 3 wave periods to the start of the signal
Tw_b             = 2 * pi / omega_inter(1) ;
n_b              = round( 3 * Tw_b / dt ) ;
t_b              = [ -n_b : -1 ] * dt ;
a_b              = gladys2( [0:n_b-1]/n_b ) * a_inter(1) ;
omega_b          = repmat( omega_inter(1), 1, n_b ) ;
k_b              = repmat( k_inter(1),     1, n_b ) ;
Cg_b             = repmat( Cg_inter(1),    1, n_b ) ;
psi_b            = -omega_inter(1) * t_b + psi(1) ;

% Make a slow end of 2 wave periods at the end of the signal, the first period with constant
amplitude
Tw_e             = 2 * pi / omega_inter(N) ;
n_e              = round( 2 * Tw_e / dt ) ;
t_e              = [ 1 : n_e ] * dt ;
a_e              = ( 1 - gladys2( [0:n_e-1]/n_e ) ) * a_inter(N) ;
omega_e          = repmat( omega_inter(N), 1, n_e ) ;
k_e              = repmat( k_inter(N),     1, n_e ) ;
Cg_e             = repmat( Cg_inter(N),    1, n_e ) ;
psi_e            = -omega_inter(N) * t_e + psi(N) ;
t_e              = t_e + t_inter(N) ;                                  % correct t_e

% Add slow start and end to signals
t_inter          = [ t_b,     t_inter,     t_e     ] ;
a_inter          = [ a_b,     a_inter,     a_e     ] ;
omega_inter      = [ omega_b, omega_inter, omega_e ] ;
k_inter          = [ k_b,     k_inter,     k_e     ] ;
Cg_inter         = [ Cg_b,    Cg_inter,    Cg_e    ] ;
psi              = [ psi_b,   psi,         psi_e   ] ;


% Correct the wave phase with psi_nul
psi              = psi - psi_nul-(0.75*pi) ;

% Lagrangian horizontal position
sigma_inter      = tanh( k_inter * h ) ;
ksi_0            = -a_inter ./sigma_inter .* sin( psi ) ;

% Compute the surface elevation at x_nul
zeta             = a_inter .* cos( psi - k_inter.*ksi_0) ;

% Compute the wavemaker motion (provided it is located at x_nul)
X_0              = - k_inter .* Cg_inter .* a_inter ./ ( omega_inter .* sigma_inter ) ...
                  .* sin( psi ) ;
X                = - k_inter .* Cg_inter .* a_inter ./ ( omega_inter .* sigma_inter ) ...
```

```
                .* sin( psi - k_inter.*X_0 ) ;


% Reset the begin of t_inter to zero
t_focus         = t_focus - t_inter(1) ;
t_inter         = t_inter - t_inter(1) ;

% Some integral quantities
E               = 0.5 * rho * g * a_inter.^2 ;      % Wave energy per unit area
E_flux          = E .* Cg_inter ;                   % Wave energy flux per meter flume width
W               = cumsum( E_flux ) * dt ;           % Work performed by wave maker
W_tot           = W( length(W) ) ;
E_b             = ( W_tot / lambda_b ) ;
H_b             = sqrt( 8 * E_b / (rho * g ) ) ;

% Round the duration of the signal to a multiple of 10 s
m               = ceil( max(t_inter+dt) / 10 ) * ( 10 / dt ) - length( t_inter ) ;
t_write         = [ [-500:-1]*dt, t_inter, ( max(t_inter) + [1:m] * dt ) ] ;
zeta_write      = [ zeros(1,500), zeta, zeros(1,m) ] ;
X_write         = [ zeros(1,500), X,    zeros(1,m) ] ;

% Write the surface elevation signal to file
fid             = fopen( f_name, 'w' ) ;
%count          = fprintf( fid, '%7.2f %9.6f\n', [ t_write ; zeta_write ] ) ;
count           = fprintf( fid, '%9.6f\r\n', [ zeta_write ] ) ;
fclose( fid ) ;
%save f_name zeta_write -ASCII zeta_write;

% Write wavemaker signal to file
X_cal           = 1 / ( setp_res * amplif ) ;     % calibration factor for wavemaker signal (units/m)
fid=fopen( [ f_name '.dat' ], 'w') ;
fwrite( fid, round( X_cal * X_write ), 'int16' ) ;
fclose( fid ) ;

% and associated .ifg-file
fid=fopen( [ f_name '.ifg' ], 'w' ) ;
fprintf( fid, 'FACILITY -FILE,TUGOOTML.pos\r\n' ) ;
fprintf( fid, 'SETPOINT-RESOLUTION,%7.5f\r\n', setp_res ) ;
fprintf( fid, 'FREQUENCY,%10.6f\r\n', 1/dt ) ;
fprintf( fid, 'AMPLIFICATION,%4.2f\r\n', amplif ) ;
fprintf( fid, 'TIME-SAMPLES,%7.7i\r\n', length(X_write) ) ;
fprintf( fid, 'CYCLIC,YES\r\n' ) ;
fprintf( fid, 'WAVEBOARD,TUGOOTML \r\n' ) ;
fprintf( fid, '  USE,YES\r\n' ) ;
fprintf( fid, '  SEGMENTS,001\r\n' ) ;
fprintf( fid, '  IDLE,n\r\n' ) ;
fprintf( fid, '  ARC-MODE,NONE\r\n' ) ;
fprintf( fid, 'END:WAVEBOARD\r\n' ) ;
fclose( fid ) ;

% Write some properties of the signal to screen
fprintf( 1, '\n' ) ;
fprintf( 1, 'The wave is expected to break after %.3g s at x = %3g m\n', t_focus, x_focus ) ;

fprintf( 1, 'The expected breaking wave height is %.3g m\n', H_b ) ;
```

```
fprintf( 1, 'The total wave energy input by the wave maker is %.3g J/m\n', W_tot ) ;
fprintf( 1, 'The total duration of the signal is %.4g s\n', length(t_write)*dt ) ;
fprintf( 1, 'The number of records written to file is %i\n', length(t_write) ) ;
```

% Plot the results

```
t_min = min( t_inter ) ;
t_max = max( t_inter ) ;
```

figure(1)

```
subplot(411) ;                                          % surface elevation
plot( t_inter, zeta, t_inter, 0*t_inter );
ylabel( \zeta (m)' ) ;
axis( [ t_min t_max -1.2*max(a_inter) 1.2*max(a_inter) ] ) ;
title( 'surface elevation, wave amplitude, frequency and phase vs. time' ) ;

subplot(412) ;                                          % wave amplitude
plot( t_inter, a_inter ) ;
ylabel( 'a (rad/m)' ) ;
axis( [ t_min t_max 0 1.2*max(a_inter) ] ) ;

subplot(413) ;                                          % angular frequency
plot( t_inter, omega_inter ) ;
ylabel( \omega (rad/s)' ) ;
axis( [ t_min t_max 0 1.2*max(omega_inter) ] ) ;

subplot(414) ;                                          % wave phase
plot( t_inter, psi ) ;
ylabel( \Psi (rad)' ) ;
axis( [ t_min t_max 1.2*min(psi) 1.2*max(psi) ] ) ;
xlabel( 't (s)' ) ;
```

figure(2)

```
plot( t_inter, zeta, '-', ...
      t_inter, X,    '--', ...
      t_inter, 0*t_inter, 'b-' ) ;
xlabel( 't (s)' ) ;
ylabel( \zeta, X (m)' ) ;
legend( { '\zeta', 'X' } ) ;
```

Appendix I

Classification of the control signals resulting from the experiments by words

Control signal	Software package	x	h	f_0	r	beta	Etot	duration	H_b	Judgement by words (including the gain factor)
bhhc3502	chirp19c	20	0.7	0.3	5	0.2	695	40.4	0.26	0.8 breekt ervoor wel goede plaats 0.7 breekt ervoor 0.65 breekt niet wel goede plaats (niet hoog)
bhhc5502	chirp19c	20	0.7	0.5	5	0.2	441	65.2	0.279	0.8 breekt ervoor niet mooie breking)
ehhh3502	chirp19c	20	0.6	0.3	5	0.2	581	40.4	0.247	zie ehhh3503
ehhh3503	chirp19c	20	0.6	0.3	5	0.3	1310	40.4	0.37	0.45 goed niet hoog
fhhh3503	chirp19c	25	0.6	0.3	5	0.3	1470	50	0.392	
bhc03502	chirp_20	20	0.7	0.3	5	0.2	695	40.4	0.26	0.8 breekt ervoor en iets te ver; 0.75 idem 0.7 breekt er net voor; 0.65 vrij goed
bhc03503	chirp_20	20	0.7	0.3	5	0.3	1590	40.4	0.394	0.7 breekt ervoor en laatste breekt te ver 0.65 idem
bhc35016	chirp_20	20	0.7	0.3	5	0.1625	469	40.4	0.214	goed (0.65/0.8)*0.2=0.1625
bhcb3502	chirp20b	20	0.7	0.3	5	0.2	695	40.4	0.26	0.8 breekt goede plaats niet mooi + golf erna (slecht)
bhcc3502	chirp20c	20	0.7	0.3	5	0.2	695	40.4	0.26	0.8 breekt ervoor. wel goede plaats (niet hoog) 0.75 breekt ervoor 0.65 breekt niet ervoor 0.7 breet NET ervoor
bhcc5502	chirp20c	20	0.7	0.5	5	0.2	196	65.2	0.186	0.8 breekt net ervoor (geen mooie breking) 1 minder
ehcc3502	chirp20c	20	0.6	0.3	5	0.2	581	40.4	0.247	0.4 goede plaats breekt niet; 0.6 ok (kleine breking) 0.8 ok breekt net ervoor; 0.75 idem 0.7 beste
ehcc3525	chirp20c	20	0.6	0.3	5	0.25	970	40.4	0.308	0.4 breekt niet wel goede plaats; 0.6 breekt net 0.57 breekt net; 0.55 beste
ehcc3503	chirp20c	20	0.6	0.3	5	0.3	1310	40.4	0.37	0.4 goed; 0.5 breekt ervoor; 0.45 beste
fhcc3502	chirp20c	25	0.6	0.3	5	0.2	632	50	0.257	0.4 breekt niet; 0.6 goed; 0.65 breekt ervoor; 0.62 breekt net ervoor
fhcc3525	chirp20c	25	0.6	0.3	5	0.25	1000	50	0.323	0.4 breekt net; 0.6 breekt ervoor (2x) 0.5 breekt net; 0.45 beste
fhcc3503	chirp20c	25	0.6	0.3	5	0.3	1470	50	0.392	0.4 breekt goed; 0.45 breekt ervoor
bdcc3502	chirp22c	20	0.7	0.3	5	0.2	695	40.4	0.26	1 mooi (beta op 0.25)
bdcc3525	chirp22c	20	0.7	0.3	5	0.25	1080	40.4	0.324	0.4 breekt niet 0.6 breekt net ervoor 0.8 breekt net ervoor wel mooie breking en goede plaats
cdcc3525	chirp22c	25	0.7	0.3	5	0.25	1190	50	0.34	0.4 breekt net 0.6 breekt mooi goede plaats 0.65 breekt net ervoor
bdcc5502	chirp22c	20	0.7	0.5	5	0.2	193	65.2	0.184	0.6 "plopje" 0.8 breekt net ervoor
bdcc5503	chirp22c	20	0.7	0.5	5	0.3	427	65.2	0.274	0.8 slecht
edcc3502	chirp22c	20	0.6	0.3	5	0.2	564	40.4	0.243	0.8 breekt ervoor maar wel mooie breking 0.75 ok , mooi 0.77 ok, mooi
edcc3525	chirp22c	20	0.6	0.3	5	0.25	870	40.4	0.302	0.4 breekt niet; 0.6 breekt mooi; 0.8 breekt ervoor wel mooi 1 slecht breekt veel te vroeg
edcc3503	chirp22c	20	0.6	0.3	5	0.3	1290	40.4	0.367	0.4 breekt ok goede plaats; 0.6 breekt ervoor wel mooi 0.8 slecht breekt ervoor; 0.55 breekt net ervoor; 0.5 ok
fdcc3502	chirp22c	25	0.6	0.3	5	0.2	630	50	0.257	0.4 breekt niet top wel op 25m; 0.6 mooi wel rustige breking 0.8 breekt ervoor (wel mooi); 0.75 en 0.7 idem; 0.65 mooi
fdcc3525	chirp22c	25	0.6	0.3	5	0.25	996	50	0.323	0.4 ok kleine breking; 0.6 mooi kleine breking ervoor 0.7 idem; 0.75 breekt ervoor (wel mooi) ; 0.55 ok
fdcc3503	chirp22c	25	0.6	0.3	5	0.3	1410	50	0.384	0.4 mooi geen "grote" breking; 0.6 breekt ervoor(2x) (wel mooi) 0.57 en 0.55 idem; 0.45 breekt net ervoor
edcf3502	chirp22cfirstapprox	20	0.6	0.3	5	0.2	564	40.4	0.243	0.8 ok
edcf3503	chirp22cfirstapprox	20	0.6	0.3	5	0.3	1290	40.4	0.367	0.6 breekt ervoor (wel mooi)
fdcf3503	chirp22cfirstapprox	25	0.6	0.3	5	0.3	1410	50	0.384	0.45 mooi
edcs3503	chirp22cdiscussion2	20	0.6	0.3	5	0.3	1320	40.4	0.372	0.45
fdcs3503	chirp22cdiscussion2	25	0.6	0.3	5	0.3	1440	50	0.388	0.45 breekt net ervoor
edcd3502	chirp22d	20	0.6	0.3	5	0.2	548	40.4	0.239	0.4 breekt niet; 0.6 breekt ok (niet erg hoog) 0.8 mooi (breekt net ervoor) vrij hoog
edcd3525	chirp22d	20	0.6	0.3	5	0.25	847	40.4	0.298	0.4 breekt niet; 0.5 mooi goede plaats 0.6 idem 0.7 breekt er net voor (mooie breking) (beste)
edcd3503	chirp22d	20	0.6	0.3	5	0.3	1170	40.4	0.35	0.4 ok (niet erg hoog) 0.5 mooi 0.55 breekt net ervoor (wel mooie breking) beste
fdcd3502	chirp22d	25	0.6	0.3	5	0.2	608	50	0.252	0.4 breekt niet 0.6 ok (niet erg hoog)

Control signal	Software package	x	h	f_0	r	beta	Etot	duration	H_b	Judgement by words (including the gain factor)
cd3525	chirp22d	25	0.6	0.3	5	0.25	940	50	0.314	0.5 goed 0.6 breekt net ervoor
fdcd3503	chirp22d	25	0.6	0.3	5	0.3	1320	50	0.371	0.4 goed 0.5 breekt net ervoor (wel mooi) 0.48 idem 0.45 mooi iets te laat
edcn3502	chirp22dfirstapprox	20	0.6	0.3	5	0.2	548	40.4	0.239	mooi
edcn3503	chirp22dfirstapprox	20	0.6	0.3	5	0.3	1170	40.4	0.35	0.6 breekt ervoor en iets te vroeg (wel mooi)
edcn5503	chirp22dfirstapprox	20	0.6	0.5	5	0.3	356	65.2	0.258	0.4 erg laag "plopje" 0.8 breekt ervoor 0.6 breekt ervoor
edcn1503	chirp22dfirstapprox	20	0.6	1	5	0.3	33.4	129	0.133	0.4 erg laag 0.3 breekt 2 a 3 ker ervoor en focused niet goed
edcn1553	chirp22dfirstapprox	20	0.6	1.5	5	0.3	5.47	193	0.0802	0.6 slecht 0.5 slecht
edcn3203	chirp22dfirstapprox	20	0.6	0.3	2	0.3	1100	17.8	0.339	0.4 slecht 0.65 focused niet 0.7 breekt wel op 20m maar 1 ervoor
edcn3303	chirp22dfirstapprox	20	0.6	0.3	3	0.3	1180	24.2	0.351	0.4 breekt niet 0.6 mooi (iets te vroeg) 0.7 beste (iets te vroeg)
edcn3603	chirp22dfirstapprox	20	0.6	0.3	6	0.3	1190	47.8	0.353	0.45 ok (iets te vroeg) 0.6 breekt ervoor 0.5 breekt ervoor
edcn5303	chirp22dfirstapprox	20	0.6	0.5	3	0.3	352	40.4	0.257	0.4 breekt niet 0.45 breekt net niet ervoor wel erg laag
fdcn5503	chirp22dfirstapprox	25	0.6	0.5	5	0.3	418	81.3	0.28	0.4 laag wel goede plaats
fdcn1503	chirp22dfirstapprox	25	0.6	1	5	0.3	40.9	161	0.147	0.3 slecht focused niet
fdcn1553	chirp22dfirstapprox	25	0.6	1.5	5	0.3	6.77	241	0.0892	0.4 slecht focused niet
fdcn3303	chirp22dfirstapprox	25	0.6	0.3	3	0.3	1280	29.5	0.365	0.65 breekt mooi goede plaats maar misschien golven erna 0.7 idem. maar mooiere breking
fdcn3603	chirp22dfirstapprox	25	0.6	0.3	6	0.3	1340	59.3	0.374	0.45 ok breekt net ervoor
fdcn3203	chirp22dfirstapprox	25	0.6	0.3	2	0.3	1200	21	0.354	0.65 slecht focused niet
fdcn5303	chirp22dfirstapprox	25	0.6	0.5	3	0.3	417	50	0.279	0.43 ok laag
fdcn3503	chirp22dfirstapprox	25	0.6	0.3	5	0.3	1320	50	0.371	0.45 mooi
edns3503	chirp22ddiscussion2	20	0.6	0.3	5	0.3	1240	40.4	0.36	0.4
edns5503	chirp22ddiscussion2	20	0.6	0.5	5	0.3	371	65.2	0.263	0.3 heeeel klein
edns3303	chirp22ddiscussion2	20	0.6	0.3	3	0.3	1200	24.2	0.354	0.4 breekt niet 0.6 breekt niet ervoor redelijk hoog wel laat 0.67 beste
fdns3503	chirp22ddiscussion2	25	0.6	0.3	5	0.3	1370	50	0.379	0.4 iets te laat
fdns5503	chirp22ddiscussion2	25	0.6	0.5	5	0.3	438	81.3	0.286	0.4 slecht 0.3 ok "plopje" erg laag
fdns3303	chirp22ddiscussion2	25	0.6	0.3	3	0.3	1310	29.4	0.37	0.65 ok breekt wel na laatste hoogtemeter 0.7 beste wel te laat
edca3503	chirp22analy	20	0.6	0.3	5	0.3	1080	40.4	0.335	0.4 breekt net; 0.6 breekt ervoor (wel mooi);

Control signal	Software package	x	h	f_0	r	beta	Etot	duration	H_b	Judgement by words (including the gain factor)
fdfa1503	chirp22firstapprox	25	0.6	1	5	0.3	40.9	161	0.147	0.4 slecht breekt te vroeg focused niet goed
fdfa1553	chirp22firstapprox	25	0.6	1.5	5	0.3	6.84	241	0.0896	0.45 erg slecht focused niet
fdfa3303	chirp22firstapprox	25	0.6	0.3	3	0.3	1490	29.5	0.395	0.65 mooi veel te vroeg
fdfa3603	chirp22firstapprox	25	0.6	0.3	6	0.3	1560	59.3	0.405	0.4 breekt NET ervoor + te vroeg
fdfa3203	chirp22firstapprox	25	0.6	0.3	2	0.3	1400	21	0.383	0.65 slecht focused niet
fdfa1303	chirp22firstapprox	25	0.6	1	3	0.3	40.6	97.1	0.147	0.4 slecht focussed niet goed
fdfa5303	chirp22firstapprox	25	0.6	0.5	3	0.3	435	50	0.285	0.4 ok iets te vroeg en vrij laag
edgm3502	chirp22firstapproxumass	20	0.6	0.3	5	0.2	597	40.4	0.25	zie edgm3503
edgm3503	chirp22firstapproxumass	20	0.6	0.3	5	0.3	1310	40.4	0.37	0.6 breekt ervoor en te vroeg
fdgm3503	chirp22firstapproxumass	25	0.6	0.3	5	0.3	1480	50	0.394	0.4 breekt iets te vroeg. ok
eddu3503	chirp22discussion2	20	0.6	0.3	5	0.3	1430	40.4	0.387	0.4 te vroeg verder ok laag
fddu3503	chirp22discussion2	25	0.6	0.3	5	0.3	1610	50	0.411	0.4 ok
edug3503	chirp22discussion2umass	20	0.6	0.3	5	0.3	1380	40.4	0.38	0.4 ok laag + iets te vroeg
fdug3503	chirp22discussion2umass	25	0.6	0.3	5	0.3	1510	50	0.398	0.4 ok vrij laag
edcl3502	chirp22lin	20	0.6	0.3	5	0.2	548	40.4	0.239	0.4 breekt niet; 0.6 ok (niet hoog); 0.7 mooi
										0.8 breekt net ervoor (wel mooi)
edcl3525	chirp22lin	20	0.6	0.3	5	0.25	847	40.4	0.298	0.4 breekt net; 0.5 ok (niet hoog); 0.6 mooi;
										0.7 breekt ervoor (mooie breking) 0.8 breekt net ervoor(wel ok)
edcl3503	chirp22lin	20	0.6	0.3	5	0.3	1170	40.4	0.35	0.3 breekt niet; 0.4 goed (niet hoog);
										0.6 breekt ervoor (2x) wel mooi
edcl5502	chirp22lin	20	0.6	0.5	5	0.2	165	65.2	0.176	0.6 heel laag "plopje" ; 0.8 beter nog laag
										1 betere breking maar wel 2x ervoor gebroken
edcl5503	chirp22lin	20	0.6	0.5	5	0.3	356	65.2	0.258	0.6 breekt (2x) ervoor (lage breking);
										0.8 breekt beter wel iets te laat; 1 slecht
fdcl3502	chirp22lin	25	0.6	0.3	5	0.2	608	50	0.252	0.4 breekt niet; 0.6 goed; 0.8 breekt er voor wel mooiere breking
										0.9 breekt net 2x ervoor.breking mooi; 1 te laat + ervoor gebroken
fdcl3525	chirp22lin	25	0.6	0.3	5	0.25	940	50	0.314	0.6 breekt ervoor wel gode breking; 0.7 idem;
										0.8 breekt veel ervoor. wel mooie breking uiteindelijk
fdcl3503	chirp22lin	25	0.6	0.3	5	0.3	1320	50	0.371	0.4 breekt (laag) 0.6 iets te ver+ breekt ervoor (wel mooier)
										0.8 1 ervoor al redelijk hoog (slecht)
fdcl5502	chirp22lin	25	0.6	0.5	5	0.2	193	81.3	0.19	0.6 breekt (erg laag); 0.8 ok; 1 breekt ervoor
fdcl5503	chirp22lin	25	0.6	0.5	5	0.3	418	81.3	0.28	0.6 breekt ervoor (laag); 0.5 goed , wel kleine breking
edlf3502	chirp22linfirstapprox	20	0.6	0.3	5	0.2	548	40.4	0.239	0.8 mooi
edlf3503	chirp22linfirstapprox	20	0.6	0.3	5	0.3	1170	40.4	0.35	0.6 breekt er net voor (wel mooi) en hoog en goede plaats
fdlf3503	chirp22linfirstapprox	25	0.6	0.3	5	0.3	1320	50	0.71	0.45 ok iets te laat
edlt3503	chirp22lindiscussion2	20	0.6	0.3	5	0.3	1240	40.4	0.36	0.45 beste 0.4 goed wel laag 0.6 wel hoog breekt 2 keer ervoor
										0.5 breekt 1 keer ervoor en lager
fdlt3503	chirp22lindiscussion2	25	0.6	0.3	5	0.3	1370	50	0.379	0.4 te laat
bucc3502	chirp23c	20	0.7	0.3	5	0.2	687	40.4	0.259	1 mooi 0.9 breekt ervoor
										0.8 breekt er net voor en golf veel later (slecht)
bucc5502	chirp23c	20	0.7	0.5	5	0.2	196	65.2	0.186	0.6 ok (niet erg mooi) 0.8 breekt ervoor
										0.7 ok (wel golf erachter maar hoort er denk niet bij)
eucc3502	chirp23c	20	0.6	0.3	5	0.2	562	40.4	0.243	0.4 breekt niet; 0.5 breekt net; 0.6 breekt goed
										0.7 breekt ervoor; 0.65 breekt net ervoor
eucc3525	chirp23c	20	0.6	0.3	5	0.25	845	40.4	0.297	0.4 breekt net; 0.6 goed; 0.7 breekt ervoor
										0.65 breekt ervoor
eucc3503	chirp23c	20	0.6	0.3	5	0.3	1230	40.4	0.359	0.4 goed; 0.45 mooi 0.5 breekt net ervoor
eucc3303	chirp23c	20	0.6	0.3	3	0.3	1190	24.2	0.352	0.6 ok iets te laaat
eucc3603	chirp23c	20	0.6	0.3	6	0.3	1240	47.8	0.361	0.48 breekt net ervoor focused ok

Control signal	Software package	x	h	f_0	r	beta	Etot	duration	H_b	Judgement by words (including the gain factor)
fucc3525	chirp23c	25	0.6	0.3	5	0.25	966	50	0.318	0.4 breekt net; 0.6 breekt ervoor en te ver weg
fucc3503	chirp23c	25	0.6	0.3	5	0.3	1360	50	0.377	0.4 breekt maar iets te laat; 0.5 breekt ervoor en te laat
fucc3303	chirp23c	25	0.6	0.3	3	0.3	1330	29.4	0.373	0.6 ok maar te laat
										0.7 breekt ervoor 0.67 beste
fucc3603	chirp23c	25	0.6	0.3	6	0.3	1390	59.3	0.381	0.4 breekt ervoor en te laat 0.35 ok
fucc3203	chirp23c	25	0.6	0.3	2	0.3	1210	20.9	0.356	0.65 focused en brekt niet 0.7 focused niet en breekt ervoor
										0.67 focused niet
fucc5503	chirp23c	25	0.6	0.5	5	0.3	438	81.3	0.286	0.4 breekt ervoor 0.35 slecht laag iets te laat
fucc1503	chirp23c	25	0.6	1	5	0.3	39.8	161	0.145	0.4 breekt maar erg laag + slecht
fucc1553	chirp23c	25	0.6	1.5	5	0.3	6.75	241	0.0891	0.4 slecht
fucc1303	chirp23c	25	0.6	1	3	0.3	39.5	97.1	0.145	0.4 redelijk
fucc5303	chirp23c	25	0.6	0.5	3	0.3	432	50	0.284	0.4
bucd3502	chirp23d	20	0.7	0.3	5	0.2	687	40.4	0.259	breekt te laat wel mooie breking
ehcl3502	chirp23d	20	0.6	0.3	5	0.2	562	40.4	0.243	mooi
ehcl3503	chirp23d	20	0.6	0.3	5	0.3	1230	40.4	0.359	0.5 breekt ervoor
fhcl3503	chirp23d	25	0.6	0.3	5	0.3	1360	50	0.377	zie fhcl3502
fhcl3502	chirp23d	25	0.6	0.3	5	0.2	624	50	0.256	0.6 slecht 0.4 slecht focused niet
bacc3502	chirp24c	20	0.7	0.3	5	0.2	760	40.4	0.272	1 te laat maar vrij mooie breking
eacc3502	chirp24c	20	0.6	0.3	5	0.2	621	40.4	0.255	0.6 ok; 0.8 breekt ervoor ; 0.75 breekt net ervoor
eacc3525	chirp24c	20	0.6	0.3	5	0.25	962	40.4	0.317	0.4 breekt niet 0.6 breekt er net voor (wel goed);
										0.55 goed
eacc3503	chirp24c	20	0.6	0.3	5	0.3	1410	40.4	0.384	0.4 goed (vrij laag); 0.45 ok (wel iets te vroeg)
facc3502	chirp24c	25	0.6	0.3	5	0.2	678	50	0.266	0.4 breekt niet; 0.6 ok (kleine breking) 0.7 breekt ervoor(laag)
										0.65 breekt er net voor (laag)
facc3525	chirp24c	25	0.6	0.3	5	0.25	1080	50	0.336	0.4 breekt net "plop"; 0.6 breekt ervoor (2x) wel betere breking
										0.55 breekt ervoor (mindere breking)
facc3503	chirp24c	25	0.6	0.3	5	0.3	1590	50	0.408	0.4 breekt (laag); 0.5 breekt (2x) ervoor
ehat3502	chirp29	20	0.6	0.3	5	0.2	621	40.4	0.255	0.4 breekt niet; 0.6 breekt net + golf (2x) erna
										0.8 idem (SLECHT)
ehaw3503	chirp290(-3/4pi) subharm=0	20	0.6	0.3	5	0.3	1410	40.4	0.384	0.4 wel laag
fhaw3503	chirp290(-3/4pi) subharm=0	25	0.6	0.3	5	0.3	1590	50	0.408	0.4 goed
ehmt3502	chirp30	20	0.6	0.3	5	0.2	562	40.4	0.243	0.6 2x golf erna slecht breking
ehmt3503	chirp30	20	0.6	0.3	5	0.3	1230	40.4	0.359	zie ehmt3503
fhmt3502	chirp30	25	0.6	0.3	5	0.2	624	50	0.255	0.6 slecht focused niet 0.7 breekt maar 1 golf veel te laat
fhmt3503	chirp30	25	0.6	0.3	5	0.3	1360	50	0.377	zie fhmt3502
ehaa3502	chirp31	20	0.6	0.3	5	0.2	621	40.4	0.255	0.6 breekt net wel golf erna; 0.8 beter
ehaa3503	chirp31	20	0.6	0.3	5	0.3	1410	40.4	0.384	0.6 breekt ervoor (wel mooie breking)+ golf erna
ehaa5502	chirp31	20	0.6	0.5	5	0.2	176	65.2	0.182	0.6 breekt net + 1 ervoor (laag);
										0.8 beter (laag) + breekt ervoor
ehaa5503	chirp31	20	0.6	0.5	5	0.3	395	65.2	0.272	0.6 breekt ervoor + laag (slecht)
fhaa3502	chirp31	25	0.6	0.3	5	0.2	678	50	0.266	zie fhaa3503
fhaa3503	chirp31	25	0.6	0.3	5	0.3	1590	50	0.408	0.4 ok wel te vroeg + laag
ehtt3502	chirp32	20	0.6	0.3	5	0.2	581	40.4	0.247	0.4 breekt niet; 0.6 breekt net;
										0.8 breekt ervoor + te laat+2 erna (slecht)

Control signal	Software package	x	h	f_0	r	beta	Etot	duration	H_b	Judgement by words (including the gain factor)
ehtt3503	chirp32	20	0.6	0.3	5	0.3	1310	40.4	0.37	zie ehtt3502
fhtt3502	chirp32	25	0.6	0.3	5	0.2	632	50	0.257	0.6 slecht focused niet en een golf te laat
fhtt3503	chirp32	25	0.6	0.3	5	0.3	1470	50	0.392	zie fhtt3502
fdnn3503	chirp33	25	0.6	0.3	5	0.3	1410	50	0.384	0.48 mooi
ednt3502	chirp33firstapprox	20	0.6	0.3	5	0.2	564	40.4	0.243	0.8 ok
ednt3503	chirp33firstapprox	20	0.6	0.3	5	0.3	1290	40.4	0.367	0.6 breekt ervoor en te vroeg (wel mooi)
ednt3519	chirp33firstapprox	20	0.6	0.3	5	0.188	504	40.4	0.23	zie ednt3503
fdnt3503	chirp33firstapprox	25	0.6	0.3	5	0.3	1410	50	0.384	0.5 breekt NET ervoor
edkk3503	chirp33discussion2	20	0.6	0.3	5	0.3	1320	40.4	0.372	0.4 goed maar laag breekt net niet ervoor 0.6 breekt twee keer ervoor wel hoog
edkk3517	chirp33discussion2	20	0.6	0.3	5	0.169	414	40.4	0.208	0.4 goed maar laag breekt net niet ervoor 0.6 breekt 2 x ervoor wel hoog
fdkk3503	chirp33discussion2	25	0.6	0.3	5	0.3	1440	50	0.388	0.45 breekt net ervoor 0.4 ok iets te laat
fdat3503	chirp340 subharm=0	25	0.6	0.3	5	0.3	1600	50	0.41	0.4 slecht breekt net wel ervoor laag en te vroeg
edtf3502	chirp34firstapprox	20	0.6	0.5	5	0.2	596	40.4	0.25	0.8 breekt ervoor niet mooi
edtf3503	chirp340firstapprox subharm=0	20	0.6	0.5	5	0.3	1390	40.4	0.381	0.6 te vroeg en breekt ervoor (wel mooie breking)
fdtf3503	chirp340firstapprox subharm=0	25	0.6	0.3	5	0.3	1550	50	0.403	0.48 breekt net ervoor eigenlijk 0.45 wel goede plaats
edtr3503	chirp340discusion2	20	0.6	0.3	5	0.3	1430	40.4	0.387	0.4 laag
fdtr3503	chirp340discusion2	25	0.6	0.3	5	0.3	1610	50	0.411	0.4
edmt3503	chirp350 subharm=0	20	0.6	0.3	5	0.3	1170	40.4	0.35	edmt3517 te laat
fdmt3503	chirp350 subharm=0	25	0.6	0.3	5	0.3	1320	50	0.71	
fdmt5503	chirp35	25	0.6	0.5	5	0.3	418	81.3	0.28	0.4 ok
edmf3502	chirp35firstapprox	20	0.6	0.3	5	0.2	548	40.4	0.239	slecht
edmf3503	chirp350firstapprox subharm=0	20	0.6	0.3	5	0.3	1170	40.4	0.35	erg grote laatste golf breekt aan het begin verder ok
fdmf3503	chirp350firstapprox subharm=0	25	0.6	0.3	5	0.3	1320	50	0.371	0.4 ok
edms3503	chirp35discussion2	20	0.6	0.3	5	0.3	1240	40.4	0.36	0.45
fdms3503	chirp350discussion2	25	0.6	0.3	5	0.3	1370	50	0.379	0.4 te laat
fdaa3503	chirp36	25	0.6	0.3	5	0.3	1600	50	0.41	0.4 ok breekt net niet ervoor. . niet erg hoog
edaf3502	chirp36firstapprox	20	0.6	0.3	5	0.2	596	40.4	0.25	zie edaf3503
edaf3503	chirp36firstapprox	20	0.6	0.3	5	0.3	1390	40.4	0.381	0.6 ok breekt ervoor en te vroeg (wel mooi)
fdaf3503	chirp36firstapprox	25	0.6	0.3	5	0.3	1550	50	0.403	0.4 ok breekt erg vroeg (voor de 1ste hoogte meter) (24.6m)
eded3503	chirp36discussion2	20	0.6	0.3	5	0.3	1230	40.4	0.359	
fded3503	chirp36discussion2	25	0.6	0.3	5	0.3	1610	50	0.411	0.4 breekt NET wel ervoor maar verder ok
fdtt3503	chirp370	25	0.6	0.3	5	0.3	1410	50	0.384	0.4 ok niet erg hoog
edff3502	chirp37firstapprox	20	0.6	0.3	5	0.2	564	40.4	0.243	0.8 breekt te laat
edff3519	chirp37firstapprox	20	0.6	0.3	5	0.19	504	40.4	0.23	breekt ervoor
edff3503	chirp370firstapprox subharm=0	20	0.6	0.3	5	0.3	1290	40.4	0.367	0.6 breekt te vroeg
fdff3503	chirp370firstapprox subharm=0	25	0.6	0.3	5	0.3	1410	50	0.384	0.6 breekt ervoor 0.5 breekt net ervoor 0.48 ok iets te vroeg

Control signal	Software package	x	h	f_0	r	beta	Etot	duration	H_b	Judgement by words (including the gain factor)
eddt3503	chirp370discussion2	20	0.6	0.3	5	0.3	1320	40.4	0.372	0.4
eddt3515	chirp370discussion2	20	0.6	0.3	5	0.15	318	40.4	0.182	zie eddt3503
fddt3503	chirp370discussion2	25	0.6	0.3	5	0.3	1440	50	0.388	0.4 ok breekt net niet evoor
fhmg3503	chirp380 subharm=0	25	0.6	0.3	5	0.3	1360	50	0.377	0.4 ok iets te laat
fdtg3503	chirp390 subharm=0	25	0.6	0.3	5	0.3	1460	50	0.39	0.4 ok wel iets te laat kleine breking
edfg3502	chirp39firstapprox	20	0.6	0.3	5	0.2	571	40.4	0.245	vrij slecht (breekt te laat)
edfg3503	chirp390firstapprox subharm=0	20	0.6	0.3	5	0.3	1290	40.4	0.367	erg slecht
fdfg3503	chirp390firstapprox subharm=0	25	0.6	0.3	5	0.3	1460	50	0.39	0.45 breekt NET ervoor. slecht. laag en te laat
edgt3503	chirp390discussion2	20	0.6	0.3	5	0.3	1290	40.4	0.367	0.45
fdgt3503	chirp390discussion2	25	0.6	0.3	5	0.3	1460	50	0.39	0.45 slecht breekt NET ervoor + iets te laat en laag
elll3503	chirp40	20	0.6	0.3	5	0.3	1440	40.4	0.388	0.4 erg laag iets te laat
flll3503	chirp40	25	0.6	0.3	5	0.3	1580	50	0.406	0.4 wel laag verder ok
ella3503	chirp41	20	0.6	0.3	5	0.3	1350	40.4	0.376	0.45 erg laag golfjes revoor
flla3503	chirp41	25	0.6	0.3	5	0.3	1460	50	0.391	0.4 slecht focused goed????? (video bekijken)
ellc3503	chirp42	20	0.6	0.3	5	0.3				0.4 erg laag en golf vlak achter (hoort er misshien bij??)
fllc3503	chirp42	25	0.6	0.3	5	0.3	1580	50	0.406	0.4 erg laag
elca3503	chirp43	20	0.6	0.3	5	0.3				0.42 erg laag
flca3503	chirp43	25	0.6	0.3	5	0.3	1460	50	0.391	0.4
elcn3503	chirp44	20	0.6	0.3	5	0.3				0.45
flcn3503	chirp44	25	0.6	0.3	5	0.3	1460	50	0.39	0.4
elnn3503	chirp45	20	0.6	0.3	5	0.3				0.45
flnn3503	chirp45	25	0.6	0.3	5	0.3	1460	50	0.39	0.4

Appendix J

Data acquisition

All the control signals of the performed experiments can be found on the CD. The names of these control signals consist of eight characters. The first four characters are letters and the last four are numbers. The choice for the different characters is explained below:

The first letter: Represents the distance of the theoretical focus point to the wave board:
- e symbolizes the theoretical focus point at 20m
- f symbolizes the theoretical focus point at 25m

The next three letters : With these letters the used theories are tried to be symbolised. Because of the large amount of experiments this could not be done consequently and therefore no further explanation is given.

The first number: Represents the used peak frequency:
- 3 symbolizes the peak frequency of 0,3 Hz.
- 5 symbolizes the peak frequency of 0,5 Hz.
- 1 symbolizes the peak frequency of 1,0 Hz.
- 15 symbolizes the peak frequency of 1,5 Hz

The use of the peak frequency of 1,5 Hz results in the use of the first and second number.

The second number Represents the used ratio between the maximum frequency to the peak frequency:
- 2 symbolizes a ratio of 2.
- 3 symbolizes a ratio of 3.
- 5 symbolizes a ratio of 5.
- 6 symbolizes a ratio of 6.

For the experiments with a peak frequency of 1,5 Hz the ratio becomes the third number.

The third and fourth number Represent the used relative wave height:
- 02 symbolizes a relative wave height of 0,2.
- 25 symbolizes a relative wave height of 0,25.
- 03 symbolizes a relative wave height of 0,3.

For the experiments with a peak frequency of 1,5 Hz the relative wave height becomes the fourth number only.
- 2 symbolizes a relative wave height of 0,2.
- 3 symbolizes a relative wave height of 0,3.

The use of the relative wave height of 0,25 in combination with a peak frequency of 1,5 Hz. has not been carried out.

An example:

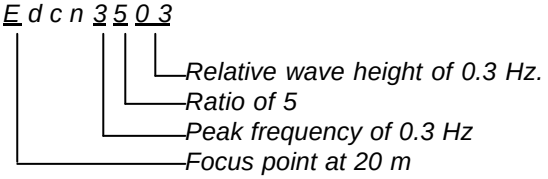

Appendix G shows the different names of the control signals and the accompanying used software package (including the used theories) and the used values of the variables.

The data of the surface elevation measurements are stored in files for each experiment and the names of these files are the same as the accompanying control signals only before this name there are four or five characters added:

19h3 are added for the experiments with the theoretical focus point at 20 meters.
24h25 are added for the experiments with the theoretical focus point at 25 meters.

For each experiment two kind of files are created one with the extension *.asci, which includes only the data of the measurements. The other one with the extension *.doc, which includes only the picture of the measurements, both are stored on the CD and the pictures can also be found in the accompanying appendices-rapport.

Appendix K

Implementation of the theories

This appendix describes the different step of figure 4-9.

- Define the parameters.
  - Request the users input (depth (h), outputname, focus distance (x_{focus}), peak frequency (f_0), ratio of maximum frequency to the peak frequency (ratio) and the relative wave height (β)).
  - Define the constants required for the computations, like the starting point (x_0) and the density etc.
  - Compute the following parameters:

$$f_{\max} = ratio * f_0 \quad \text{(K-1)}$$

$k_{\max}$ = iterative computation with the linear dispersion relation($w = 2pf_{\max}$,h,g)

The wave with the highest frequency ($f_{\max}$) travels with the lowest velocity, the minimum group velocity can therefore be calculated with this frequency (with the linear theory):

$$C_{group,\min} = \frac{1}{2}\frac{2pf_{\max}}{k_{\max}}\left[1 + k_{\max}h\frac{1-\tanh^2(k_{\max}h)}{\tanh(k_{\max}h)}\right] \quad \text{(K-2)}$$

All the waves of the wave train have to arrive at the focus point at the same time (the focus time). Consequently the wave with the lowest velocity is decisive for the focus time. This time can be computed with the minimum group velocity:

$$t_{focus} = \frac{x_{focus} - x_0}{C_{group\min}} \quad \text{(K-3)}$$

- Compute maximum and minimum angular frequency and create an array with equidistant frequency steps
  - The minimum and maximum wave angular frequency can be computed with:

$$w_{\min} = 2pf_0 \quad \text{(K-4)}$$

$$w_{\max} = 2pf_{\max} \quad \text{(K-5)}$$

  - A first estimate for the angular wave frequency has been generated by linearly spacing between the maximum- and minimum angular frequency with equidistant frequency steps.

- Compute the wave number with the linear dispersion relation
  - The wave number will be calculated iterative with the linear dispersion relation:

$$w = \sqrt{gk\tanh(kh)}$$

Furthermore the wave number array will stay fixed.

- Initialise the amplitude equal to zero

The run will start with an array of the amplitude, which is set to zero. Therefore in the first iteration all the nonlinear terms are not included.

To compute the desired angular wave frequency with the accompanying group velocity, time and amplitude arrays, a loop will follow. This loop will end when the relative differences of the angular wave frequency between the iterations is small enough (<1e-6)

***Begin Loop**:*

- Compute a new angular frequency (ω) with the chosen dispersion relation
  - The angular wave frequency will be computed with the desired dispersion relation, for example, Hedges (equation 2-17):

    Hedges: $$w = \sqrt{gk\left(1+e^{2}\right)\tanh\left(\frac{kh+e}{1+e^{2}}\right)}$$

- Compute the group velocity

  The group velocity could be evaluated from the dispersion relation and is a function of the wave number:

  - $$C_{group} = \frac{dw}{dk}$$

- Compute the time
  - to travel the same distance and have to arrive in the focus point at exactly the same time. So the time array will be computed with:

$$C_{group} = \frac{x_{focus} - x_0}{t_{focus} - t} \qquad \Rightarrow \qquad t = t_{focus} - \frac{x_{focus} - x_0}{C_{group}} \qquad \text{(F-6)}$$

- Compute the amplitude
  - The amplitude will be calculated with the Miche criterion (equation 2-53):

$$a(t) = \frac{1/2 * b * 0{,}88}{k}$$

End loop

- Compute the phase shift (to get the wave crest of the last wave at the focus point)
  - The phase shift can be computed with equation 2-56:

$$q_0 = k\left(x_{focus} - x_0\right) - w\left(t_{focus} - t_{lastwave}\right)$$

- Compute the wave phase
  - The wave phase can be computed with equation 2-77:

$$y = -\int w dt - q_0 - phase\_correction$$

After the required arrays has been computed the values at the beginning and the end of the arrays are described by a varying function in order to avoid discontinuities. These values extend over three wave periods at the beginning and two wave periods at the end.

- Compute the water surface elevation at x =0 m
  - Compute the water elevation at x = 0 m with:

$$z = a\cos[y] \qquad \text{(F-7)}$$

- Compute the wave board motion at x = 0 m
  - Compute the wave board motion at x = 0 m with equation 3-4:

$$X = -\frac{kC_{group}a}{w\tanh(kh)}\sin(y)$$

- Write the computed signal to file and write some characteristic properties to screen (incl. some plots)
  - The calculated surface water elevation and wave board motion, as a function of time will be written to a file.
  - Some characteristic properties are computed en written to screen:

Wave energy per unit area:	$E = \frac{1}{2}rga^2$	(4.53)
Wave energy flux per meter flume width:	$E_{flux} = EC_{group}$	(4.54)
Work performed by wave maker:	$W = \int E_{flux}dt$	(4.55)
Expected wave length of the breaking wave:	$l_{break} = \frac{2p}{k}$	(4.56)
Total wave energy input by the wave maker:	$H_{break} = \sqrt{\frac{8W}{l_{break}rg}}$	(4.57)

The corrections and the second-order theory are described below:

Compute the mass correction
If a correction for the mass transport velocity is required, first the correction will be computed with:
Compute the correction for the mass-transport velocity with equation 2-84

$$U_{correction} = -\frac{1}{2}\frac{gka^2}{wh}$$

Compute dispersion relationship including the mass correction with equation 2-85:

$$w_{ucorr} = w + kU$$

where:

w_{ucorr} = The corrected angular wave frequency (due to the mass-transport velocity)

Compute the Lagrangian correction
To apply the lagrangian correction to the wave frequency focussing signal the following steps has to be carried out:

Compute the orbital displacement of the Lagrangian point with respect to the still position x:

$$x_0 = -\frac{a}{\tanh(kh)}\sin(y) \qquad (2\text{-}78)$$

Compute the non-linear corrected water surface elevation:

$$z_E(t) = a\cos(y - kx_0) \qquad (2\text{-}79)$$

Compute the linear-theory wave maker motion:

$$X_0(t) = -\frac{C_g}{C}\frac{1}{\tanh(kh)}a\sin(-wt) \qquad (2\text{-}80)$$

Compute the non-linear corrected wave maker motion:

$$X_E(t) = -\frac{C_g}{C}\frac{1}{\tanh(kh)}a\sin\left(-kX_0(t) - wt\right) \qquad (2\text{-}81)$$

Apply the second-order wave maker theory:
This will not be repeated here. The whole theory used for getting the second-order wave signal is described in 3.3.

The Cauchy-Poisson theory programmed by G. Klopman and explained in appendix D will not be further described here.